Review of Iberia-Eurasia plate-boundary basins: Role of sedimentary burial and salt tectonics during rifting and continental breakup

Nicolas Saspiturry, Philippe Razin, Thierry Baudin, Riccardo Asti, Yves Lagabrielle, Cécile Allanic, Olivier Serrano, Thibault Duretz

Review of Iberia-Eurasia plate-boundary basins: Role of sedimentary burial and salt tectonics during rifting and continental breakup

Nicolas Saspiturry[1*], Benoit Issautier[2], Philippe Razin[1], Thierry Baudin[2], Riccardo Asti[3], Yves Lagabrielle[3], Cécile Allanic[2], Olivier Serrano[2] and Thibault Duretz[2]

[1] Université Bordeaux Montaigne / EA 4592 Géoressources & Environnement, 1 allée Fernand Daguin, 33607 Pessac cedex, France

[2] Université Rennes, CNRS, Géosciences Rennes - UMR 6118, F-35000, Rennes, France

[3] BRGM-French Geological Survey, 3 Avenue Claude Guillemin, 45100 Orléans, France

*Corresponding author (e-mail: saspiturry.nicolas@gmail.com)

Data sharing is not applicable to this article as no new data were created or analysed in this study.

Acknowledgement

This work is part of Saspiturry's Ph.D. research conducted as part of the OROGEN project, cofunded by Total S.A., Bureau de Recherches Géologiques et Minières (BRGM), and Institut National de Sciences de l'Univers (INSU). We thank OROGEN project managers Sylvain Calassou (Total), Emmanuel Masini (Total), Olivier Vidal (CNRS, Centre National de la Recherche Scientifique) and Isabelle Thinon (BRGM). We specially thank Basin Research's deputy editor Kerry Gallagher and the three reviewers, Tiago M. Alves, Per Terje Osmundsen and Nicholas Christie-Blick for their constructive comments, which significantly improved the initial manuscript.

Keywords

Iberian-European boundary; Sedimentary burial; Salt tectonics; Depth-dependent thinning; Ductile regime; HT/LP metamorphism

Abstract

We document the role of sedimentary burial and salt tectonics in controlling the deformation style of continental crust during hyperextension. The Iberian-European boundary records a complex history of Cretaceous continental extension, which has led to the development of so-called smooth-slope type basins. Based on the review of the available geological constraints (crustal-balanced cross sections, sedimentary profile evolution, RSCM thermometer, low-temperature thermochronology) and geophysical data (Bouguer anomaly, Moho depth, seismic reflection profiles, and Vp/Vs velocity models) on the Tartas, Arzacq, Cameros, Parentis, Columbrets, Mauléon, Basque-Cantabrian and Internal Metamorphic Zone basins, we shed light on the main characteristics of this type of basin. This synthesis indicates that crustal thinning was influenced by two decoupling horizons: the middle crust and Triassic pre-rift salt, initially located between the basement and pre-rift sedimentary cover. These two horizons remained active throughout basin formation and were responsible for depth-dependent thinning of the crust and syn-rift salt tectonics. We therefore identify several successive deformation phases involving (1) pure shear dominated thinning, (2) simple shear dominated thinning and (3) continental breakup. In the first phase, distributed deformation resulted in the development of a symmetric basin. Field observations indicate that the middle and lower crust were under dominantly ductile conditions at this stage. In the second phase, deformation was localized along a crustal detachment rooted between the crust and the mantle and connecting upwards with Triassic pre-rift salt. During continental breakup, basin shoulders recorded the occurrence of brittle deformation while the hyperextended domain remained under predominantly ductile thinning. The formation of smooth-slope type extensional basins was intrinsically linked to the combined deposition of thick syn-rift and breakup sequences, and regional salt tectonics. They induced significant burial and allowed

the continental crust and the pre-rift sequence to deform under high temperature conditions from the rifting to continental breakup stages.

1 Introduction

Recent models and concepts related to hyperextended continental margins have been defined on North Atlantic passive margins such as West Iberia/Newfoundland (Boillot et al., 1980, 1995; Reston et al., 1995; Whitmarsh et al., 2001; Péron-Pinvidic & Manatschal, 2009; Péron-Pinvidic et al., 2015), Norway/Greenland (Osmundsen et al., 2002; Osmundsen & Ebbing, 2008; Osmundsen & Péron-Pinvidic, 2018), and the Alps (Lemoine et al., 1987; Froitzheim & Manatschal, 1996; Manatschal & Nievergelt, 1997; Manatschal et al., 2006; Masini et al., 2011; Mohn et al., 2014). They describe the mechanisms responsible for continental crust thinning and subcontinental mantle exhumation at the ocean-continent transition, and have shown that the hyperextended domain of continental margins is characterized by (1) sediment starved conditions with very thin pre-rift and syn-rift sedimentary sequences, (2) asymmetric margins, and (3) coupled deformation between the basement and sedimentary cover resulting in the formation of extensional allochthons. The syn-rift and post-rift units have been respectively defined as strata deposited during (1) the last extension episode leading to continental breakup and (2) a period of relative tectonic quiescence above a regional breakup unconformity (Driscoll et al., 1995; Wilson et al., 2001). DSDP and ODP drilling expeditions along the West-Iberia margin have also contributed to a more complete understanding of how continental breakup is recorded in syn-rift to post-rift sedimentary sequences (Alves & Cunha, 2018), and how it evolves through time along the strike of continental margins (Alves et al., 2009). Indeed, such data allowed the identification of syn-rift, breakup and post-rift sequences as correlating with major phases of crustal thinning, mantle denudation and oceanic spreading (Alves et al., 2009; Soares et al., 2012; Soares, 2014; Alves & Cunha, 2018; Alves et al.,

2020). Continental breakup is thus defined as the deposits that are correlated with the phases of hyperextension and mantle denudation on magma-poor continental margins (Soares et al., 2012). Alves et al. (2020) have demonstrated that continental breakup is only possible along magma-poor Type I margins (sensu Huismans & Beaumont, 2003, 2008, 2011, 2014). Indeed, the upper lithosphere in Type I margins is much more coupled to the continental crust than in Type II margins (Alves et al., 2020). Thus, along Type II margins, the upper lithosphere is laterally subtracted and mantle denudation cannot occur. Syn-rift and breakup sequences are delimited by major unconformities corresponding (from bottom to top) to the base syn-rift unconformity (BSU; base of syn-rift sequence), the lithospheric breakup surface (LBS; base of the breakup sequence) and the base post-rift unconformity (BPU; base of the post-rift sequence) as defined by Soares et al. (2012) and Soares (2014). While Atlantic-type margins develop under conditions of high mantle heat flow, as the product of asthenosphere upwelling and subsequent denudation of subcontinental mantle (e.g., Huismans & Beaumont, 2003, 2008, 2011, 2014; Lavier & Manatschal, 2006; Brune et al., 2014, 2016), the North Pyrenean hyperextended rift system differs from the Atlantic type by the presence of high-temperature/low-pressure (HT/LP) metamorphism (Albarède & Michard-Vitrac, 1978a, 1978b; Golberg et al., 1986; Montigny et al., 1986; Golberg & Maluski, 1988; Golberg & Leyreloup, 1990; Thiébaut et al., 1992). The North Pyrenean rift basins were affected by a syn-rift stage throughout the Early Cretaceous that evolved to continental breakup and mantle denudation during the Latest Albian to Early Cenomanian (Debroas et al., 2010; Saspiturry et al., 2019a; Espurt et al., 2019; Labaume & Teixell, 2020). Thus, these margins can be defined as Type I margins as mantle denudation occured during continental breakup (sensu Huismans & Beaumont, 2003, 2008, 2011, 2014). The hyperextended domain of these basins is interpreted to have stretched under high-temperature conditions under a predominantly ductile regime, resulting in the generation of large-scale boudins whose formation was controlled by

a strong thermal and structural inheritance (Clerc & Lagabrielle, 2014; Clerc et al., 2015, 2015b; Corre et al., 2016; de Saint Blanquat et al., 2016; Teixell et al., 2016; Lagabrielle et al., 2016, 2019; Asti et al., 2019). The major difference between the hyperextended Atlantic-type and Pyrenean Cretaceous rift margins is the rare occurrence of tilted crustal blocks and related stepping fault scarps in the central parts of the basins, thus defining a dominantly symmetrical basement profile with smooth slopes (see Lagabrielle et al., 2020 for a review). Several other rift basins apart from the North Pyrenean rift basins exist along the plate boundary separating Iberia from the Eurasia plate and share several features in common with the Pyrenean system. They include the Tartas, Arzacq, Columbrets, Cameros and Parentis syn-rift basins, which developed during Late Jurassic to Early Cretaceous rifting (more details in the review section). The development of these basins is time-equivalent to the Late Jurassic–Aptian rifting and Albian-Cenomanian breakup sequence of the V-shaped Bay of Biscay margin (Montadert et al., 1979; Barbier et al., 1986; Thinon, 1999; Vergés & García-Senz, 2001; Thinon et al., 2003; Tugend et al., 2014) and the NW-Iberia margin (Soares et al., 2012; Alves & Cunha, 2018; Alves et al., 2020). All of these basins share similarities that include (1) a small amount of brittle deformation affecting the upper crust, (2) a pre-rift cover that is efficiently decoupled from its substratum thanks to the thick layer of Late Triassic to earliest Jurassic evaporites, (3) hyperthinned continental crust resulting from a polyphase rifting history, (4) a thick pre-rift to syn-rift sedimentary pile and (5) HT/LP syn-rift metamorphism. This paper presents a structural and sedimentological review of these smooth-slope type basins that sheds light on the major role of sedimentary burial and decoupling levels in controlling the ductile crustal thinning of the Iberia-Eurasia plate boundary basins during the syn-rift and breakup stages. We also compare the processes responsible for continental crust thinning and discuss the timing of formation of the smooth-slope type basins

with respect to the evolution of the West Iberia and Bay of Biscay hyperextended continental margins.

2 Mesozoic basins of Iberia and Europe

2.1 Aquitaine basin and the Tartas and Arzacq basins

The Aquitaine basin started to develop during the Late Permian in an extensional context related to the breakup of Pangea (Burg et al., 1994). During the Triassic and earliest Jurassic (Hettangian), extension led to an aborted rift basin filled with clastic rocks, carbonates, and an evaporite sequence ~1–2 km thick (Curnelle et al., 1982; Curnelle, 1983; Curnelle & Dubois, 1986). The Jurassic was a tectonically stable period marked by the development of a widespread carbonate platform (Peybernès, 1976). At the end of the Jurassic, the entire platform was confined as suggested by the deposition of restricted dolomite and anhydrite facies (BRGM et al., 1974; Serrano et al., 2006). The Jurassic pre-rift carbonate platform was uplifted, weathered and partly eroded (Combes et al., 1998; James, 1998; Canérot et al., 1999) in response to asthenosphere upwelling that preceded Early Cretaceous rifting (Saspiturry et al., 2019a). The Early Cretaceous was a structurally active time in which the Aquitaine basin evolved into different syn-rift basins characterised by very rapid subsidence (up to 130 m/Myr; Désaglaux & Brunet, 1990; Brunet, 1991), including the symmetric Arzacq and Tartas basins. A ~1–3 km thick Early Cretaceous syn-rift sedimentary sequence unconformably overlies pre-rift deposits of Triassic and Jurassic age totalling 2–3 km in thickness (Serrano et al., 2006).

2.1.1 Tartas basin

The Tartas basin is located in the southern part of the Aquitaine domain (Fig. 1). It is bounded to the north by the Celtaquitaine Flexure (BRGM et al., 1974), which separates the Tartas Basin and the North Aquitaine Platform, and to the south by the Audignon-Pécorade-Antin

Maubourguet ridge. The Tartas basin is a relatively narrow (20 km) east-west elongated trough (Serrano et al., 2006) that lies on slightly thinned continental crust (20–25 km; Wang et al., 2016). It formed symmetrically during the Berriasian with the development of widespread shallow-water facies and continued this pattern throughout Early Cretaceous continental rifting. Sediments from this period range from marginal littoral facies (Berriasian to Barremian; e.g., Issautier et al., 2018) to inner-platform facies (Aptian and Albian; e.g., Delfaud, 1969; Arnaud-Vanneau et al., 1979; Bouroullec et al., 1979; Peybernès, 1979, 1982). Throughout the Early Cretaceous rifting, the balance between carbonate production and basin subsidence in the Tartas basin led to the aggradation of a shallow-marine carbonate succession 2500 m thick. The resulting palaeogeography was a homogeneous, flat-floored basin with no major brittle deformation recorded within the basin. High subsidence rates are consistent with ductile pure shear thinning of the lower/middle crust and formation of a symmetric syn-rift basin (Issautier et al., 2020). This regime was probably enhanced by the presence of a thick evaporite layer of Rhaetian-Hettangian age that favoured mechanical decoupling between the pre-rift sediments and the basement. This salt blanket may account for the lack of illustrated brittle structures in the syn-rift succession of the Tartas basin (Issautier et al., 2020).

2.1.2 Arzacq basin

The Arzacq syn-rift basin lies to the south of the Tartas basin (Fig. 1). Similarly to the Tartas basin, it is 40 km wide, elongated in the N110° direction and overlies slightly thinned continental crust nearly 25 km thick (Wang et al., 2016). The Arzacq basin is bounded to the north by the Audignon-Pécorade-Antin Maubourguet ridge (Mauriaud, 1987; Mediavilla, 1987; Serrano et al., 2006) and to the south by the North Pyrenean Frontal Thrust (Choukroune & ECORS Team, 1989; Daignières et al., 1994; Bourrouilh et al., 1995). Its southern flank coincides with north-dipping normal faults on the south side of the Grand Rieu

ridge (Fig. 2) (e.g., Serrano et al., 2006; Masini et al., 2014; Gómez-Romeu et al., 2019; Saspiturry et al., 2019a). Early Mesozoic rifting (Triassic to Hettangian) was responsible for a high subsidence rate and the deposition of a thick anhydrite sequence (Curnelle, 1983). The basin's subsequent rifting history was characterised by two successive extensional regimes, the first one symmetric (Berriasian to Aptian) and the second one slightly asymmetric (Albian) (Issautier et al., 2020). The symmetric syn-rift stage, identical to that of the Tartas basin, was accommodated by ductile flow of the lower/middle continental crust. Again, no brittle structures are recorded, probably because deformation was decoupled by the thick salt blanket (Canérot et al., 2005; Duretz et al., 2019). From Berriasian to Barremian times, the palaeogeography was dominated by a shallow marginal carbonate platform (e.g., Bouroullec & Deloffre, 1970; Peybernès & Combes, 1994; Biteau et al., 2006; Biteau & Canérot, 2007). In late Aptian times, the basin differentiated with the growth of a median marl flanked by carbonate-reef and inner-platform deposits (Delfaud & Gautier, 1967; Delfaud & Villanova, 1967). This second stage began during the Albian with a sudden change in both palaeogeography and basin geometry, when the depositional profile became asymmetric and salt tectonics affected its flanking ridges (Fig. 2; Issautier et al., 2020). Halokinesis consisted of gliding displacement of the Grand Rieu sedimentary cover on the southern side of the basin (Fig. 2), leading to the development of salt-detached ramp synclines as defined by Jackson and Hudec, (2005) and Pichel et al. (2018). Salt diapirism in the Audignon district in the northern side of the basin accompanied this stage (Mauriaud, 1987; Mediavilla, 1987; Issautier et al., 2020). As the syn-rift stage continued, the gliding of the sedimentary cover occurred. Motion resulted from simple shear strain localisation along an Albian detachment fault that followed ductile pure shear thinning of the lower/middle crust during the Barremian-Aptian interval (Issautier et al., 2020). The subsidence history of the Arzacq syn-rift basin also shows that the second stage coincided with an unusually steep geothermal gradient that

ended around the initiation of the Pyrenean compression (Angrand et al., 2018). The post-rift stage was marked by the deposition of Cenomanian shallow-water carbonates resting unconformably on Albian strata. Although this basin underwent simple shear thinning during the Albian, it did not reach the stage of continental breakup.

2.2 Cameros basin

The Cameros basin, on the northwestern edge of the Iberian mountain chain (Fig. 1), is a WNW-ESE trending synclinorium 80 km wide and 120 km long resulting mostly from Early Cretaceous rifting (Guimerà et al., 1995) (Fig. 3). The basin infill has been thrusted onto neighbouring Cenozoic basins, the Ebro basin to the north and the Duero basin to the south (Fig. 3E). It underwent separate rifting stages from Permian to Triassic (Alvaro et al., 1979) and Late Jurassic to Early Cretaceous times (Platt, 1990; Mas et al., 1993; Casas-Sainz & Gil-Imaz, 1998; Salas et al., 2001). The Late Jurassic to Early Cretaceous rifting stage was followed by Late Albian thermal subsidence recording the post-rift stage (Omodeo Salè et al., 2014; Omodeo-Salé et al., 2014, 2017). The associated Late Jurassic to Early Cretaceous syn-rift sequence ranges from 6.5 to 8 km in thickness (Fig. 3) (Casas-Sainz & Gil-Imaz, 1998; Mas et al., 2011; Omodeo-Salé et al., 2014; García-Lasanta et al., 2017).

The base of the Mesozoic sedimentary pile of the Cameros basin is a 500 m thick Late Triassic salt sequence (Fig. 3) (Casas Sainz, 1993; Casas-Sainz & Gil-Imaz, 1998). A pre-rift Jurassic sequence reaching 800 m in thickness, composed of shallow marine carbonate platform deposits, lies unconformably over both the Triassic salt and the Paleozoic basement (Valladares, 1980; Platt, 1990; Aurell & Meléndez, 1993; Aurell et al., 2003). The syn-rift sequence begins with 3–6 km of fluvial to lacustrine deposits and rare unconformable marine layers of Late Jurassic to Barremian age (Guiraud & Séguret, 1985; Platt, 1990; Alonso & Mas, 1993; Mas et al., 1993, 2011; Quijada et al., 2010; Suárez González et al., 2010). The late Barremian to early Aptian depositional profile is characterized by lithologies typical of

coastal wetlands with both freshwater and marine influences, grading laterally to alluvial and fluvio-lacustrine deposits (Platt, 1989, 1986). These syn-rift deposits show that the basin was continuously shallow. The syn-rift sequence thins gradually toward the basin's flanks, where it laps onto the pre-rift Jurassic sequence (Fig. 3). An apparent northward migration of the depocenter suggests a slight asymmetry in the basin (Casas-Sainz & Gil-Imaz, 1998; Guimerà et al., 1995; Mas et al., 1993; Omodeo-Salé et al., 2014, 2017). This northward migration of the depocenter likely indicates that simple shear deformation was concentrated along a detachment fault. This fault was reactivated as a reverse fault during the Pyrenean compression, inducing the northward thrusting of the Cameros basin onto the Ebro flexural basin (Fig. 3) (Omodeo-Salé et al., 2014).

The Cameros basin is characterised by (1) the perfect continuity of the pre-rift Jurassic sequence, that is not fragmented along the reactivated detachment (Fig. 3), (2) the absence of normal faulting affecting both basement and cover (Fig. 3) and (3) a lack of significant offset of the top of the basement (Casas-Sainz & Simón-Gómez, 1992; Casas Sainz, 1993; Casas-Sainz & Gil-Imaz, 1998; Casas et al., 2000, 2009; Omodeo-Salé et al., 2014). The basin has therefore been interpreted as an extensional ramp syncline, formed above a décollement in the Late Triassic evaporites rooting at depth on a blind south-dipping extensional ramp or crustal detachment (Mas et al., 1993, 2011; Guimerà et al., 1995; Casas-Sainz & Gil-Imaz, 1998; Casas et al., 2009; García-Lasanta et al., 2017; Omodeo-Salé et al., 2017). This interpretation explains the northward migration of the syn-rift depocenter and associated edgeward onlap onto the pre-rift deposits, and the development of a synformal rift basin (Fig. 3). The pre-rift Jurassic deposits were stretched by this fault movement, but remained continuous (Casas et al., 2009). The Triassic evaporite layer accommodated most of the shear strain during extension, leaving both cover and basement well preserved. The resulting basinward gliding

of the pre-rift cover was accompanied by thinning of the Triassic evaporites and by salt diapirism (Casas Sainz, 1993; Casas-Sainz & Gil-Imaz, 1998; Rat et al., 2019).

The Cameros syn-rift basin exhibits effects of HT/LP metamorphism in its deepest part, with temperatures that reached around 350–400°C (Fig. 3E) (Guiraud & Séguret, 1985; Golberg et al., 1988; Rat et al., 2019). The rifting stage developed under a high thermal gradient estimated at around 70°C/km, assuming a sediment thickness of 8 km (Mata et al., 2001; Del Río et al., 2009). Toward the basin's northern edge, the palaeogeothermal gradient decreases to 41.5°C/km, along with the intensity of the HT/LP metamorphism (Fig. 3F) (Omodeo-Salé et al., 2017). This lower thermal gradient is consistent with an estimated heat flow of approximately 60–65 mW/m^2 (Omodeo-Salé et al., 2017). The HT/LP metamorphism reached its peak temperature during the early post-rift stage and developed coevally with continental breakup in the North Pyrenean Zone basins (Golberg et al., 1988; Casquet et al., 1992; Casas-Sainz & Gil-Imaz, 1998; Mata et al., 2001).

2.3 Parentis Basin

The E-W elongated Parentis basin lies between the Landes High (Ferrer et al., 2009) to the south and the Armorican Arc to the north (Lefort & Agarwal, 1999). This wedge-shaped basin opens westward to the eastern edge of the Bay of Biscay continental margin characterized by exhumed subcontinental mantle at the ocean-continent transition (Fig. 1) (Pinet et al., 1987; Bois & ECORS Scientific team, 1990; Bois & Gariel, 1994; Jammes, 2009; Tugend et al., 2014). The south edge of the basin is defined by the north-dipping Ibis fault (Fig. 4; Ferrer et al., 2008). The continental crust of the future Parentis basin underwent several extensional deformations during the Permian to Early Triassic period (Dardel & Rosset, 1971; Mathieu, 1986; Ferrer et al., 2009; Biteau et al., 2006). Extension was accompanied by the deposition of a 1–3 km thick sequence of Late Triassic to Early Jurassic evaporites (Fig. 4D; Curnelle,

1983; Ferrer et al., 2009). The basin was subsequently filled with a 10 km thick sequence of pre-rift Jurassic and Early Cretaceous syn-rift shallow platform carbonates and terrigenous sediments that rests upon the Late Triassic evaporites (Fig. 4D; Montadert & Winnock, 1971; Bourrouilh et al., 1995; Bois et al., 1997). Tectonic subsidence occurred in the Parentis basin during a latest Jurassic to Early Albian syn-rift stage, followed by post-rift thermal subsidence during a latest Albian to Late Cretaceous post-rift stage (Brunet, 1994; Ferrer et al., 2008).

The Parentis basin is characterised by a hyperextended continental crust with a Moho depth of about 10 km in the thinnest portion (Bois & ECORS Scientific team, 1990; Bois, 1992; Ferrer et al., 2008). The overall basin geometry shows gently dipping margins lacking major normal fault scarps (Fig. 4D). The lower continental crust appears to be absent or very thin in the hyperextended domain, while the proximal margins include both upper and lower crust (Fig. 4D; Pinet et al., 1987b; Marillier et al., 1988; Tomassino & Marillier, 1997; Ruiz, 2007). A positive Bouguer gravity anomaly coincides with the hyperextended domain of the Parentis rift basin (Pinet et al., 1987a), which originated during the latest Jurassic to Early Cretaceous rifting affecting the peri-Pyrenean realm (Jammes et al., 2009; Tugend et al., 2015).

The ECORS deep seismic profiling project documented the symmetrical synclinal shape of the Parentis basin and the paucity of normal faults in the stretched crust as well as in the proximal rift margins (Fig. 4D) (Pinet et al., 1987b; Bois et al., 1997; Bois & Courtillot, 1988). Once the syn-rift stage was well established, the Parentis basin sedimentary profile became slightly asymmetrical in response to simple shear localization along a crustal detachment during Albian time (Fig. 4D; Pinet et al., 1987a; Jammes, 2009). This evolution stage is comparable to the one identified in the Arzacq basin (Issautier et al., 2020). The southern and northern margins of the rift have been interpreted by various workers as parts of an asymmetric opening system (Jammes et al., 2010a, 2010b, 2010c; Masini et al., 2014; Tugend et al., 2014). However, Pinet et al. (1987b) argued that the location and the geometry

of the thinned zone make it difficult to apply a classical simple shear model to the Parentis basin. They proposed that mantle uplift induced stretching (i.e. active rifting) and ductile flow in the lower crust and consequently a decoupling between the upper and lower crust. This depth-dependent crustal thinning explains the discrepancy between the slight extension at the surface and the substantial thinning of the lower/middle crust (thinning ratio greater than 6) at depth (Fig. 4D). This interpretation implies that the crust beneath the Parentis basin reached the ductile strain regime and was thinned under high-temperature conditions, as was the case in the adjacent North Pyrenean Zone. Finally, according to various authors, the Parentis basin first developed as a latest Jurassic–Aptian symmetrical rift that became asymmetrical when thinning progressively occurred through simple shear concentrated along a ductile crustal shear zone during Albian time. This suggests that the processes responsible for the Parentis basin continental crust thinning bear similarities with the ones defined in the Arzacq and Cameros syn-rift basins.

Jammes et al. (2010c) highlighted the major role played by the thick pre-rift salt sequence in decoupling the deformation between the basement and the rest of the Mesozoic sedimentary cover. The southern margin of the Parentis basin underwent gravity-driven cover gliding followed by syn-rift thin-skinned extensional faulting along a décollement plane within the salt (Fig. 4D; Tugend et al., 2014). This process induced the development of syn-rift salt anticlines and welded diapirs affecting the Mesozoic sedimentary pile (Fig. 4D; Mathieu, 1986; Mediavilla, 1987; Ferrer et al., 2008). Moreover, Ferrer et al. (2012) reported that salt structures are mainly localised on basin flanks (Fig. 2).

2.4 Columbrets basin

The Columbrets offshore basin is the southwestern part of the Valencia Trough between Spain and the Balearic Islands (Figs. 1 & 5A). This ENE-WSW trending basin represents a mildly

inverted and thus exceptionally preserved hyperextended rift of Late Jurassic to Early Cretaceous age (Fig. 5; e.g., Etheve et al., 2018). The pre-rift and syn-rift successions occupy a large-scale synclinal basin with thinned borders, shaped by displacement along extensional detachments (Figs. 5D-E). This domain underwent a polyphase rifting history that spanned three major rifting events. During the Late Permian to Early Triassic, distributed deformation formed an intracontinental rift basin filled by continental deposits (Arche & López-Gómez, 1996; Vargas et al., 2009). This first rifting stage was followed by a Late Triassic–Early Jurassic rifting event related to the opening of the Alpine-Ligurian Tethys (Jiménez-Munt et al., 2010; Frizon de Lamotte et al., 2011; Schettino & Turco, 2011). The climax of this rifting event was marked by the deposition of a thick layer of evaporites that became a major décollement during subsequent events (Ortí, 1974; Ortí et al., 2017). The Jurassic post-rift sequence is mainly composed of shallow-water limestone (e.g., Roca, 1996). Partial crustal thinning occurred during the first rifting stage (Salas et al., 2001; Nebot & Guimerà, 2016; Etheve, 2016; Etheve et al., 2018; Roma et al., 2018).

The main rifting stage leading to the hyperthinning of the continental crust in the Columbrets basin (Fig. 5D) occurred during the Late Jurassic to early Albian. The syn-rift succession consists of platform carbonate deposits, which grade basinward into deep-water marl and give way locally toward the basin's flanks to fluvial and deltaic deposits (Etheve et al., 2018 and references therein). The platform limestones preserve the record of post-rift thermal subsidence from the middle Albian to the Late Cretaceous (Salas et al., 2001; Nebot & Guimerà, 2016; Etheve et al., 2018).

The Moho depth is 25–30 km under the margins of the Columbrets basin and only 8–10 km under the central portion (Fig. 5A; Gallart et al., 1990; Banda & Santanach, 1992; Dañobeitia et al., 1992; Torné et al., 1996; Vidal et al., 1997; Ayala et al., 2003, 2015; Gomez-Ortiz et al., 2011; Etheve et al., 2018). The thickness of the continental crust reaches a minimum of

3.5 km in the hyperextended domain (Fig. 5D; Etheve et al., 2018), where it coincides with an unusually strong Bouguer gravity anomaly ranging in amplitude between 60 and 80 mGal (Fig. 5B; Ayala et al., 2015). Both features are consistent with the shallowing of the lithosphere-asthenosphere boundary (60–65 km depth) indicated by geoid modelling and 3-D gravity data consistent with extreme crustal thinning (Zeyen & Fernàndez, 1994; Ayala et al., 1996, 2003; Carballo et al., 2015).

The Columbrets basin has been interpreted as a salt-detached syn-rift ramp-syncline basin (Roma et al., 2018). The eastern side of the basin features an extensional detachment fault, rooting at depth in the continental crust beneath the hyperextended rift domain (Figs. 5D-E; Etheve et al., 2018) that coincides with the Triassic salt décollement. This detachment is responsible for the overall thin-skinned extensional deformation of the pre-rift sedimentary cover experiencing basinward halokinetic gliding (Etheve et al., 2018). Nevertheless, finite motion along the detachment imaged in seismic reflection profiles is not enough to account for the extreme crustal thinning identified in the basin core and the large discrepancy in thinning ratios between the lower and upper crust (Etheve et al., 2018). In fact, the reflective lower crust becomes thinner toward the axis of the Columbrets basin, where it appears to be either absent or no thicker than 1–2 km (Gallart et al., 1990, 1994; Dañobeitia et al., 1992; Torné et al., 1992; Sàbat et al., 1997; Vidal et al., 1997). These observations highlight the differences in the rheological response of the upper and lower crust to crustal stretching as deduced from the Parentis basin architecture. Etheve et al. (2018) suggested that the lower crust underwent large-scale ductile deformation/boudinage during the Late Jurassic to Early Cretaceous syn-rift stage followed by simple shear along a single crustal detachment at the end of the syn-rift stage. In summary, the evolution of the Columbrets rift system was controlled by shallow decoupling in the Triassic pre-rift evaporites and deep decoupling in the middle crust (Etheve et al., 2018). Thus, its syn-rift evolution shares similarities with the

behaviour of the Arzacq, Cameros and Parentis basins, which first experienced homogeneous ductile crustal thinning of the lower crustal levels passing to the activation of a shallower crustal detachment.

The present-day surface heat flow in the southwestern Valencia Trough is about 65 to 100 mW/m^2 (e.g., Ayala et al., 2015; Carballo et al., 2015). That area also displays the thinnest continental crust section (Banda & Santanach, 1992; Fernandez et al., 1995; Ayala et al., 2015), demonstrating that a stable high thermal regime was inherited from the Late Jurassic to Cretaceous rifting despite the fact that rifting ended in the Cenozoic.

2.5 North Pyrenean Zone basins

In the Pyrenees, late Hercynian (Permian) post-orogenic extension led to the development of continental deposits in endorheic extensional basins (Bixel & Lucas, 1983, 1987; Bixel, 1984). At the same time, magmatic and granulitic rocks were exhumed all along the North Pyrenean Zone (de Saint Blanquat, 1993; Olivier et al., 2004; Cochelin, 2016; Cochelin et al., 2017; Saspiturry et al., 2019b). A consequence of the Hercynian collapse stage was major thinning of previously hot lithosphere, an important structural inheritance regarding the following Mesozoic stages. Recent studies have proposed that the continental crust was partly thinned before the onset of Early Cretaceous hyperextension. Restorations of Iberian-European crustal sections across the Mauléon basin (western Pyrenees) and the Ballongue basin (central Pyrenees) show that the Moho was already very shallow (~20 km depth) by the end of the Jurassic (Asti et al., 2019; Espurt et al., 2019; Saspiturry et al., 2020a). Thus, the latest Paleozoic thinning stage, as well as the Late Triassic regional extensional stage, should not be neglected when estimating the Cretaceous thinning in the North Pyrenean Zone.

The Triassic deposits of the Western Pyrenees are typical of the German-type succession, ending with a thick evaporite and ophite complex (Curnelle, 1983; Lucas, 1985; Rossi et al.,

2003). The salt unit has played a major role in the Pyrenees, acting as a décollement layer at the base of the Mesozoic sedimentary cover that controlled the deformational style during Early Cretaceous hyperextension (Canérot, 1988, 1989; Canérot & Lenoble, 1993; James & Canérot, 1999; Canérot et al., 2005; Jammes et al., 2010b; Lagabrielle et al., 2010, 2020; Duretz et al., 2019). Unlike the previously described basins, the North Pyrenean Zone typically lacks Berriasian and Valanginian deposits (Combes et al., 1998; James, 1998; Canérot, 2008), a witness of the emersion of the area during the earliest Cretaceous. From Barremian to Aptian times, the Iberian and European margins of the North Pyrenean Zone basins were carbonate platforms grading to distal marls toward the basin axis. In summary, the North Pyrenean Zone hyperextended basins are characterised by sedimentary sequences consisting of (1) Late Triassic to Early Jurassic pre-rift evaporites 1–3 km thick (Curnelle, 1983), (2) Jurassic pre-rift carbonate platform rocks 0.5–2 km thick deposited in a relatively stable tectonic context (Delfaud & Henry, 1967; Lenoble, 1992; James, 1998), (3) Barremian to Aptian syn-rift carbonates and marls up to 1.6 km thick (Delfaud & Villanova, 1967, Arnaud-Vanneau et al., 1979), (4) syn-rift Albian flysch-like deposits (the Black Flysch or "Flysch Ardoisier") 1–5 km thick (Debroas, 1978, 1987, 1990; Boirie, 1981; Boirie & Souquet, 1982; Fixari, 1984; Roux, 1983; Souquet et al., 1985; Debroas et al., 2010) and (5) post-rift turbidites 2–4 km thick (Casteras, 1971; Henry et al., 1987; Le Pochat et al., 1976; Razin, 1989).

In this section we discuss the reconstructed architecture of the Mauléon and Basque-Cantabrian basins, together with that of basins present within the Internal Metamorphic Zone. We show that similarly to the previously described basins, the North Pyrenean Zone basins is affected by a syn-rift stage characterised by pure shear ductile thinning of the lower middle crust. The North Pyrenean Zone basins are characterised by the presence of positive Bouguer gravity anomalies above their inverted hyperextended domain, as evidenced by the Basque-

Cantabrian, Mauléon and Saint-Gaudens anomalies (Fig. 6). These anomalies reflect the presence of subcontinental mantle at shallow depth that was exhumed during the climax of the Mesozoic extension. With the exception of the Columbrets basin, the North Pyrenean Zone rift basins record continental breakup and mantle exhumation from the latest Albian to Early Cenomanian (breakup sequence, sensu Soares et al., 2012).

2.5.1 Mauléon basin

The Mauléon basin, located south of the Arzacq basin (Figs. 1 & 7), coincides with a strong positive gravity anomaly centred upon the basin axis (Figs. 6 & 7A; Gottis, 1972; Boillot et al., 1973). First interpreted as lower crustal material (Grandjean, 1994; Vacher & Souriau, 2001; Pedreira et al., 2007), the anomaly is currently attributed to the presence at shallow depth (~10 km) of a dome of subcontinental mantle (Fig. 7B; Casas et al., 1997; Jammes et al., 2010a). This interpretation has gained support from recent work documenting P-wave velocities of ~7.3 km/s in this deep material (Fig. 7B; Wang et al., 2016; Chevrot et al., 2018). Above the mantle dome, the thickness of the crust is assumed to be roughly 5 km (Fig. 7B). Mantle exhumation apparently occurred during Cretaceous hyperextension, when the Mauléon basin developed as a hyperextended rift (Jammes et al., 2009; Lagabrielle et al., 2010; Masini et al., 2014; Tugend et al., 2014; Corre et al., 2016; Teixell et al., 2016; Lagabrielle et al., 2019a; Labaume & Teixell, 2020). The basin was inverted during Eocene shortening and is a pop-up structure at present, bordered to the north and south by conjugate thrusts (Fig. 7B; Saspiturry et al., 2020a).

The Mauléon basin began as a symmetric syn-rift basin that subsided in response to pure shear ductile thinning of the lower/middle crust during the Early Cretaceous (Saspiturry et al., 2019a) (Fig. 7E). Its structural style changed from Albian to early Cenomanian time, leading to asymmetric basin morphology and sedimentary facies distribution. Gravity-flow conglomerates accumulated at the foot of the Iberian margin slope, forming the Mendibelza

fan conglomerates (Boirie, 1981; Fixari, 1984; Souquet et al., 1985), in response to activity on steep north-dipping normal faults (South Arbailles and North Arbailles faults; Saspiturry et al., 2019a). These rocks originated in fan deltas reworking freshly uplifted Paleozoic substratum. Restoration of syn-rift geometries indicates that the Iberian substratum was tilted 30° toward the north in Albian time (Saspiturry et al., 2019a). This implies a thickening of syn-rift deposits to the north toward the steep south-dipping Saint-Palais fault, where the conglomerates reach a maximum thickness of around 5 km (Fig. 7). This fault separated the marls of the central basin from the European proximal margin to the north, where a carbonate platform developed (Saspiturry et al., 2019a). The gentle southward slope of the European margin contrasts with the steep northward slope of the Iberian margin. This geometry points to the Saint-Palais fault as a major normal fault that was responsible for the change to asymmetric basin margins during Albian to early Cenomanian time. In this scheme, the steep north-dipping slope of the Iberian margin can be interpreted as a rollover structure in the hanging-wall of the Saint-Palais fault. The rollover structure is also accommodated by minor north-dipping normal faults that propagated toward the south.

Facies distribution significantly changed from the mid-Cenomanian to the late Santonian in the Mauléon basin as shallow carbonate platforms developed on the Iberian and European margins (Souquet, 1967; Alhamawi, 1992; Ternet et al., 2004; Serrano et al., 2006). On the European side, the transition from platform to basin coincided with the steep south-dipping South Grand Rieu fault (Fig. 7). The Iberian carbonate platform graded northward rather abruptly to deep-sea calcareous breccias at the site of the Lakhoura normal fault, which appears to have acted as a significant northward detachment during mid-Cenomanian times. This detachment, responsible for a southward tilt of the Iberian basement, crosscuts the lower part of the older Saint-Palais structure, which was inactive at that time. Thus, the Mauléon basin was affected by ductile pure shear thinning of the lower/middle crust from the

Barremian to the Aptian, followed by Albian simple shear concentrated along two major crustal detachments: (1) the south-verging Saint-Palais fault accommodating the thinning of the European margin and (2) the north-verging Lakhoura detachment crosscutting the Saint-Palais fault (Fig. 7C3). Along strike, the Mauléon basin was affected by continental breakup from the latest Albian to the Early Cenomanian (Fig. 7D) as evidenced by the presence of subcontinental mantle clasts into the latest Albian to Early Cenomanian Urdach breccias (Roux, 1983; Duée et al., 1984; Fortané et al., 1986; Debroas et al., 2010) as well as by the formation of ophicalcites at the surface of the denudated mantle (Jammes et al., 2009; Lagabrielle et al., 2010, 2019a; Debroas et al., 2010).

Rifting and continental breakup in the Mauléon basin developed, from the Early Cretaceous to the mid-Cenomanian (Fig. 7E), under a high geothermal gradient, as indicated by (1) Raman spectroscopy of carbon materials (RSCM) showing peak temperatures consistent with a gradient of 60–75°C/km (Corre, 2017; Saspiturry, 2019; Saspiturry et al., 2020b), (2) detrital zircon fission-track data indicating a 80°C/km gradient (Vacherat et al., 2014) and (3) (U-Th-Sm)/He thermochronology data indicating a 80–100°C/km gradient (Hart et al., 2017). Numerical thermal models suggest that the base of the hyperextended domain had a mantle heat flow of 100 mW/m^2 and a maximum temperature of 600°C during continental breakup (Saspiturry, 2019; Saspiturry et al., 2020b). Vitrinite reflectance values from the Mauléon basin also weigh in favour of HT/LP syn-rift metamorphism (Lescoutre, 2019; Lescoutre et al., 2019). It should be noted that the peak temperature was reached in the lower part of the basin during the post-rift period (Vacherat et al., 2014; Saspiturry, 2019), similar to the Cameros basin. Due to Pyrenean thrusting, a detached slice of mantle rock crops out in the eastern part of the basin (Urdach area). In that location, crustal material in contact with the Urdach lherzolites shows ductile shearing, suggesting that the upper/middle crust was extruded laterally from the basin axis at temperatures between 350°C and 450°C (Asti et al.,

2019). Hydrothermal fluid circulation sheds light on the ductile shearing of the Mauléon basin pre-rift cover during continental breakup at ~94 Ma (Incerpi et al., 2020). The thermal regime of the Mauléon basin from the end of the syn-rift stage (Albian, Fig. 7E) to the breakup sequence (latest Albian to Early Cenomanian; Fig. 7E) attests a ductilely stretched sedimentary cover and crystalline basement.

2.5.2 Basque-Cantabrian basin

The Basque-Cantabrian basin records a similar Mesozoic history as the North Pyrenean Zone rift basins, although it developed to the eastern termination and south of the Pyrenean Axial Zone (AZ in Fig. 1). The rift axis is characterised by a succession of Upper Jurassic and Cretaceous sediments around 8–10 km thick with interlayered basic volcanic rocks of Aptian to Santonian age (Figs. 8A-B; Azambre & Rossy, 1976; Rat et al., 1983; Rat, 1988; García Mondéjar et al., 1996; Castañares et al., 1997; Castañares & Robles, 2004). The lithosphere is extremely thin in the western central part of the basin, as suggested by a positive Bouguer anomaly recorded in the Biscay Synclinorium (Fig. 6; Pedreira et al., 2007) that is interpreted as the consequence of lithospheric mantle exhumed at shallow depth (Figs. 8A-B; Pedrera et al., 2017, 2020; Garcia-Senz et al., 2019). Field observations and seismic interpretations indicate that the Basque-Cantabrian basin has an overall symmetric shape characterised by brittle deformation on its flanks and ductile deformation on its axis (DeFelipe et al., 2017; Pedrera et al., 2017; Ducoux et al., 2019).

The basin continental crust was stretched during the Early Cretaceous rifting stage. Locally, mantle denudation occurred during early Cenomanian continental breakup as revealed by the presence of a strongly weathered mantle fragment near the inverted Leiza major detachment fault (Mendia & Ibarguchi, 1991; DeFelipe et al., 2017; Ducoux, 2017; Ducoux et al., 2019). Hyperextension was also recorded by the development of Cretaceous HT/LP metamorphism (Golberg & Leyreloup, 1990; Cuevas & Tubia, 1999). Mineral assemblages and RSCM data

517 from the Nappes des Marbres, which represents the inverted eastern part of the Basque-
518 Cantabrian basin, indicate that temperature in the pre-rift sedimentary cover locally reached
519 500–600°C during hyperextension (Figs. 8C-D; Lamare, 1936; Martínez-Torres, 1989;
520 Mendia & Ibarguchi, 1991; Ducoux et al., 2019). Thus, the felsic crust and its sedimentary
521 cover underwent ductile stretching during the Albian syn-rift stage and Cenomanian
522 continental breakup. Interpretations of geophysical data have shown that decoupling between
523 basement and cover rocks occurred in low-strength Triassic evaporites and mudstones and
524 induced coeval formation of cover gliding, mini-basins, turtle salt anticlines, expulsion
525 rollovers, and salt diapirs in the cover strata (Fig. 8; Pedrera et al., 2017, Ducoux et al., 2019;
526 Cámara, 2020). The association of exhumed mantle along the Leiza fault with rift and post-
527 rift structural geometries suggests that a major south-dipping ramp-flat-ramp extensional
528 detachment was active from Albian to early Cenomanian time (Lagabrielle et al., 2020).

529 **2.5.3 Internal Metamorphic Zone basins**

530 The central and eastern portions of the North Pyrenean Zone include a narrow Internal
531 Metamorphic Zone along their southern borders (Fig. 1). They consist of a east-west-trending
532 stretched zone of Variscan basement and pre-rift to syn-rift metamorphic rocks (Casteras,
533 1933; Mattauer, 1968; Choukroune, 1974) with several outcrops of subcontinental mantle
534 rocks (Monchoux, 1970; Choukroune & Mattauer, 1978; Fabriès et al., 1991, 1998;
535 Lagabrielle et al., 2010). Recent studies have shown that the Internal Metamorphic Zone is an
536 inverted domain of continental crust that was hyperextended during Early Cretaceous rifting
537 (Lagabrielle & Bodinier, 2008; Lagabrielle et al., 2010; Clerc & Lagabrielle, 2014; Clerc et
538 al., 2014, 2015; de Saint Blanquat et al., 2016; Teixell et al., 2018; Dielforder et al., 2019;
539 Espurt et al., 2019; Garcia-Senz et al., 2019). In the central Pyrenees, the Internal
540 Metamorphic Zone coincides with the Saint-Gaudens positive Bouguer anomaly (Fig. 9A)
541 and corresponds to the inverted Early Cenomanian continental breakup domain (Figs. 9B-C).

It has been shown that the whole continental crust of the North Pyrenean Zone was affected by large-scale ductile boudinage during Early Cretaceous hyperextension, with E-W trending rift basins exhibiting a relatively symmetrical profile (Clerc et al., 2015; Lagabrielle et al., 2020). The presence of a thick pre-rift salt layer led to basinward gliding of the overlying Jurassic cover during hyperextension (Lagabrielle et al., 2010; Clerc & Lagabrielle, 2014; Clerc et al., 2015; Duretz et al., 2019; Lagabrielle et al., 2020).

Evidence of HT/LP metamorphism has been reported along the entire North Pyrenean Zone (Ravier, 1957; Albarède & Michard-Vitrac, 1978a, 1978b; Golberg et al., 1988; Golberg & Maluski, 1988; Golberg & Leyreloup, 1990; Clerc et al., 2015). This metamorphism resulted from Early Cretaceous continental-crust thinning and an associated increase in thermal gradient and burial (Choukroune & Mattauer, 1978; Vielzeuf & Kornprobst, 1984; Debroas, 1990; Clerc et al., 2015). RSCM peak temperatures reached 400–600°C in the marbles of the Internal Metamorphic Zone, where some of the highest temperatures were recorded close to exhumed mantle outcrops (Fig. 9D; Clerc, 2012; Clerc et al., 2015; Boulvais, 2016; Chelalou et al., 2016; Lagabrielle et al., 2016; Ducoux, 2017). During the Albian syn-rift stage and the Early Cenomanian breakup event, the crust was homogeneously and ductilely stretched in the hyperextended domain, while detachment faults at the transition between the mantle and the crust/sedimentary cover accommodated the thinning of the whole system (Lagabrielle et al., 2019a). Likewise, mineral assemblages indicate that maximum temperatures of 550–650°C and pressures of 3–4 kbar were reached locally (Bernus-Maury, 1984; Golberg & Leyreloup, 1990; Vauchez et al., 2013). Previous authors have established that this metamorphic event was linked to high syn-rift geothermal gradients (Dauteuil & Ricou, 1989; Golberg & Leyreloup, 1990; Clerc et al., 2015; Lagabrielle et al., 2016). Finally, these data collectively indicate that the Jurassic to Early Cretaceous metacarbonate cover forming the current Internal Metamorphic Zone corresponds to pre-rift to basal syn-rift sediments located in the

deepest part of the former North Pyrenean Zone basin, which was also characterised by a thin continental crust.

The WNW-ESE trending Lourdes and Saint-Gaudens positive Bouguer anomalies coincide with the maximum thickness of the Albian syn-rift turbidites (Figs. 9A-B; Casas et al., 1997). Espurt et al. (2019) interpreted the Saint-Gaudens anomaly as a body of allochthonous mantle pushed northward onto the European margin on the North Pyrenean Frontal Thrust. It corresponds to an allochthonous body of subcontinental mantle that was previously exhumed during Early Cretaceous time (Fig. 9B).

3 Discussion: Tectono-sedimentary evolution of smooth-slope extensional basins

3.1 Syn-rift

3.1.1. Pure-shear dominated thinning

All the basins reviewed in this work are characterised by a strong heterogeneous structural pattern inherited from the Late Carboniferous to Triassic rifting events related to the collapse of the Variscan belt and the breakup of Pangea. These events ended with the deposition of ~1–3 km thick Late Triassic to Early Jurassic salt deposits. Thus, Mesozoic hyperextension initiated within a continental crust that was previously thinned to less than 30 km thick (Fig. 10A). Unfortunately, the precise thickness of the crust at the end of the Triassic remains undetermined. The Late Jurassic to Early Cretaceous syn-rift stage was driven by distributed deformation characterised by the lateral extraction of the lower/middle crust (Fig. 10B). During this stage, thinning of the lower/middle crust triggered progressive subsidence. Our review shows that homogeneous subsidence was partly balanced by the production of syn-rift carbonates in most of the studied basins. The result is a relatively smooth basin floor profile characterised by carbonate platform deposits with marls in a central trough. During this early

591 stage, the basin was symmetric and marked by edgeward onlap of the syn-rift deposits (Fig.
592 10B). The pre-rift cover was efficiently decoupled from its substratum thanks to the thick
593 layer of Keuper evaporites at its base. This rheological layering and the progressive sinking of
594 the central part of the rift system eventually led to the breakup of the pre-rift lid on the
595 external margins of the basin. This resulted in a large-scale pre-rift cover which remained in
596 the central part of the extensional system throughout the whole basin lifetime, while the
597 continental crust was progressively thinned below it (Fig. 10B and C). In contrast to all other
598 reviewed basins, the Tartas basin exemplifies this syn-rift stage since continental crust
599 thinning was not followed by the activation of extensional detachments, allowing the basin
600 floor profile to remain symmetric. During this first rift regime, the upper crust might have
601 been affected by very minor brittle deformation beneath the salt décollement level that led to
602 superficial salt diapirism affecting the pre-rift to syn-rift sedimentary cover (Fig. 10B), as
603 evidenced in the Arzacq (Issautier et al., 2020), Parentis (Ferrer et al., 2012), Columbrets
604 (Etheve et al., 2018), and Mauléon (Canérot et al., 2005) basins during Late Jurassic to Aptian
605 time. However, during this syn-rift stage, continental crustal thinning was mainly
606 accommodated by distributed ductile thinning within the lower/middle continental crust. This
607 process was first suggested in the case of the Parentis basin (Pinet et al., 1987a). It was then
608 put forward by Clerc and Lagabrielle (2014) in their interpretation of the architecture of the
609 eastern North Pyrenean Zone basins and used by Corre et al. (2016) in the reconstruction of
610 the eastern Mauléon basin border. It has more recently been applied to the central Mauléon
611 basin (Saspiturry et al., 2019a; Asti et al., 2019), Arzacq basin (Issautier et al., 2020) and
612 Columbrets basin (Etheve et al., 2018). It consists of a distributed thinning stage in which the
613 lower/middle crust was homogeneously and symmetrically thinned without major brittle
614 deformation of the upper crust. Interpretation of seismic profiles sheds light on the wide
615 discrepancy in thinning ratios between the lower and upper crust in the Columbrets (Etheve et

al., 2018) and Parentis (Pinet et al., 1987a) basins as they were slightly inverted. Such a discrepancy in the amount of continental thinning has been numerically modelled and defined as depth-dependent continental crust thinning (Huismans & Beaumont, 2008, 2011, 2014). This pure shear dominated thinning stage is applicable to all the North Pyrenean Zone basins since (1) their sedimentary profile was symmetric throughout the Barremian to Aptian beginning of the syn-rift stage and (2) they do not record exhumation of the lower crust during Mesozoic hyperextension in their central part (see section 2.5 for more details).

3.1.2. Simple shear dominated thinning

As thinning of the lower/middle crust continued, isostatic subsidence occurred in the centre of the basin. The early smooth synclinal-shape basin progressively deepened, triggering steepening of pre-to- syn-rift sequences. Deformation became localised and a simple shear regime initiated along a crustal detachment connecting upward to the Late Triassic pre-rift salt décollement. With the progression of extension, the pre-rift sequence was progressively dissected in several large-scale boudins and turtle structures separated by intervening salt diapirs (Fig. 10C and D). The top basement surface is steeper in the basin flanks than in the basin core, therefore portions of the pre-rift cover may undergone gravity-driven gliding leading to local syn-extensional thrusting (layer-parallel shortening). From a general point of view, gliding was controlled by thickness variations of the sedimentary pile that cause differential loading on the salt layer (Lundin, 1992; Liro & Coen, 1995; Rouby et al., 2002) and basinward tilting of the proximal margin (Cobbold & Szatmari, 1991; Demercian et al., 1993; Gaullier et al., 1993; Fort et al., 2004a, 2004b). The gravity gliding unroofed the basement of the proximal rift margin. As the pre-rift and syn-rift sequences glided along the décollement, salt was expelled both marginward and basinward as well as upward by buoyancy. Thus, in the reviewed basins, halokinesis led to (1) the development of salt-detachment synclines, salt rollovers or diapirs affecting and controlling syn-rift depocentres

and (2) the denudation of the proximal margin basement that was subsequently overlain by syn-rift sediments. This scenario is reported from most of the studied basins.

(1) In the Arzacq basin, the southern margin recorded northward cover gliding (Fig. 2; Issautier et al., 2020).

(2) In the Parentis basin, major diapirism (Pelican borehole, Fig. 4D; Ferrer et al., 2008, 2009, 2012) and denudation of its southern margin basement (Fig. 4D: Jammes, 2019) were documented.

(3) In the Columbrets basin, the SE margin basement was denudated (Etheve et al., 2018).

(4) In the Mauléon basin, the proximal margin basement was locally denudated on both edges of the rift (Fig. 7C3 & 7D; Teixell et al., 2016; Saspiturry et al., 2020a).

(5) In the Basque-Cantabrian basin, the prerift cover was removed from its proximal margins (Fig 8A; Pedrera et al., 2017).

(6) In the Internal Metamorphic Zone, the pre-rift allochthonous cover remained in its central part (Fig. 9C-D; Espurt et al., 2019).

Denudation of the basement proximal margin has also appeared in thermo-mechanical numerical models of lithospheric-scale extension that integrate recent data collected along the North Pyrenean Zone basins (Duretz et al., 2019). This process resulted in the formation of syn-gliding wedge-shaped sedimentary geometries and syn-rift sequence depocenter migration, as seen in (a) the Arzacq and Parentis basins, which display southward syn-rift depocenter migration (Fig. 2 and 4D; Jammes, 2009; Issautier et al., 2020), and (b) the Cameros, Columbrets and Mauléon basins which display northward, north-westward and northward syn-rift depocenter migration, respectively (Figs. 3F, 4D and 7C2-C3; Omodeo-Salé et al., 2014; Etheve et al., 2018; Saspiturry et al., 2020a). In the Mauléon basin, the

increasing northward slope-deepening of the Iberian margin is interpreted as a rollover effect linked to the Saint-Palais detachment. Increasing tilting of the Iberian margin led to cover gliding, immediately followed by the accumulation of deep basin gravity deposits. These latter consist of reworked sediment from rafts of the pre-rift sedimentary cover and the freshly exposed proximal margin basement (Teixell et al., 2016; Saspiturry et al., 2019a; Labaume & Teixell, 2020). A similar evolution cannot be clearly reconstructed for the Basque-Cantabrian and Internal Metamorphic Zone basins, which experienced severe inversion during the compressional stages of the Pyrenean orogeny (e.g. Pedrera et al., 2017, Fig. 8A; Espurt et al., 2019, Fig. 9C). In contrast to the Tartas basin, which did not reach the second syn-rift extensional stage, all the other basins became asymmetric, as evidenced by shifts of the basin depocenter.

Seismic profiles display clear images of crustal detachments in the Parentis (Fig. 4D; Jammes, 2009; Jammes et al., 2010c; Tugend et al., 2014) and Columbrets (Figs. 5D & 5E; Etheve et al., 2018) basins. Both basins exhibit an asymmetric outline associated with a very thin crust in their axial regions. This sheds light on the fact that important crustal thinning was partly accommodated by simple shear deformation along the imaged detachments (Fig. 2B; Issautier et al., 2020). In the Arzacq and Cameros basins, detachment faults have not been imaged but only inferred, although both basins evolved with cover gliding and depocenter migration during the syn-rift stage. For instance, the northern thrust edging the Cameros basin has been interpreted as a reactivated syn-rift southward deepening ramp-flat structure corresponding to an extensional detachment (Figs. 5E-F; Omodeo-Salé et al., 2014). Although the Arzacq, Cameros, Parentis and Columbrets basins did not record continental breakup like the North Pyrenean basins, crustal thinning was fairly advanced, developing under warm thermal conditions during the simple shear stage. Indeed, mature mantle exhumation is evidenced by a positive Bouguer anomaly and a current shallow Moho depth in the Parentis (Figs. 4A & 4D;

689 Jammes, 2009) and Columbrets basins (Figs. 5A-D; Ayala et al., 2015; Etheve et al., 2018).
690 Due to progressive burial and continental crust thinning, the sedimentary cover in the centre
691 of some smooth-slope basins experienced warm thermal regimes as typically shown by the
692 HT/LP metamorphism of the North Pyrenean Basins (more than 400°C). This is also
693 documented in the Cameros basin by mineralogical analysis, thermochronology and fluid
694 inclusion studies (Fig. 3F; Rat et al., 2019), as well as in the Columbrets basin by an elevated
695 mantle heat flow of around 100 mW/m^2 (Ayala et al., 2015; Carballo et al., 2015).

696 **3.2 Breakup stage**

697 The North Pyrenean Basins first underwent significant pure shear ductile thinning of the
698 lower/middle crust throughout the Barremian to Aptian, followed by simple shear localization
699 on detachment faults during the Albian (Saspiturry et al., 2019a). In concept, continental
700 breakup occurs once the sedimentary cover is removed from the proximal margins and the
701 lower crust fully withdrawn from the basin centre (Fig. 10D). This results in the development
702 of brittle deformation on the basin flanks and the formation of tilted basement blocks devoid
703 of sedimentary cover, while the central hyperextended domain records dominantly ductile
704 thinning and mantle exhumation (Fig. 10D). As previously shown by Soares et al. (2012),
705 while the upper continental crust deforms in a brittle manner in the hyperextended domain
706 during dominantly pure-shear thinning, the deformation regime switches during dominantly
707 simple-shear thinning and subsequent mantle exhumation. As the lower and middle crust is
708 removed from the basin centre during the syn-rift sequence, the isotherms rise under the most
709 highly extended parts of the rift. The 300°C to 500°C isotherms can be traced above the top of
710 the Variscan basement and overlying pre-rift and syn-rift sediments. This implies that large
711 volumes of the basement and cover were in a ductile regime during this stage (Fig. 10D).
712 Thus, during the breakup sequence, thinning of the crust is first controlled by the elevation of
713 the thermal conditions in relation with mantle exhumation. An additional parameter triggering

temperature elevation is the progressive burial of the continental crust under a thick sedimentary cover that accumulates in the basin during the syn-rift stage. Both causes significantly increase the temperature at the base of the basin. This process has also been demonstrated by numerical modelling of the North Pyrenean Zone basins (Duretz et al., 2019). In the hyperextended domain, extension is localised along a ductile shear zone at the transition between mantle and continental crust/sedimentary cover.

Our review highlights important characteristics of the thinning processes in the most evolved basins. We confirm that the conditions of HT/LP metamorphism evident along the hyperextended domains of the North Pyrenean basins account for the ductile behaviour of the crust. The climax of this thermal metamorphism occurred during continental breakup (Albarède & Michard-Vitrac, 1978a; Montigny et al., 1986; Golberg et al., 1986; Golberg & Maluski, 1988; Thiébaut et al., 1992). The peak temperature reached in the Jurassic to Albian sedimentary cover varies between 500° and 600°C, as documented in various places: (1) the Mauléon basin (Figs. 7C4-D; Corre, 2017; Saspiturry, 2019), (2) the Nappes des Marbres in the Basque-Cantabrian basin (Fig. 8D; Lamare, 1936; Martínez-Torrez, 1989; Mendia & Ibarguchi, 1991; Ducoux, 2017; Ducoux et al., 2019) and (3) the Internal Metamorphic Zone basins in the central and eastern Pyrenees (Fig. 9D; Bernus-Maury, 1984; Golberg & Leyreloup, 1990; Azambre et al., 1992; Clerc, 2012; Vauchez et al., 2013; Clerc et al., 2015; Chelalou et al., 2016).

The Internal Metamorphic Zone and the Nappes des Marbres have been interpreted as the inverted base of the North Pyrenean hyperextended rift domain (Clerc, 2012; Clerc & Lagabrielle, 2014; Clerc et al., 2015; Lagabrielle et al., 2016; Ducoux, 2017). In these settings, continental crust thinning resulted in a high geothermal gradient estimated at around 60–100°C/km in the Mauléon basin (Vacherat et al., 2014; Corre, 2017; Hart et al., 2017; Saspiturry, 2019). The maximum temperature reached in the sedimentary cover increased

739 from the margins to the hyperextended domain. Thus, the thermal gradient increased together
740 with the thickness of the sedimentary pile (Saspiturry, 2019). Numerical thermal modelling
741 has shown that this thermal gradient was associated, in the Mauléon basin, with an elevated
742 mantle heat flow of around 100 mW/m^2 (Saspiturry, 2019). The basinward gliding of the pre-
743 rift cover contributed significantly to the burial and thus to the peak temperature increase at
744 the base of the hyperextended domain.

745 The coupled effects of heating by mantle exhumation and burial under the thick pre-rift (salt
746 tectonic) to syn-rift sedimentary sequence prevented crustal normal faults from propagating
747 into the hyperextended domain, as evidenced in the Nappes des Marbres (Fig. 8D; Ducoux et
748 al., 2019) and the Internal Metamorphic Zone (Fig. 9D; Espurt et al., 2019). Thinning of both
749 the Variscan basement and the allochthonous sedimentary pile occurred in the hyperextended
750 domain within a thick zone of dominantly ductile shear (Lagabrielle et al., 2019a). This
751 process led to the formation of large-scale boudins and lenses of continental crust and
752 strongly sheared metasedimentary rocks (Clerc & Lagabrielle, 2014; Clerc et al., 2015b;
753 Corre et al., 2016; Asti et al., 2019; Duretz et al., 2019; Lagabrielle et al., 2019a). These
754 mature basins then took the shape of typical pseudo-symmetric hyperextended rift basins;
755 their margins were affected by brittle normal faulting and their centres were dominated by
756 ductile stretching as observed along the most evolved smooth-slope basins of the North
757 Pyrenean Zone. As shown by the presence of clasts of mantle rocks in the Cretaceous
758 turbidite breakup sequence of the Urdach area, these basins underwent local denudation of
759 subcontinental mantle thanks to motion along a major detachment during the Late Albian to
760 Early Cenomanian continental breakup (Roux, 1983; Duée et al., 1984; Fortané et al., 1986;
761 Jammes et al., 2009; Debroas et al., 2010; Lagabrielle et al., 2010, 2019a, b). Although the
762 Mauléon basin displays clasts of mantle rocks reworked in its breakup sequence sensu Soares
763 et al. (2012), it underwent heterogeneous amounts of mantle denudation and seems to show a

764 less advanced stage of continental breakup than the Basque-Cantabrian and Internal
765 Metamorphic Zone basins. According to Saspiturry et al. (2019a, 2020a), the amount of
766 mantle denudation under the Mauléon basin varied along strike as a consequence of Permian
767 inheritance along N20° transverse structures (Fig. 7C3; Saspiturry et al., 2019b). It was
768 maximal in the eastern part (Urdach) but almost nonexistent in its western part (Fig. 7D;
769 Teixell et al., 2016; Labaume & Teixell, 2020). In addition, the Internal Metamorphic Zone
770 basin displayed a more advanced breakup sequence than the Basque-Cantabrian basin as
771 evidenced by the widths of exhumed mantle along two restored crustal-balanced cross-
772 sections, which are ~45 km (Fig. 9C; Espurt et al., 2019) and ~15 km (Fig. 8A; Pedrera et al.,
773 2017) long, respectively. The Bilbao, Mauléon and Saint-Gaudens positive Bouguer
774 anomalies (Fig. 6) represent the remains of continental breakup stages now buried at depth, as
775 they correspond to major pieces of mantle exhumed during the latest Albian to Early
776 Cenomanian breakup sequence and more recently inverted during the Pyrenean orogeny
777 (Figs. 7A-B, 8A-B & 9A-B).

778 Based on the observations listed in this section, we may conclude that the reviewed smooth-
779 slope extensional basins represent different degrees of hyperextension that occurred along the
780 Iberia-Eurasia plate boundary during the Cretaceous drift of Iberia. We thus propose to rank
781 these basins from least mature to most mature as follows: (1) Tartas, (2) Arzacq/Cameros, (3)
782 Parentis/Columbrets, (4) Mauléon, (5) Basque-Cantabrian and (6) Internal Metamorphic Zone
783 (Fig. 11). This ranking indicates that as the amount of extension increases in these basins, the
784 intensity of various fundamental processes also increases. These processes are lower/middle
785 crust lateral extraction, thermal gradient and heat flow, HT/LP metamorphism, ductile
786 thinning of the crust and its sedimentary cover, relative gliding of the pre-rift cover and
787 mantle exhumation.

A major consequence of all these processes is the formation of a succession of basins with smooth basement slopes, which differ significantly from rift basins controlled by dominantly normal faulting that affects both their borders and centres. These smooth-slope basins were the locus of gentle, homogeneous subsidence that led to the deposition of syn-rift flysch-like sediments a few kilometers thick. Therefore the response of the smooth-slope basins to extensional stress was the accumulation of sediments that in turn increased the thermal burial effect in the basin centres. Such burial appears to have been a key factor in the syn-rift evolution of smooth-slope basins, along with parameters that were critical earlier at the initiation of rifting, such as the Variscan-Triassic inheritance of thin crust (Asti et al., 2019) and the presence of a very thick (average 2 km) layer of evaporites and shale of the Keuper group that allowed the decoupling of the pre-rift cover and its stagnation within the centre of the studied basins (Lagabrielle et al., 2020). Syn-rift deposits of mature smooth-slope basins are well known in the North Pyrenean Zone as the "Flysch Noir" group (Souquet et al., 1985; Debroas et al., 1990). Pioneer authors such as Ravier (1959) have shown that this sequence locally experienced HT/LP metamorphism and deduced from microstructural analysis that a large part of this evolution was static and necessarily linked to passive burial in the Flysch Noir basins. These authors clearly showed that the thermal pulse did not affect the Cenomanian sediments, leading to the concept of a "phase ante-cénomanienne" (e.g. Casteras, 1933). In contrast, further studies pointed to the synkinematic character of some HT/LP mineral assemblages and claimed that Pyrenean metamorphism was linked to the orogenic evolution of the belt (e.g. Choukroune, 1976). Later detailed studies revisited the link between thermal metamorphism and the opening of the North Pyrenean basins (e.g. Golberg & Leyreloup, 1990). However, these studies did not consider the role of sedimentary burial. Therefore, in this review, we note the existence of pioneer works that despite the rudimentary

geological knowledge of the time deduced 60 years ago that sediment burial was a key factor in the thermal evolution of the basins at the Iberia-Eurasia plate boundary.

4 Comparison of smooth-slope type basins with Atlantic type margins: West Iberia and Bay of Biscay margins

4.1. Review of the timing of the main Mesozoic events and unconformities

In this section we address the timing of formation of the syn-rift, breakup, post-rift and drifting sequences in the reviewed basins as well as in the adjacent Northwest Iberia and Bay of Biscay margins (Fig. 12). As a reminder, the syn-rift, breakup, post-rift and drifting sedimentary sequences record respectively crustal thinning, mantle denudation, post-rift thermal cooling and oceanic spreading (e.g. Alves et al., 2009, 2020; Soares et al., 2012; Alves & Cunha, 2018). These sequences are delimited by major unconformities corresponding (from bottom to top) to the base syn-rift unconformity (BSU; base of syn-rift sequence), the lithospheric breakup surface (LBS; base of the breakup sequence) and the base post-rift unconformity (BPU; base of the post-rift sequence) as defined by Soares et al. (2012) and Alves and Cunha (2018).

All the reviewed basins as well as the West Iberia and Bay of Biscay margins are characterised by the onset of Mesozoic rifting between the Late Jurassic and earliest Cretaceous as they are all related to Iberia plate motion associated with the North Atlantic opening (e.g. Alves et al., 2009; Nirrengarten et al., 2017; Angrand et al., 2020). The beginning of rifting is slightly diachronous among these basins as evidenced by the timing of formation of their BSU (Fig. 12). Nearly all of the rifting sequences in the Tartas and Arzacq (Désaglaux & Brunet, 1990; Brunet, 1991; Serrano et al., 2006; Issautier et al., 2020), Parentis (Brunet, 1994; Ferrer et al., 2008; Jammes et al., 2009; Tugend et al., 2015) and Columbrets (Salas et al., 2001; Nebot & Guimerà, 2016; Etheve, 2016; Etheve et al., 2018; Roma et al.,

2018) basins end at the same time, in the Early or Middle Cenomanian (Fig. 12). The North Pyrenean Zone basins end their syn-rift sequence slightly earlier, as they are characterised by a breakup sequence developing between the latest Albian and the Early Cenomanian (Fig. 12; Masini et al., 2014; Teixell et al., 2016; Pedrera et al., 2017; Espurt et al., 2019; Labaume and Teixell, 2020). Thus, the North Pyrenean Zone basins are characterised by the development of a LBS surface (sensu Soares et al., 2012) separating the Early Cretaceous syn-rift sequence and the Latest Albian to Early Cenomanian breakup sequence. Hence the syn-rift sequence of the reviewed basins lasts around 35–45 Myr according to the timing of formation of the different basins whereas the breakup sequence of the North Pyrenean Zone basins lasts about 5 Myr (Fig. 12). In contrast to the reviewed basins, the West Iberia margins have a relatively short (~20 Myr) syn-rift sequence and a longer (~15 Myr) breakup sequence (Soares et al., 2012; Pereira & Alves, 2012; Alves & Cunha, 2018; Alves et al., 2020), and the Bay of Biscay margins have equally long syn-rift and breakup sequences (~20 Myr) (Fig. 12; Montardet et al., 1979; Brunet, 1994; Thinon, 1999; Thinon et al., 2001, 2003; Tugend et al., 2015). This is consistent with interpretations of the West Iberia margin as having a syn-rift sequence getting longer to the north and a continental breakup sequence becoming shorter to the north (Alves et al., 2002, 2006, 2009).

All the reviewed basins record a post-rift thermal cooling stage in which a post-rift sequence overlaps the syn-rift sequence in the Tartas, Arzacq, Cameros, Parentis and Columbrets basins and the breakup sequence in the North-Pyrenean Zone basins, where they record a more advanced Mesozoic extension. The post-rift unconformity is clearly visible in the reviewed basins as erosional truncation of the syn-rift/breakup sequences and onlap of the post-rift sequence, as seen in a seismic profile in the Arzacq (Fig. 2; Issautier et al., 2020), Parentis (Fig. 4D; Jammes, 2019), and Columbrets (Figs. 5C-E; Etheve et al., 2018) basins, and in field observations in the Cameros (Omodeo-Salé et al., 2014, 2017), Mauléon (e.g. Saspiturry

et al., 2019a), Basque-Cantabrian (Rat, 1988) and Internal Metamorphic Zone (Debroas, 1978, 1987, 1990) basins. Although the North Pyrenean Zone basins underwent continental breakup, it did not progress to oceanic spreading. It is conceivable that the Pyrenean compression may have obliterated the stratigraphic evidence for a drifting stage in the North Pyrenean Zone basins. However, (1) the entire mid-Cenomanian to Late Santonian post-rift sequence is fully preserved above the North Pyrenean Zone hyperextended domain and clearly records a post-rift thermal cooling stage, (2) there is no evidence of subducted oceanic crust in a passive seismic Vp/Vs model of the Mauléon basin (Fig. 7B, Wang et al., 2016) and Internal Metamorphic Zone basins (Fig. 9B, Chevrot et al., 2018) or in a crustal-scale 3D gravity inversion of the Basque-Cantabrian basin (Pedrera et al., 2017). In contrast to the North Pyrenean Zone basins, oceanic spreading occurred during mid-Cenomanian time in the eastern Bay of Biscay margins (Fig. 12; Montadert et al., 1979; Brunet 1994; Thinon, 1999; Thinon et al., 2001, 2003; Gong et al., 2008; Tugend et al., 2015) and at the Cenomanian-Turonian boundary in the Northwest Iberia margin and western Bay of Biscay margins (Fig. 12; Gong et al., 2008; Soares et al., 2012; Pereira & Alves, 2012; Alves & Cunha, 2018; Alves et al., 2020). Although the duration of the breakup sequence differs strongly between the North Pyrenean Zone basins and the Bay of Biscay and West Iberia margins, the breakup affected all of these regions simultaneously from the mid-Cenomanian to the earliest Turonian (Fig. 12).

4.2 Architectural contrasts and discrepancies in the modes of crustal thinning

Atlantic-type margins such as West Iberia (Boillot et al., 1980, 1995; Reston et al., 1995; Whitmarsh et al., 2001; Péron-Pinvidic & Manatschal, 2009; Sutra et al. 2013; Péron-Pinvidic et al., 2015) or the Bay of Biscay margins (Jammes, 2009; Jammes et al., 2010a, 2010b, 2010c; Tugend et al., 2014) are characterized by five distinctive features: (1) deformation coupling that occurs when the ductile layer has been removed and deformation in the strong

and brittle upper crust couples with deformation in the strong lower crust/upper mantle, (2) detachment faults at the top of the basement that accommodate crustal extension through tilting of blocks of the basement and their pre-rift cover showing a coupled deformation, (3) formation of continental crust extensional allochthons, made up of upper crust and pre-rift cover, tectonically placed over exhumed lower crust or serpentinized mantle, (4) a wide domain of exposed subcontinental mantle at the ocean-continent transition and (5) large-scale serpentinization of the exhumed mantle that was still active at ambient seawater temperatures (Fig. 13A). Numerical models of such systems reproduce the palaeoarchitecture of the continental margins and the detachment faults responsible for crustal thinning (Lavier & Manatschal, 2006; Huismans & Beaumont, 2011). Numerical studies have also shown that continental crust thinning develops under conditions of high heat flow from the mantle due to asthenospheric upwelling. In these sediment-starved Atlantic-type margins, only small volumes of syn-rift sedimentary cover can be found in the hyperextended domain (Masini et al., 2011, 2012; Péron-Pinvidic et al., 2015; Ribes et al., 2019) (Fig. 13A).

Palaeogeographic reconstructions (Ziegler, 1982; Dercourt et al., 1986; Ortí et al., 2017; Soto et al., 2017) show that the distribution of the Pyrenean and peri-Pyrenean smooth-slope extensional basins corresponds closely to the distribution of Late Triassic evaporites and claystones (Lagabrielle et al., 2020). Numerical modelling shows that these Triassic deposits played a major role at the onset of continental rifting as zones of decoupling between the Palaeozoic basement and the Jurassic to Albian sedimentary cover (Duretz et al., 2019). Thus Triassic salt does not allow the coupling of the basement and its sedimentary cover during crustal extension characteristic of Atlantic-type margins. Moreover, in smooth-slope basins, the lower/middle crust is not exhumed during the breakup sequence, unlike Atlantic-type margins, as it has been laterally extracted during initial rifting. In fact, the only lower crustal rocks cropping out along the Cretaceous North Pyrenean Rift axis are quite old, having been

911 previously exhumed during Permian time (de Saint-Blanquat, 1993; Olivier et al., 2004;
912 Cochelin et al., 2018a, 2018b; Saspiturry et al., 2019b).

913 Finally, unlike Atlantic-type margins, the hyperextended domain of smooth-slope basins
914 deforms under ductile conditions and HT/LP conditions due to (1) the displaced cover
915 remaining preserved in the centre of the basin while the lower crust is thinned ductilely and
916 (2) the continental crust being buried under a very thick pre-rift to syn-rift sedimentary cover.
917 However, as in Atlantic-type margins, the proximal margins become subject to extensional
918 brittle faulting as the crust acquires a normal thermal gradient of ~30°C/km (Saspiturry, 2019)
919 and the proximal sedimentary cover is thinned or removed (Fig. 13B). Thus in smooth-slope
920 basin margins, the proximal margins undergo brittle deformation while the hyperextended
921 domain undergoes ductile thinning due to a complex interaction between salt beds,
922 sedimentary burial and changes in the syn-rift thermal gradient (Fig. 13B). This elevated
923 thermal regime is associated with intense metasomatism and fluid circulation affecting both
924 the continental basement and the sedimentary cover at temperatures of 500–600°C (Corre et
925 al., 2016; Quesnel et al., 2019; Lagabrielle et al., 2019a, 2019b). The peak syn-rift
926 temperature is mainly controlled by burial but can be locally influenced by fluid circulation.
927 Indeed, adiabatic temperatures in the sedimentary cover have been interpreted as the presence
928 of local fluid generation and convective cells in the Mauléon (Saspiturry, 2019) and
929 Boucheville (Boulvais et al., 2016) basins.

930 An important difference between the two geological settings is the fact that Atlantic-type
931 margin are sediment-starved (less than 2 km of burial) while smooth-slope basins are
932 sediment-rich (syn-rift sequence is more than 5 km thick). In addition, in the reviewed basins,
933 the pre-rift cover remaining in the central part of the basin, thanks to the Late Triassic salt
934 décollement, contributes significantly to the increase in burial and thus the peak temperature
935 at the base of the hyperextended domain by adding around 2–3 km of pre-rift sediments to

preexisting syn-rift and breakup sedimentary sequences that are nearly 5 km thick. Therefore, the thinned continental basement and the exhumed mantle may be buried under 7–10 km of pre-rift to syn-breakup sediments. This allows the crust to deform in a ductile way. Finally, the pre-rift salt, which is mostly absent along Atlantic-type margins, is also a major contributor to sedimentary burial. Thus, it participates in the ductile thinning of the continental crust and its sedimentary cover, as pointed out by Lagabrielle et al. (2020).

The review of the sequence of the main tectono-stratigraphic events presented in section 4.1 (Fig. 12) also sheds light on another possible controlling factor. Indeed, the duration of syn-rift sequences in smooth-slope basins (~35–45 Myr) is significantly longer than those of the West Iberia and Bay of Biscay margins (~15–20 Myr). Thus, the long lifetime of smooth-slope extensional basins could favour the depth-dependent ductile thinning of the lower/middle crust by pure shear at the beginning of the rifting stage and may prevent brittle structures from forming within the upper crust.

5 Conclusions

We infer the evolution of smooth-slope type basins in the Iberian-Eurasian plate junction from the rifting to the breakup stage. At the beginning of the syn-rift stage, depth-dependent crustal thinning is dominantly controlled by distributed pure shear thinning within the lower/middle crust due to the presence of two decoupling levels: (1) the middle crust, which allows the lower crust to be extracted laterally without disturbing significantly the upper crust, and (2) within pre-rift Triassic salt beds, which act as a décollement between the upper crust and the overlying sedimentary cover. Then simple shear becomes localized along a crustal detachment connecting upward with the Late Triassic décollement layer, inducing shearing in the pre-rift salt. When continental breakup occurs, the basin flanks are affected by brittle deformation while the hyperextended domain undergoes dominantly ductile thinning. The rise

of the 300°C to 500°C isotherms in the hyperextended domain, from the syn-rift to the continental breakup stage, implies that the originally crystalline upper continental crust and the overlying pre-rift and syn-rift sedimentary pile are affected by depth-dependent ductile thinning. The deformation style during rifting and continental breakup is mainly controlled by burial that results from the complex interaction between the syn-rift sedimentary sequence and the pre-rift salt beds that indirectly contribute to the burial by preserving from disruption the pre-rift sequence in the basin core.

To summarize, hyperextension in Atlantic-type margins leads to a progressive embrittlement of the continental crust due to progressive extraction of the ductile middle crust (e.g. Pérez-Gussinyé et al., 2001; Reston, 2009; Sutra et al., 2013; Mohn et al., 2015). In margins with smooth-slope basins, in contrast, crustal thinning is mostly ductile. The latter is favoured by the lateral extraction of the deep crust and the occurrence of thick sedimentary cover (Asti et al., 2019; Duretz et al., 2019; Lagabrielle et al., 2020). This implies that in the distal domain of smooth-slope margins deformation coupling never occurs, thanks to progressive upward migration of the brittle/ductile transition during rifting. Finally, in the reviewed basins, sedimentary burial coupled to the presence of pre-rift salt and a long-lived rifting sequence allow the continental crust to stretch in a dominantly ductile regime from rifting until breakup.

References

Albarède, F., & Michard-Vitrac, A., 1978a. Datation du metamorphisme des terrains secondaires des Pyrenees par les methodes 39 Ar-40 Ar et 87 Rb-87 Sr; ses relations avec les peridotites associees. Bull. Société Géologique Fr. 7, 681–687.

Albarède, Francis, & Michard-Vitrac, A., 1978b. Age and Significance of the North Pyrenean Metamorphism. Earth Planet. Sci. Lett. 327–332.

Alhamawi, M., 1992. Sédimentologie, pétrographie sédimentaire et diagenèse des calcaires Crétacé supérieur de la marge ibérique, Vallées d'Ossau - Vallée d'Aspe, Haute Chaîne, Pyrénées Atlantiques. Université Bordeaux 1.

Alonso, A., & Mas, J.R., 1993. Control tectónico e influencia del eustatismo en la sedimentación del Cretácico inferior de la cuenca de Los Cameros.

Alvaro, M., del Villar, R.C., & Vegas, R., 1979. Un modelo de evolución geotectónica para la Cadena Celtibérica. Acta Geológica Hispánica 14, 172–177.

Alves, T. M., R. L. Gawthorpe, D. H. Hunt, and J. H. Monteiro., 2002, Jurassic tectono-sedimentary evolution of the Northern Lusitanian Basin (offshore Portugal), Mar. Pet. Geol., 19, 727–754, doi:10.1016/S0264-8172(02)00036-3.

Alves, T. M., C. Moita, F. Sandnes, T. Cunha, J. H. Monteiro, and L. M. Pinheiro (2006), Mesozoic – Cenozoic evolution of North Atlantic continental slope basins: The Peniche basin, western Iberian margin, AAPG Bull., 90, 31 – 60, doi:10.1306/08110504138.

Alves, T.M., Moita, C., Cunha, T., Ullnaess, M., Myklebust, R., Monteiro, J.H., Manupella, G., 2009. Diachronous evolution of Late Jurassic–Cretaceous continental rifting in the northeast Atlantic (west Iberian margin). Tectonics 28. https://doi.org/10.1029/2008TC002337.

Alves, T.M., Cunha, T.A., 2018. A phase of transient subsidence, sediment bypass and deposition of regressive–transgressive cycles during the breakup of Iberia and Newfoundland. Earth Planet Sci. Lett. 484, 168–183. https://doi.org/10.1016/j.epsl.2017.11.054.

Alves, T.M., Fetter, M., Busby, C., Gontijo, R., Cunha, T., Mattos, N.H., 2020, A tectono-stratigraphic review of continental breakup on intraplate continental margins and its impact on resultant hydrocarbon systems. Marine and Petroleum Geology, 117. https://doi.org/10.1016/j.marpetgeo.2020.104341

Angrand, P., Ford, M., & Watts, A.B., 2018. Lateral Variations in Foreland Flexure of a Rifted Continental Margin: The Aquitaine Basin (SW France): Flexure of the Aquitaine Foreland Basin. Tectonics 37, 430–449. https://doi.org/10.1002/2017TC004670

Angrand, P., Mouthereau, F., Masini, E., Asti, R., 2020. A reconstruction of Iberia accounting for W-Tethys/N-Atlantic kinematics since the late Permian-Triassic, Solid Earth. 10.5194/se-2020-24.

Arche, A., & López-Gómez, J., 1996. Origin of the Permian-Triassic Iberian Basin, central-eastern Spain. Tectonophysics 266, 443–464. https://doi.org/10.1016/S0040-1951(96)00202-8

Arnaud-Vanneau, A., Arnaud, H., Charollais, J., Conrad, M.-A., Cotillon, P., Ferry, S., Masse, J.-P., & Peybernès, B., 1979. Paléogéographie des calcaires urgoniens du sud de la France. Géobios 3, 363–383.

Asti, R., Lagabrielle, Y., Fourcade, S., Corre, B., & Monié, P., 2019. How Do Continents Deform During Mantle Exhumation? Insights From the Northern Iberia Inverted Paleopassive Margin, Western Pyrenees (France). Tectonics 2018TC005428. https://doi.org/10.1029/2018TC005428

Aurell, M., & Meléndez, A., 1993. Sedimentary evolution and sequence stratigraphy of the Upper Jurassic in the central Iberian Chain, northeast Spain. Spec. Publ. Int. Ass. Sediment.

Aurell, M., Robles, S., Bádenas, B., Rosales, I., Quesada, S., Meléndez, G., & García-Ramos, J.., 2003. Transgressive–regressive cycles and Jurassic palaeogeography of northeast Iberia. Sediment. Geol. 162, 239–271. https://doi.org/10.1016/S0037-0738(03)00154-4

Ayala, C., Pous, J., & Torné, M., 1996. The lithosphere-asthenosphere boundary of the Valencia Trough (western Mediterranean) deduced from 2D Geoid and Gravity Modelling. Geophys. Res. Lett. 23, 3131–3134. https://doi.org/10.1029/96GL03005

Ayala, C., Torne, M., & Pous, J., 2003. The lithosphere–asthenosphere boundary in the western Mediterranean from 3D joint gravity and geoid modeling: tectonic

implications. Earth Planet. Sci. Lett. 209, 275–290. https://doi.org/10.1016/S0012-821X(03)00093-1

Ayala, C., Torne, M., & Roca, R., 2015. A review of the current knowledge of the crustal and lithospheric structure of the Valencia Trough Basin. Bol. Geológico Min. 126, 533–552.

Azambre, B., & Rossy, M., 1976. Le magmatisme alcalin d'age cretace, dans les Pyrenees occidentales et l'Arc basque; ses relations avec le metamorphisme et la tectonique. Bull. Société Géologique Fr. 7, 1725–1728.

Banda, E., & Santanach, P., 1992. The Valencia trough (western Mediterranean): An overview. Tectonophysics 208, 183–202. https://doi.org/10.1016/0040-1951(92)90344-6

Barbier, F., Duvergé, J., & Le Pichon, X., 1986. Structure profonde de la marge Nord Gascogne. Implications sur le mécanisme de rifting et de formation de la marge continentale. Bull Cent Rech Explor Prod Elf Aquitaine 10, 105–121.

Bernus-Maury, C., 1984. Etude des paragéneses caractéristiques du métamorphisme mésozoïque dans la partie orientale des Pyrénées. Pierre et Marie Curie, Paris.

Biteau, J., & Canérot, J., 2007. La Chaine des Pyrenees et ses avant-pays d'Aquitaine et de l'Ebre: caracteristiques structurales, evolution geodynamique et tectono-sedimentaire. Geol.-PARIS- 155, 16.

Biteau, J.-J., Le Marrec, A., Le Vot, M., & Masset, J.-M., 2006. The Aquitaine Basin. Pet. Geosci. 12, 247–273.

Bixel, F., 1984. Le volcanisme stéphano-permien des Pyrénées. Université Paul Sabatier de Toulouse (Sciences).

Bixel, F., & Lucas, C.L., 1983. Magmatisme, tectonique et sédimentation dans les fossés stéphano-permiens des Pyrénées occidentales. Rev. Géologie Dyn. Géographie Phys. 24, 329–342.

Bixel, F., & Lucas, C., 1987. Approche Géodynamique du Permien et du Trias des Pyrénées dans le cadre du sud-ouest européen. Cuad. Geol. Ibérica 11, 57–81.

Boillot, G., Beslier, M.O., Krawczyk, C.M., Rappin, D., & Reston, T.J., 1995. The formation of passive margins: constraints from the crustal structure and segmentation of the deep Galicia margin, Spain. Geol. Soc. Lond. Spec. Publ. 90, 71–91.

Boillot, G., Capdevilla, R., Hennequin-Marchand, I., Lamboy, M., & Lepretre, J.P., 1973. La zone nord-pyrénéenne, ses prolongements sur la marge continentale nord-espagnole et sa signification structurale. Comptes Rendus Acad. Sci. Paris 227, 2629–2632.

Boillot, G., Féraud, G., Recq, M., & Girardeau, J., 1989. Undercrusting by serpentinite beneath rifted margins: the example of the west Galicia margin (Spain). Nature 341, 523–525.

Boillot, G., Grimaud, S., Mauffret, A., Mougenot, D., Kornprobst, J., Mergoil-Daniel, J., & Torrent, G., 1980. Ocean-continent boundary of the Iberian margin: a serpentinite diapir west of the Galicia Bank. Earth Planet. Sci. Lett. 48, 23–34.

Boillot, G., Recq, M., Winterer, E.L., Meyer, A.W., Applegate, J., Baltuck, M., . . . Dunham, K., & others, 1987. Tectonic denudation of the upper mantle along passive margins: a model based on drilling results (ODP leg 103, western Galicia margin, Spain). Tectonophysics 132, 335–342.

Boirie, J.-M., 1981. Etude Sédimentologique des Poudingues de Mendibelza (Pyrénées Atlantiques). Université Paul Sabatier de Toulouse (Sciences), Toulouse.

Boirie, J.-M., & Souquet, P., 1982. Les poudingues de Mendibelza: dépôts de cônes sous-marins du rift albien des Pyrénées. Bull. Cent. Rech. Explor.-Prod. Elf-Aquitaine 6, 405–435.

Bois, C., 1992. The evolution of the layered lower crust and the Moho through geological time in Western Europe: contribution of deep seismic reflection profiles. Terra Nova 4, 99–108.

Bois, C., & Courtillot, V., 1988. Deep Seismic Profiling of the Crust and Evolution of the Lithosphere 69, 987–988.

Bois, C., & ECORS Scientific team, 1990. Major geodynamic processes studied from the ECORS deep seismic profiles in France and adjacent areas. Tectonophysics 173, 397–410.

Bois, C., Gabriel, O., Lefort, J.-P., Rolet, J., Brunet, M.-F., Masse, P., & Olivet, J.-L., 1997. Geologic contribution of the Bay of Biscay deep seismic survey: a summary of the main scientific results, a discussion of the open questions and suggestions for further investigation. Mém Soc Géol Fr. 193–309.

Bois, C., & Gariel, O., 1994. Deep Seismic Investigation in the Parentis Basin (Southwestern France), in: Mascle, A. (Ed.), Hydrocarbon and Petroleum Geology of France. Springer Berlin Heidelberg, Berlin, Heidelberg, pp. 173–186. https://doi.org/10.1007/978-3-642-78849-9_13

Boulvais, P., 2016. Fluid generation in the Boucheville Basin as a consequence of the North Pyrenean metamorphism. Comptes Rendus Geosci. 348, 301–311. https://doi.org/10.1016/j.crte.2015.06.013

Bouroullec, J., Delfaud, J., & Deloffre, R., 1979. Organisations sédimentaire et paléocologique de l'Aptien supérieur a faciès urgonien dans les Pyrénées occidentales et l'Aquitaine méridionale. Geobios 12, 25–43.

Bouroullec, J., & Deloffre, R., 1970. Interprétation sédimentologique et paléogéographique par microfaciès du Crétacé inférieur basal d'Aquitaine Sud-Ouest. Bull. Cent. Rech. Pau-SNPA 4, 381–429.

Bourrouilh, R., Richert, J.-P., & Zolnaï, G., 1995. The North Pyrenean Aquitaine Basin, France: Evolution and Hydrocarbons. AAPG Bull. 79, 831–853.

BRGM, Elf, Esso, & SNPA, 1974. Géologie du Bassin d'aquitaine. BRGM Editions, Paris.

Brune, S., Heine, C., Pérez-Gussinyé, M., & Sobolev, S.V., 2014. Rift migration explains continental margin asymmetry and crustal hyper-extension. Nat. Commun. 5. https://doi.org/10.1038/ncomms5014

Brune, S., Williams, S.E., Butterworth, N.P., & Müller, R.D., 2016. Abrupt plate accelerations shape rifted continental margins. Nature 536, 201–204. https://doi.org/10.1038/nature18319

Brunet, M.-F., 1991. Subsidence et géodynamique du Bassin d'Aquitaine. Relations avec l'ouverture de l'Atlantique.

Brunet, M. F., 1994, Subsidence in the Parentis Basin (Aquitaine, France): Implications of the Thermal Evolution, ed, *in* Mascle, A., Hydrocarbon and Petroleum Geology of France: Special Publication of the European Association of Petroleum Geoscientists, Volume 4, p.187–198.

Burg, J.-P., Van Den Driessche, J., & Brun, J.-P., 1994. Syn- to post-thickening extension : mode and consequences. Comptes Rendus Académie Sci. Sér. 2 Sci. Terre Planètes 319, 1019–1032.

Cámara, P., 2020. Inverted turtle salt anticlines in the Eastern Basque-Cantabrian basin, Spain. Marine and Petroleum Geology. 117. https://doi.org/10.1016/j.marpetgeo.2020.104358

Canérot, J., 1988. Manifestations de l'halocinèse dans les chaînons béarnais (zone Nord-Pyrénéenne) au Crétacé inférieur. Comptes Rendus Académie Sci. Sér. 2 Mécanique Phys. Chim. Sci. Univers Sci. Terre 306, 1099–1102.

Canérot, J., 1989. Rifting éocrétacé et halocinèse sur la marge ibérique des Pyrénées Occidentales (France). Conséquences structurales. Bull. Cent. Rech. Explor.-Prod. Elf-Aquitaine 13, 87–99.
Canérot, J., 2008. Les Pyrénées: Histoire géologique. Atlantica.
Canérot, J., Hudec, M.R., & Rockenbauch, K., 2005. Mesozoic diapirism in the Pyrenean orogen: Salt tectonics on a transform plate boundary. AAPG Bull. 89, 211–229. https://doi.org/10.1306/09170404007
Canérot, J., & Lenoble, J.-L., 1993. Diapirisme crétacé sur la marge ibérique des Pyrénées occidentales; exemple du pic de Lauriolle; comparaisons avec l'Aquitaine, les Pyrénées centrales et orientales. Bull. Société Géologique Fr. 164, 719–726.
Canérot, J., Majesté-Menjoulas, C., & Ternet, Y., 1999. Le cadre stratigraphique et géodynamique des altérites et des bauxites sur la marge ibérique des Pyrénées occidentales (France). Comptes Rendus Académie Sci.-Ser. IIA-Earth Planet. Sci. 328, 451–456.
Carballo, A., Fernandez, M., Torne, M., Jiménez-Munt, I., & Villaseñor, A., 2015. Thermal and petrophysical characterization of the lithospheric mantle along the northeastern Iberia geo-transect. Gondwana Res. 27, 1430–1445. https://doi.org/10.1016/j.gr.2013.12.012
Casas, A., Kearey, P., Rivero, L., & Adam, C.R., 1997. Gravity anomaly map of the Pyrenean region and a comparison of the deep geological structure of the western and eastern Pyrenees. Earth Planet. Sci. Lett. 150, 65–78.
Casas, A.M., Cortés, A.L., & Maestro, A., 2000. Intra-plate deformation and basin formation during the Tertiary at the Northern Iberian Plate: origin and evolution of the Almazán Basin. Tectonics 19, 258–289.
Casas, A.M., Villalaín, J.J., Soto, R., Gil-Imaz, A., del Río, P., & Fernández, G., 2009. Multidisciplinary approach to an extensional syncline model for the Mesozoic Cameros Basin (N Spain). Tectonophysics 470, 3–20. https://doi.org/10.1016/j.tecto.2008.04.020
Casas Sainz, A.M., 1993. Oblique tectonic inversion and basement thrusting in the Cameros Massif (Northern Spain). Geodin. Acta 6, 202–216. https://doi.org/10.1080/09853111.1993.11105248
Casas-Sainz, A.M., & Gil-Imaz, A., 1998. Extensional subsidence, contractional folding and thrust inversion of the eastern Cameros basin, northern Spain. Geol. Rundsch. 86, 802–818. https://doi.org/10.1007/s005310050178
Casas-Sainz, A.M., & Simón-Gómez, J., 1992. Stress field and thrust kinematics: a model for the tectonic inversion of the cameros massif (Spain). J. Struct. Geol. 14, 521–530. https://doi.org/10.1016/0191-8141(92)90154-O
Casquet, C., Galindo, C., González-Casado, J.M., Alonso, A., Mas, R., Rodas, M., García, E., & Barrenechea, J.F., 1992. El metamorfismo en la cuenca de los Cameros; geocronologia e implicaciones tectonicas. Geogaceta 11, 22–25.
Castañares, L.M., & Robles, S., 2004. El vulcanismo del Albiense-Santoniense en la Cuenca Vasco-Cantábrica. Geol. Esp.
Castañares, L.M., Robles, S., & Vicente Bravo, J.C., 1997. Distribución estratigráfica de los episodios volcánicos submarinos del Albiense-Santoniense en la Cuenca Vasca (sector Gernika-Plentzia, Bizkaia).
Casteras, M., 1933. Recherches sur la structure du versant nord des Pyrénées centrales et orientales. Libraire Polytechnique, C. Béranger.
Casteras, M., 1971. Carte géologique de la France à 1/50 000: feuille de Tardets–Sorholus, Orléans, France.

Chelalou, R., Nalpas, T., Bousquet, R., Prevost, M., Lahfid, A., Poujol, M., Ringenbach, J.-C., & Ballard, J.-F., 2016. New sedimentological, structural and paleo-thermicity data in the Boucheville Basin (eastern North Pyrenean Zone, France). Comptes Rendus Géoscience 348, 312–321.

Chevrot, S., Sylvander, M., Diaz, J., Martin, R., Mouthereau, F., Manatschal, G., ... Ruiz, M., 2018. The non-cylindrical crustal architecture of the Pyrenees. Sci. Rep. 8, 9591. https://doi.org/10.1038/s41598-018-27889-x

Choukroune, P., 1974. Structure et évolution tectonique de la zone nord-pyrénéenne: analyse de la déformation dans une portion de chaîne à schistosité sub-verticale.

Choukroune, P., & ECORS Team, 1989. The ECORS Pyrenean deep seismic profile reflection data and the overall structure of an orogenic belt. Tectonics 8, 23–39.

Choukroune, P., & Mattauer, M., 1978. Tectonique des plaques et Pyrenees; sur le fonctionnement de la faille transformante nord-pyreneenne; comparaisons avec des modeles actuels. Bull. Société Géologique Fr. 7, 689–700.

Clerc, C., 2012. Evolution du domaine nord-pyrénéen au Crétacé: amincissement crustal extrême et thermicite élevée: un analogue pour les marges passives. Paris 6.

Clerc, C., Boulvais, P., Lagabrielle, Y., & de Saint Blanquat, M., 2014. Ophicalcites from the northern Pyrenean belt: a field, petrographic and stable isotope study. Int. J. Earth Sci. 103, 141–163. https://doi.org/10.1007/s00531-013-0927-z

Clerc, C., Lahfid, A., Monié, P., Lagabrielle, Y., Chopin, C., . . . de St Blanquat, M., 2015. High-temperature metamorphism during extreme thinning of the continental crust: a reappraisal of the North Pyrenean passive paleomargin. Solid Earth 6, 643–668.

Clerc, C., & Lagabrielle, Y., 2014. Thermal control on the modes of crustal thinning leading to mantle exhumation: Insights from the Cretaceous Pyrenean hot paleomargins. Tectonics 33, 1340–1359. https://doi.org/10.1002/2013TC003471

Clerc, C., Lagabrielle, Y., Labaume, P., Ringenbach, J.-C., Vauchez, A., Nalpas, T., . . . Fourcade, S., 2016. Basement – Cover decoupling and progressive exhumation of metamorphic sediments at hot rifted margin. Insights from the Northeastern Pyrenean analog. Tectonophysics 686, 82–97. https://doi.org/10.1016/j.tecto.2016.07.022

Cobbold, P.R., & Szatmari, P., 1991. Radial gravitational gliding on passive margins. Tectonophysics 188, 249–289.

Cochelin, B., 2016. Champ de déformation du socle paléozoïque des Pyrénées. Géosciences Environnement Toulouse (GET).

Cochelin, B., Chardon, D., Denèle, Y., Gumiaux, C., & Le Bayon, B., 2017. Vertical strain partitioning in hot Variscan crust: Syn-convergence escape of the Pyrenees in the Iberian-Armorican syntax. Bull. Société Géologique Fr. 188, 39.

Cochelin, B., Lemirre, B., Denèle, Y., Blanquat, M. de S., Lahfid, A., Duchêne, S., 2018a, Structural inheritance in the central Pyrenees: the variscan to Alpine tectonometamorphic evolution of the axial zone. J. Geol. Soc., v. 175, 336–351, doi:10.1144/jgs2017-066.

Cochelin, B., Gumiaux, C., Chardon, D., Denèle, Y., Le Bayon, B., 2018b, Multi-scale strainfield analysis using geostatistics: Investigating the rheological behavior of the hot Variscan crust of the Pyrenees (Axial Zone). J. Struct. Geol., v. 116, 114–130, doi:10.1016/j.jsg.2018.07.024

Combes, P.-J., Peybernès, B., & Leyreloup, A.F., 1998. Altérites et bauxites, témoins des marges européenne et ibérique des Pyrénées occidentales au Jurassique supérieur—Crétacé inférieur, à l'ouest de la vallée d'Ossau (Pyrénées-Atlantiques, France). Comptes Rendus Académie Sci.-Ser. IIA-Earth Planet. Sci. 327, 271–278.

Corre, B., 2017. La bordure nord de la plaque ibérique à l'Albo-Cénomanien: architecture d'une marge passive de type ductile (Chaînons Béarnais, Pyrénées Occidentales) (PhD Thesis). Rennes 1.

Corre, B., Lagabrielle, Y., Labaume, P., Fourcade, S., Clerc, C., & Ballèvre, M., 2016. Deformation associated with mantle exhumation in a distal, hot passive margin environment: New constraints from the Saraillé Massif (Chaînons Béarnais, North-Pyrenean Zone). Comptes Rendus Geosci. 348, 279–289. https://doi.org/10.1016/j.crte.2015.11.007

Cuevas, J., & Tubia, J.M., 1999. The discovery of scapolite marbles in the Biscay Synclinorium (Basque-Cantabrian basin, Western Pyrenees): geodynamic implications. Terra Nova 11, 259–265. https://doi.org/10.1046/j.1365-3121.1999.00255.x

Curnelle, R., 1983. Evolution structuro-sédimentaire du Trias et de l'Infra-Lias d'Aquitaine. Bull Cent Rech Explor Prod Elf-Aquitaine 7, 69–99.

Curnelle, R., & Dubois, P., 1986. Evolution mesozoique des grands bassins sedimentaires francais; bassins de Paris, d'Aquitaine et du Sud-Est. Bull. Soc. Geol. Fr. II, 529–546. https://doi.org/10.2113/gssgfbull.II.4.529

Curnelle, R., Dubois, P., Seguin, J.C., Whitaker, D., Matthews, D.H., Roberts, D.G., . . . Kholief, M.M., 1982. The Mesozoic-Tertiary Evolution of the Aquitaine Basin [and Discussion]. Philos. Trans. R. Soc. Math. Phys. Eng. Sci. 305, 63–84. https://doi.org/10.1098/rsta.1982.0026

Daignières, M., Séguret, M., Specht, M., & Team, E., 1994. The Arzacq-western Pyrenees ECORS deep seismic profile, in: Hydrocarbon and Petroleum Geology of France. Springer, pp. 199–208.

Dañobeitia, J.J., Arguedas, M., Gallart, J., Banda, E., & Makris, J., 1992. Deep crustal configuration of the Valencia trough and its Iberian and Balearic borders from extensive refraction and wide-angle reflection seismic profiling. Tectonophysics 203, 37–55.

Dardel, R.A., & Rosset, R., 1971. Histoire géologique et structurale du bassin de Parentis et de son prolongement en mer. Hist. Struct. Golfe Gasc. 2.

Dauteuil, O., & Ricou, L.-E., 1989. Une circulation de fluides de haute-température à l'origine du métamorphisme crétacé nord-pyrénéen. Geodin. Acta 3, 237–249. https://doi.org/10.1080/09853111.1989.11105190

de Saint Blanquat, M., 1993. La faille normale ductile du massif du Saint Barthélémy. Evolution hercynienne des massifs nord-pyrénéens catazonaux considérée du point de vue de leur histoire thermique. Geodin. Acta 6, 59–77.

de Saint Blanquat, M., Bajolet, F., Grand'Homme, A., Proietti, A., Zanti, M., Boutin, A., . . . Labaume, P., 2016. Cretaceous mantle exhumation in the central Pyrenees: New constraints from the peridotites in eastern Ariège (North Pyrenean zone, France). Comptes Rendus Geosci. 348, 268–278. https://doi.org/10.1016/j.crte.2015.12.003

Debroas, E.J., 1978. Evolution de la fosse du flysch ardoisier de l'Albien superieur au Senonien inferieur (zone interne metamorphique des Pyrenees navarro-languedociennes). Bull. Société Géologique Fr. 7, 639–648.

Debroas, E.-J., 1987. Modèle de bassin triangulaire à l'intersection de décrochements divergents pour le fossé albo-cénomanien de la Ballongue (zone nord-pyrénéenne, France). Bull. Société Géologique Fr. 3, 887–898. https://doi.org/10.2113/gssgfbull.III.5.887

Debroas, E.J., 1990. Le flysch noir albo-cenomanien temoin de la structuration albienne a senonienne de la Zone nord-pyreneenne en Bigorre (Hautes-Pyrenees, France). Bull. Soc. Geol. Fr. VI, 273–285. https://doi.org/10.2113/gssgfbull.VI.2.273

Debroas, E.J., Canérot, J., & Bilotte, M., 2010. Les brèches d'Urdach, témoins de l'exhumation du manteau pyrénéen dans un escarpement de faille vraconnien-cénomanien inférieur (Zone nord-pyrénéenne, Pyrénées-Atlantiques, France). Géologie Fr. 2, 53–63.

DeFelipe, I., Pedreira, D., Pulgar, J.A., Iriarte, E., & Mendia, M., 2017. Mantle exhumation and metamorphism in the Basque-Cantabrian Basin (NSpain): Stable and clumped isotope analysis in carbonates and comparison with ophicalcites in the North-Pyrenean Zone (Urdach and Lherz). Geochem. Geophys. Geosystems 18, 631–652. https://doi.org/10.1002/2016GC006690

Del Río, P., Barbero, L., Mata, P., & Fanning, C.M., 2009. Timing of diagenesis and very low-grade metamorphism in the eastern sector of the Sierra de Cameros (Iberian Range, Spain): a U-Pb SHRIMP study on monazite: U-Pb dating of diagenetic and low-grade monazite from the Iberian Range (Spain). Terra Nova 21, 438–445. https://doi.org/10.1111/j.1365-3121.2009.00900.x

Delfaud, J., 1969. Essai sur la géologie dynamique du domaine aquitano-pyrénéen durant le Jurassique et le Crétacé inférieur. Université de Bordeaux.

Delfaud, J., & Gautier, J., 1967. Evolution des milieux de dépôts au passage Jurassique–Crétacé du forage de Lacq 104 (Aquitaine, France, Sud-Ouest). Bull. Cent. Rech. Pau-SNPA 1, 77–89.

Delfaud, J., & Henry, J., 1967. Evolution des bassins jurassiques dans la zone nord-pyrénéenne occidentale. 64ème Congrès AFAS Bordx. 75–80.

Delfaud, J., & Villanova, M., 1967. Evolution des bassins pendant le Crétacé inférieur dans les Pyrénees occidentales et la bordure de l'Aquitaine. 64ème Congrès AFAS Bordx. 87–92.

Demercian, S., Szatmari, P., & Cobbold, P.R., 1993. Style and pattern of salt diapirs due to thin-skinned gravitational gliding, Campos and Santos basins, offshore Brazil. Tectonophysics 228, 393–433.

Dercourt, J., Zonenshain, L.P., Ricou, L.-E., Kazmin, V.G., Le Pichon, X., Knipper, A.L., . . . Biju-Duval, B., 1986. Geological evolution of the tethys belt from the atlantic to the pamirs since the LIAS. Tectonophysics 123, 241–315. https://doi.org/10.1016/0040-1951(86)90199-X

Désaglaux, P., & Brunet, M.-F., 1990. Tectonic subsidence of the Aquitaine basin since Cretaceous times. Bull. Société Géologique Fr. 8, 295–306.

Dielforder, A., Frasca, G., Brune, S & Ford, M., 2019. Formation of the Iberian-European Convergent Plate Boundary Fault and Its Effect on Intraplate Deformation in Central Europe. Geochemistry Geophysics Geosystems. https://doi.org/10.1029/2018GC007840.

Driscoll, N.W., Hogg, J.R., Christie-Blick, N., & Karner, G.D., 1995. Extensional tectonics in the Jeanne d'Arc Basin, offshore Newfoundland: implications for the timing of break-up between Grand Banks and Iberia. Geol. Soc. Lond. Spec. Publ. 90, 1–28. https://doi.org/10.1144/GSL.SP.1995.090.01.01

Ducoux, M., 2017. Structure, thermicité et évolution géodynamique de la Zone Interne Métamorphique des Pyrénées. Institut des Sciences de la Terre d'Orléans (ISTO).

Ducoux, M., Jolivet, L., Callot, J. -P., Aubourg, C., Masini, E., Lahfid, A., . . . Baudin, T., 2019. The Nappe des Marbres unit of the Basque-Cantabrian Basin: the tectono-thermal evolution of a fossil hyperextended rift basin. Tectonics 2018TC005348. https://doi.org/10.1029/2018TC005348

Duée, G., Lagabrielle, Y., Coutelle, A., & Fortané, A., 1984. Les lherzolites associées aux Chaînons Béarnais (Pyrénées Occidentales): Mise à l'affleurement anté-dogger et

1332 resédimentation albo-cénomanienne. Comptes-Rendus Séances Académie Sci. Sér. 2
1333 Mécanique-Phys. Chim. Sci. Univers Sci. Terre 299, 1205–1210.
1334 Duretz, T., Asti, R., Lagabrielle, Y., Brun, J., Jourdon, A., Clerc, C., & Corre, B., 2019.
1335 Numerical modelling of Cretaceous Pyrenean Rifting: The interaction between mantle
1336 exhumation and syn-rift salt tectonics. Basin Res. bre.12389.
1337 https://doi.org/10.1111/bre.12389
1338 Espurt, N., Angrand, P., Teixell, A., Labaume, P., Ford, M., de Saint Blanquat, M., &
1339 Chevrot, S., 2019. Crustal-scale balanced cross-section and restorations of the Central
1340 Pyrenean belt (Nestes-Cinca transect): Highlighting the structural control of Variscan
1341 belt and Permian-Mesozoic rift systems on mountain building. Tectonophysics 764,
1342 25–45.
1343 Etheve, N., 2016. Le bassin de Valence à la frontière des domaines ibérique et méditerranéen:
1344 Evolution tectonique et sédimentaire du Mésozoïque au Cénozoïque. Université de
1345 Cergy Pontoise.
1346 Etheve, N., Mohn, G., Frizon de Lamotte, D., Roca, E., Tugend, J., & Gómez-Romeu, J.,
1347 2018. Extreme Mesozoic Crustal Thinning in the Eastern Iberia Margin: The Example
1348 of the Columbrets Basin (Valencia Trough). Tectonics 37, 636–662.
1349 Fabriès, J., Lorand, J.-P., & Bodinier, J.-L., 1998. Petrogenetic evolution of orogenic
1350 lherzolite massifs in the central and western Pyrenees. Tectonophysics 292, 145–167.
1351 Fabriès, J., Lorand, J.-P., Bodinier, J.-L., & Dupuy, C., 1991. Evolution of the Upper Mantle
1352 beneath the Pyrenees: Evidence from Orogenic Spinel Lherzolite Massifs. J. Petrol.
1353 Special_Volume, 55–76. https://doi.org/10.1093/petrology/Special_Volume.2.55
1354 Fernandez, M., Foucher, J.P., & Jurado, M.J., 1995. Evidence for the multi-stage formation of
1355 the south-western Valencia Trough. Mar. Pet. Geol. 12, 101–109.
1356 https://doi.org/10.1016/0264-8172(95)90390-6
1357 Ferrer, O., Jackson, M.P.A., Roca, E., & Rubinat, M., 2012. Evolution of salt structures
1358 during extension and inversion of the Offshore Parentis Basin (Eastern Bay of Biscay).
1359 Geol. Soc. Lond. Spec. Publ. 363, 361–380. https://doi.org/10.1144/SP363.16
1360 Ferrer, O., Roca, E., Benjumea, B., Muñoz, J.A., Ellouz, N., & MARCONI Team, 2008. The
1361 deep seismic reflection MARCONI-3 profile: Role of extensional Mesozoic structure
1362 during the Pyrenean contractional deformation at the eastern part of the Bay of Biscay.
1363 Mar. Pet. Geol. 25, 714–730. https://doi.org/10.1016/j.marpetgeo.2008.06.002
1364 Ferrer, O., Roca, E., Jackson, M.P.A., & Muñoz, J.A., 2009. Effects of Pyrenean contraction
1365 on salt structures of the offshore Parentis Basin (Bay of Biscay). Trab. Geol. 29.
1366 Fixari, G., 1984. Stratigraphie, faciès et dynamique tecto-sédimentaire du flysch albien
1367 (flysch noir et poudingues de mendibelza) dans la région de Mauléon-Tardets
1368 (Pyrénées Atlantiques). Université Paul Sabatier de Toulouse (Sciences).
1369 Fort, X., Brun, J.-P., & Chauvel, F., 2004a. Salt tectonics on the Angolan margin,
1370 synsedimentary deformation processes. AAPG Bull. 88, 1523–1544.
1371 Fort, X., Brun, J.P., & Chauvel, F., 2004b. Contraction induced by block rotation above salt
1372 (Angolan margin). Mar. Pet. Geol. 21, 1281–1294.
1373 Fortané, A., Duée, G., Lagabrielle, Y., & Coutelle, A., 1986. Lherzolites and the western
1374 “Chaînons Béarnais” (French Pyrenees): Structural and paleogeographical pattern.
1375 Tectonophysics 129, 81–98. https://doi.org/10.1016/0040-1951(86)90247-7
1376 Frizon de Lamotte, D., Raulin, C., Mouchot, N., Wrobel-Daveau, J.-C., Blanpied, C., &
1377 Ringenbach, J.-C., 2011. The southernmost margin of the Tethys realm during the
1378 Mesozoic and Cenozoic: Initial geometry and timing of the inversion processes:
1379 TETHYS SOUTHERNMOST MARGIN. Tectonics 30, n/a-n/a.
1380 https://doi.org/10.1029/2010TC002691

Froitzheim, N., & Manatschal, G., 1996. Kinematics of Jurassic rifting, mantle exhumation, and passive-margin formation in the Austroalpine and Penninic nappes (eastern Switzerland). Geol. Soc. Am. Bull. 108, 1120–1133. https://doi.org/10.1130/0016-7606(1996)108<1120:KOJRME>2.3.CO;2

Gallart, J., Rojas, H., Diaz, J., & Dañobeitia, J.J., 1990. Features of deep crustal structure and the onshore-offshore transition at the Iberian flank of the Valencia Trough (Western Mediterranean). J. Geodyn. 12, 233–252.

Gallart, J., Vidal, N., & Danobeitia, J., 1994. Lateral variations in the deep crustal structure at the Iberian margin of the Valencia trough imaged from seismic reflection methods. Tectonophysics 232, 59–75. https://doi.org/10.1016/0040-1951(94)90076-0

García Mondéjar, J., Agirrezabala, L., M., Aranburu, A., Fernandez-Mendiola, P., A., Gomèz-Pérèz, I., Lopez-Horgue, M., & Rosales, I., 1996. Aptian—Albian tectonic pattern of the Basque—Cantabrian Basin (Northern Spain). Geol. J. 31, 13–45.

García-Lasanta, C., Casas-Sainz, A., Villalaín, J.J., Oliva-Urcia, B., Mochales, T., & Speranza, F., 2017. Remagnetizations used to unravel large-scale fold kinematics: A case study in the Cameros Basin (Northern Spain): Unfolding in Basin Inversion. Tectonics 36, 714–729. https://doi.org/10.1002/2016TC004459

Garcia-Senz, J., Pedrera, A., Ayala, C., Ruiz-Constán, A., Robador Moreno, A., Rodríguez-Fernández, R., 2019, Inversion of the North-Iberian hyperextended margin: the role of exhumed mantle indentation during continental collision. Geological Society, London, Special Publications, 490, doi: https://doi.org/10.1144/SP490-2019-112.

Gaullier, V., Brun, J.P., Gueīrin, G., & Lecanu, H., 1993. Raft tectonics: the effects of residual topography below a salt deīcollement. Tectonophysics 228, 363–381.

Golberg, J.M., Guiraud, M., Maluski, H., & Séguret, M., 1988. Caractères pétrologiques et âge du métamorphisme en contexte distensif du bassin sur décrochement de Soria (Crétacé inférieur, Nord Espagne). Comptes Rendus Académie Sci. Sér. 2 Mécanique Phys. Chim. Sci. Univers Sci. Terre 307, 521–527.

Golberg, J.M., & Leyreloup, A.F., 1990. High temperature-low pressure Cretaceous metamorphism related to crustal thinning (Eastern North Pyrenean Zone, France). Contrib. Mineral. Petrol. 104, 194–207. https://doi.org/10.1007/BF00306443

Golberg, J.-M., & Maluski, H., 1988. Données nouvelles et mise au point sur l'âge du métamorphisme pyrénéen. Comptes Rendus Académie Sci. Sér. 2 Mécanique Phys. Chim. Sci. Univers Sci. Terre 306, 429–435.

Golberg, J.M., Maluski, H., & Leyreloup, A.F., 1986. Petrological and age relationship between emplacement of magmatic breccia, alkaline magmatism, and static metamorphism in the North Pyrenean Zone. Tectonophysics 129, 275–290. https://doi.org/10.1016/0040-1951(86)90256-8

Gomez-Ortiz, D., Agarwal, B.N.P., Tejero, R., & Ruiz, J., 2011. Crustal structure from gravity signatures in the Iberian Peninsula. Geol. Soc. Am. Bull. 123, 1247–1257. https://doi.org/10.1130/B30224.1

Gómez-Romeu, J., Masini, E., Tugend, J., Ducoux, M., & Kusznir, N., 2019. Role of rift structural inheritance in orogeny highlighted by the Western Pyrenees case-study. Tectonophysics 766, 131–150. https://doi.org/10.1016/j.tecto.2019.05.022

Gottis, M., 1972. Construction d'un modèle géodynamique pyrénéen. Comptes Rendus Académie Sci. 275, 2099.

Gong, Z., C. G. Langereis, and T. A. T. Mullender, 2008, The rotation of Iberia during the Aptian and the opening of the Bay of Biscay: Earth and Planetary Science Letters, v. 273, no. 1–2, p. 80–93, doi:10.1016/j.epsl.2008.06.016.

Grandjean, G., 1994. Etude des structures crustales dans une portion de chaîne et de leur relation avec les bassins sédimentaires. Application aux Pyrénées occidentales. Bull Cent Rech Explor Prod Elf Aquitaine 18, 391–420.

Guimerà, J., Alonso, Á., & Mas, J.R., 1995. Inversion of an extensional-ramp basin by a newly formed thrust: the Cameros basin (N. Spain). Geol. Soc. Lond. Spec. Publ. 88, 433–453. https://doi.org/10.1144/GSL.SP.1995.088.01.23

Guiraud, M., & Séguret, M., 1985. A releasing solitary overstep model for the Late Jurassic-Early Cretaceous (Wealdian) Soria strike-slip basin (northern Spain). AAPG Bull.

Hart, N.R., Stockli, D.F., Lavier, L.L., & Hayman, N.W., 2017. Thermal evolution of a hyperextended rift basin, Mauléon Basin, western Pyrenees: Thermal evolution of hyperextended rift. Tectonics. https://doi.org/10.1002/2016TC004365

Henry, J., Zolnaï, G., Le Pochat, G., & Mondeilh, C., 1987. Carte géologique de la France au 1/50 000: feuille d'Orthez, Orléans, France.

Huismans, R.S., & Beaumont, C., 2003. Symmetric and asymmetric lithospheric extension: Relative effects of frictional-plastic and viscous strain softening. J. Geophys. Res. Solid Earth 108. https://doi.org/10.1029/2002JB002026

Huismans, R.S., & Beaumont, C., 2008. Complex rifted continental margins explained by dynamical models of depth-dependent lithospheric extension. Geology 36, 163. https://doi.org/10.1130/G24231A.1

Huismans, R.S., & Beaumont, C., 2011. Depth-dependent extension, two-stage breakup and cratonic underplating at rifted margins. Nature 473, 74–78. https://doi.org/10.1038/nature09988

Huismans, R.S., & Beaumont, C., 2014. Rifted continental margins: The case for depth-dependent extension. Earth Planet. Sci. Lett. 407, 148–162. https://doi.org/10.1016/j.epsl.2014.09.032

Incerpi, N., Manatschal, G., Martire, L., Bernasconi, S. M., Gerdes, A., Bertok, C., 2020. Characteristics and timing of hydrothermal fluid circulation in the fossil Pyrenean hyperextended rift system: new constraints from the Chaînons Béarnais (W Pyrenees). International Journal of Earth Sciences. https://doi.org/10.1007/s00531-020-01852-6

Issautier, B., Saspiturry, N., Serrano, O., 2020. Structural inheritance and salt tectonics controlling pseudosymmetric rift formation during Early Cretaceous hyperextension of the Arzacq and Tartas Basins (southwest France). Marine and Petroleum Geology. 10.1016/j.marpetgeo.2020.104395

Jackson, M. P., & Hudec, M. R. (2005). Stratigraphic record of translation down ramps in a passive-margin salt detachment. Journal of Structural Geology, 27(5), 889–911. https://doi.org/10.1016/j.jsg.2005.01.010

James, V., 1998. La plate-forme carbonatée ouest-pyrénéenne au jurassique moyen et supérieur stratigraphie séquentielle, stades d'évolution, relations avec la subsurface en aquitaine méridionale.

James, V., & Canérot, J., 1999. Diapirisme et structuration post-triasique des Pyrénées occidentales et de l'Aquitaine méridionale (France). Eclogae Geol. Helvetiae 92, 63–72.

Jammes, S., 2009. Processus d'amincissement crustal en contexte transtensif : l'exempe du Golfe de Gascogne et des Pyrénées basques. PhD thesis, Strasbourg University.

Jammes, S., Manatschal, G., Lavier, L., & Masini, E., 2009. Tectono-sedimentary evolution related to extreme crustal thinning ahead of a propagating ocean: Example of the western Pyrenees. Tectonics 28. https://doi.org/10.1029/2008TC002406

Jammes, S., Tiberi, C., & Manatschal, G., 2010a. 3D architecture of a complex transcurrent rift system: The example of the Bay of Biscay–Western Pyrenees. Tectonophysics 489, 210–226. https://doi.org/10.1016/j.tecto.2010.04.023

Jammes, S., Lavier, L., & Manatschal, G., 2010b. Extreme crustal thinning in the Bay of Biscay and the Western Pyrenees: From observations to modeling. Geochem. Geophys. Geosystems 11. https://doi.org/10.1029/2010GC003218

Jammes, S., Manatschal, G., & Lavier, L., 2010c. Interaction between prerift salt and detachment faulting in hyperextended rift systems: The example of the Parentis and Mauléon basins (Bay of Biscay and western Pyrenees). AAPG Bull. 94, 957–975. https://doi.org/10.1306/12090909116

Jiménez-Munt, I., Fernàndez, M., Vergés, J., Afonso, J.C., Garcia-Castellanos, D., & Fullea, J., 2010. Lithospheric structure of the Gorringe Bank: Insights into its origin and tectonic evolution: GORRINGE BANK STRUCTURE AND EVOLUTION. Tectonics 29, n/a-n/a. https://doi.org/10.1029/2009TC002458

Labaume, P., & Teixell, A., 2020. Evolution of salt structures of the Pyrenean rift (Chaînons Béarnais, France): From hyper-extension to tectonic inversion. Tectonophysics. https://doi.org/10.1016/j.tecto.2020.228451.

Lagabrielle, Y., & Bodinier, J.-L., 2008. Submarine reworking of exhumed sub-continental mantle rocks: field evidence from the Lherz peridotites, French Pyrenees: Cretaceous exhumation of pyrenean mantle. Terra Nova 20, 11–21. https://doi.org/10.1111/j.1365-3121.2007.00781.x

Lagabrielle, Y., Labaume, P., & de Saint Blanquat, M., 2010. Mantle exhumation, crustal denudation, and gravity tectonics during Cretaceous rifting in the Pyrenean realm (SW Europe): Insights from the geological setting of the lherzolite bodies. Tectonics 29. https://doi.org/10.1029/2009TC002588

Lagabrielle, Y., Clerc, C., Vauchez, A., Lahfid, A., Labaume, P., Azambre, B., Fourcade, S., & Dautria, J.-M., 2016. Very high geothermal gradient during mantle exhumation recorded in mylonitic marbles and carbonate breccias from a Mesozoic Pyrenean palaeomargin (Lherz area, North Pyrenean Zone, France). Comptes Rendus Geosci. 348, 290–300. https://doi.org/10.1016/j.crte.2015.11.004

Lagabrielle, Y., Asti, R., Fourcade, S., Corre, B., Poujol, M., Uzel, J., . . . Maury, R., 2019a. Mantle exhumation at magma-poor passive continental margins. Part I. 3D architecture and metasomatic evolution of a fossil exhumed mantle domain (Urdach lherzolite, north-western Pyrenees, France). BSGF - Earth Sci. Bull. 190, 8. https://doi.org/ 10.1016/j.earscirev.2019.103071.

Lagabrielle, Y., Asti, R., Duretz, T., Clerc, C., Fourcade, S., Teixell, A., . . Saspiturry, N., 2020. A review of cretaceous smooth-slopes extensional basins along the Iberia-Eurasia plate boundary: How pre-rift salt controls the modes of continental rifting and mantle exhumation. Earth-Science Reviews. 201. https://doi.org/10.1051/bsgf/2019007

Lamare, P., 1936. Recherches géologiques dans les Pyrénées basques d'Espagne. Société géologique de France.

Lavier, L.L., & Manatschal, G., 2006. A mechanism to thin the continental lithosphere at magma-poor margins. Nature 440, 324–328. https://doi.org/10.1038/nature04608

Le Pochat, G., Bolthenhagen, C., Lenguin, M., Lorsignol, S., & Thibault, C., 1976. Carte géologique de France au 1/50 000: Mauléon-licharre, Orléans, France.

Lefort, J.-P., & Agarwal, B.N.., 1999. Of what is the centre of the Ibero-Armorican arc composed? Tectonophysics 302, 71–81. https://doi.org/10.1016/S0040-1951(98)00275-3

Lemoine, M., Tricart, P., & Boillot, G., 1987. Ultramafic and gabbroic ocean floor of the Ligurian Tethys (Alps, Corsica, Apennines): In search of a genetic imodel. Geology 15, 622–625. https://doi.org/10.1130/0091-7613(1987)15<622:UAGOFO>2.0.CO;2

Lenoble, J.-L., 1992. Les plates-formes carbonatées ouest-pyrénéennes du dogger à l'Albien, stratigraphie séquentielle et évolution géodynamique. Université Paul Sabatier de Toulouse (Sciences).

Lescoutre, R., 2019. Formation and reactivation of the Pyrenean-Cantabrian rift system : inheritance, segmentation and thermal evolution. Strasbourg.

Lescoutre, R., Tugend, J., Brune, S., Masini, E., & Manatschal, G., 2019. Thermal Evolution of Asymmetric Hyperextended Magma-Poor Rift Systems: Results From Numerical Modeling and Pyrenean Field Observations. Geochem. Geophys. Geosystems 2019GC008600. https://doi.org/10.1029/2019GC008600

Liro, L.M., & Coen, R., 1995. Salt deformation history and postsalt structural trends, offshore southern Gabon, West Africa.

Lucas, C., 1985. Le grès rouge du versant nord des Pyrénées: essai sur la géodynamique de dépôts continentaux du permien et du trias.

Lundin, E.R., 1992. Thin-skinned extensional tectonics on a salt detachment, northern Kwanza Basin, Angola. Mar. Pet. Geol. 9, 405–411.

Manatschal, G., 2004. New models for evolution of magma-poor rifted margins based on a review of data and concepts from West Iberia and the Alps. Int. J. Earth Sci. 93. https://doi.org/10.1007/s00531-004-0394-7

Manatschal, G., Engström, A., Desmurs, L., Schaltegger, U., Cosca, M., Müntener, O., & Bernoulli, D., 2006. What is the tectono-metamorphic evolution of continental break-up: The example of the Tasna Ocean–Continent Transition. J. Struct. Geol. 28, 1849–1869. https://doi.org/10.1016/j.jsg.2006.07.014

Manatschal, G., & Nievergelt, P., 1997. A continent-ocean transition recorded in the Err and Platta nappes (Eastern Switzerland). Eclogae Geol. Helvetiae 90, 3–28.

Marillier, F., Tomassino, A., Patriat, P., & Pinet, B., 1988. Deep structure of the Aquitaine shelf: constraints from expanding spread profiles on the ECORS Bay of Biscay transect. Mar. Pet. Geol. 5, 65–74.

Martínez-Torres, L.M., 1989. El manto de los mármoles (Pirineo occidental): geología estructural y evolución geodinámica (PhD Thesis). Universidad del País Vasco-Euskal Herriko Unibertsitatea.

Mas, J.R., Alonso, A., & Guimerà, J., 1993. Evolución tectonosedimentaria de una cuenca extensional intraplaca: la cuenca finijurásica–eocretácica de Los Cameros (La Rioja–Soria). Rev. Soc. Geológica Esp. 6, 129–144.

Mas, R., Benito, M.I., Arribas, J., Alonso, A., Arribas, M.E., Lohmann, K.C., . . . Suárez, P., 2011. Evolution of an intra-plate rift basin: the latest Jurassic-early Cretaceous Cameros basin (Northwest Iberian ranges, North Spain). Geo-Guías 8, 117–154.

Masini, E., Manatschal, G., Mohn, G., Ghienne, J.-F., & Lafont, F., 2011. The tectono-sedimentary evolution of a supra-detachment rift basin at a deep-water magma-poor rifted margin: the example of the Samedan Basin preserved in the Err nappe in SE Switzerland: Tectono-sedimentary evolution of a supra-detachment rift basin. Basin Res. 23, 652–677. https://doi.org/10.1111/j.1365-2117.2011.00509.x

Masini, E., Manatschal, G., Tugend, J., Mohn, G., & Flament, J.-M., 2014. The tectono-sedimentary evolution of a hyper-extended rift basin: the example of the Arzacq–Mauléon rift system (Western Pyrenees, SW France). Int. J. Earth Sci. 103, 1569–1596. https://doi.org/10.1007/s00531-014-1023-8

Mata, M.P., Casas, A.M., Canals, A., Gil, A., & Pocovi, A., 2001. Thermal history during Mesozoic extension and Tertiary uplift in the Cameros Basin, northern Spain. Basin Res. 13, 91–111.

Mathieu, C., 1986. Histoire géologique du sous-bassin de Parentis. Bull. Cent. Rech. Explor. Elf-Aquitaine 10, 22–47.

Mattauer, M., 1968. Les traits structuraux essentiels de la chaîne Pyrénéenne. Rev. Géologie Dyn. Géographie Phys. 10, 3–11.
Mauriaud, P., 1987. La tectonique salifère d'Aquitaine. Le bassin d'Aquitaine. Rev. Pétrole Tech. 335, 38–41.
Mediavilla, F., 1987. La tectonique salifère d'Aquitaine. Le Bassin de Parentis. Rev. Pétrole Tech. 335, 35–37.
Mendia, M.S., & Ibarguchi, J.I.G., 1991. High-grade metamorphic rocks and peridotites along the Leiza Fault (Western Pyrenees, Spain). Geol. Rundsch. 80, 93–107.
Mohn, G., Karner, G.D., Manatschal, G., & Johnson, C.A., 2015. Structural and stratigraphic evolution of the Iberia–Newfoundland hyper-extended rifted margin: a quantitative modelling approach. Geol. Soc. Lond. Spec. Publ. 413, 53–89. https://doi.org/10.1144/SP413.9
Monchoux, P., 1970. Les lherzolites pyrénéennes: contribution à l'étude de leur minéralogie, de leur genèse et de leurs transformations. Université Paul Sabatier de Toulouse (Sciences).
Montadert, L., de Charpal, O., Roberts, D., Guennoc, P., & Sibuet, J.-C., 1979. Northeast Atlantic passive continental margins: Rifting and subsidence processes, in: Talwani, M., Hay, W., Ryan, W.B.F. (Eds.), Maurice Ewing Series. American Geophysical Union, Washington, D. C., pp. 154–186. https://doi.org/10.1029/ME003p0154
Montadert, L., & Winnock, E., 1971. L'histoire structurale du Golf de Gascogne. Technip.
Montigny, R., Azambre, B., Rossy, M., & Thuizat, R., 1986. K-Ar Study of cretaceous magmatism and metamorphism in the Pyrenees: Age and length of rotation of the Iberian Peninsula. Tectonophysics, The Geological Evolution of the Pyrenees 129, 257–273. https://doi.org/10.1016/0040-1951(86)90255-6
Nebot, M., & Guimerà, J.J., 2016. Structure of an inverted basin from subsurface and field data: the Late Jurassic-Early Cretaceous Maestrat Basin (Iberian Chain). Geol. Acta 14, 0155–177.
Nirrengarten, M., Manatschal, G., Tugend, J., Kusznir, N., Sauter, D., 2017. Kinematic evolution of the southern North Atlantic: implications for the formation of hyper-extended rift systems: Kinematic of hyper-extended rift systems. Tectonics. 37. 10.1002/2017TC004495
Olivier, P., Gleizes, G., & Paquette, J.L., 2004. Gneiss domes and granite emplacement in an obliquely convergent regime: New interpretation of the Variscan Agly Massif (Eastern Pyrenees, France). Spec. Pap.-Geol. Soc. Am. 229–242.
Omodeo-Salé, S., Guimerà, J., Mas, R., & Arribas, J., 2014. Tectono-stratigraphic evolution of an inverted extensional basin: the Cameros Basin (north of Spain). Int. J. Earth Sci. 103, 1597–1620. https://doi.org/10.1007/s00531-014-1026-5
Omodeo-Salé, S., Salas, R., Guimerà, J., Ondrak, R., Mas, R., Arribas, J., Suárez-Ruiz, I., & Martinez, L., 2017. Subsidence and thermal history of an inverted Late Jurassic-Early Cretaceous extensional basin (Cameros, North-central Spain) affected by very low- to low-grade metamorphism. Basin Res. 29, 156–174. https://doi.org/10.1111/bre.12142
Ortí, F., 1974. El Keuper del levante español. Estud. Geológicos 30, 7–46.
Ortí, F., Pérez-López, A., & Salvany, J.M., 2017. Triassic evaporites of Iberia: Sedimentological and palaeogeographical implications for the western Neotethys evolution during the Middle Triassic–Earliest Jurassic. Palaeogeogr. Palaeoclimatol. Palaeoecol. 471, 157–180. https://doi.org/10.1016/j.palaeo.2017.01.025
Osmundsen, P.T., & Ebbing, J., 2008. Styles of extension offshore mid-Norway and implications for mechanisms of crustal thinning at passive margins: STYLES OF EXTENSION OFFSHORE NORWAY. Tectonics 27, n/a-n/a. https://doi.org/10.1029/2007TC002242

Osmundsen, P.T., & Péron-Pinvidic, G., 2018. Crustal-Scale Fault Interaction at Rifted Margins and the Formation of Domain-Bounding Breakaway Complexes: Insights From Offshore Norway. Tectonics 37, 935–964. https://doi.org/10.1002/2017TC004792

Osmundsen, P.T., Sommaruga, A., Skilbrei, J.R., & Olesen, O., 2002. Deep structure of the Mid Norway rifted margin. Nor. J. Geol. Geol. Foren. 82.

Pedreira, D., Pulgar, J.A., Gallart, J., & Torné, M., 2007. Three-dimensional gravity and magnetic modeling of crustal indentation and wedging in the western Pyrenees-Cantabrian Mountains. J. Geophys. Res. 112. https://doi.org/10.1029/2007JB005021

Pedrera, A., García-Senz, J., Ayala, C., Ruiz-Constán, A., Rodríguez-Fernández, L.R., Robador, A., & González Menéndez, L., 2017. Reconstruction of the exhumed mantle across the North Iberian Margin by crustal-scale 3-D gravity inversion and geological cross section. Tectonics 36, 3155–3177.

Pedrera, A., García-Senz, J., Peropadre, C., Robador, A., Lopez Mir, B., Diaz Alvarado, J., & Rodríguez-Fernández, L.R., 2020. The Getxo crustal-scale cross-section: testing tectonic models in the Bay of Biscay-Pyrenean rift system. Earth-Sciences Review, doi: 10.1016/j.earscirev.2020.103429.

Pereira, R., Alves, T.M., 2012, Tectono-stratigraphic signature of multiphased rifting on divergent margins (deep-offshore Southwest Iberia, North Atlantic). Tectonics. 31. doi:10.1029/2011TC003001

Pérez-Gussinyé, M., 2013. A tectonic model for hyperextension at magma-poor rifted margins: an example from the West Iberia–Newfoundland conjugate margins. Geol. Soc. Lond. Spec. Publ. 369, 403–427. https://doi.org/10.1144/SP369.19

Péron-Pinvidic, G., Manatschal, G., Masini, E., Sutra, E., Flament, J.M., Haupert, I., & Unternehr, P., 2015. Unravelling the along-strike variability of the Angola–Gabon rifted margin: a mapping approach. Geol. Soc. Lond. Spec. Publ. 438, 49–76. https://doi.org/10.1144/SP438.1

Péron-Pinvidic, G., Manatschal, G., Minshull, T.A., & Sawyer, D.S., 2007. Tectonosedimentary evolution of the deep Iberia-Newfoundland margins: Evidence for a complex breakup history. Tectonics 26, 1–19. https://doi.org/10.1029/2006TC001970

Peybernès, B., 1976. Le Jurassique et le Crétace inferieur des Pyrénées franco-espagnoles entre la Garonne et la Méditérranée. Toulouse.

Peybernès, B., 1979. L'Urgonien des Pyrénées, Essai de synthèse. Geobios 12, 79–87.

Peybernès, B., 1982. Création puis évolution de la marge nord-ibérique des Pyrénées au Crétacé inférieur. Cuad. Geol. Ibérica 8, 987–1004.

Peybernès, B., & Combes, P.-J., 1994. Stratigraphie séquentielle du Crétacé basal (intervalle Berriasien-Hauterivien) des Pyrénées centrales et orientales franco-espagnoles. Cretac. Res. 15, 535–546. https://doi.org/10.1006/cres.1994.1032

Pichel, L. M., Peel, F., Jackson, C. A.-L., & Huuse, M. (2018). Geometry and kinematics of salt-detached ramp syncline basins. Journal of Structural Geology, 115, 208–230. https://doi.org/10.1016/j.jsg.2018.07.016

Pichel, L. M., Finch, E., & Gawthorpe, R. L. (2019). The Impact of Pre-Salt Rift Topography on Salt Tectonics: A Discrete-Element Modeling Approach. Tectonics, 38(4), 1466–1488.

Pinet, B., Montadert, L., Curnelle, R., Cazes, M., Marillier, F., Rolet, J., . . . Brunet, M.F., 1987a. Crustal thinning on the Aquitaine shelf, Bay of Biscay, from deep seismic data. Nature 325, 513.

Pinet, Bertrand, Montadert, L., & ECORS Scientific Party, 1987b. Deep seismic reflection and refraction profiling along the Aquitaine shelf (Bay of Biscay). Geophys. J. Int. 89, 305–312. https://doi.org/10.1111/j.1365-246X.1987.tb04423.x

Platt, N.H., 1986. Sedimentology and Tectonics of the Western Cameros Basin, Province of Burgos, Northern Spain (PhD Thesis). University of Oxford.

Platt, N.H., 1989. Continental sedimentation in an evolving rift basin: the Lower Cretaceous of the western Cameros Basin (northern Spain). Sediment. Geol. 64, 91–109. https://doi.org/10.1016/0037-0738(89)90086-9

Platt, N.H., 1990. Basin evolution and fault reactivation in the western Cameros Basin, Northern Spain. J. Geol. Soc. 147, 165–175. https://doi.org/10.1144/gsjgs.147.1.0165

Quijada, I.E., Suárez González, P., Isabel, B.M., Mas, J.R., & Alonso, Á., 2010. Un ejemplo de llanura fluvio-deltaica influenciada por las mareas: el yacimiento de icnitas de Serrantes (Grupo Oncala, Berriasiense, Cuenca de Cameros, N. de España). Geogaceta 15–18.

Rat, J., Mouthereau, F., Brichau, S., Crémades, A., Bernet, M., Balvay, M., . . . Gautheron, C., 2019. Tectonothermal Evolution of the Cameros Basin: Implications for Tectonics of North Iberia. Tectonics 38, 440–469. https://doi.org/10.1029/2018TC005294

Rat, P., 1988. The Basque-Cantabrian Basin between the Iberian and European plates, some facts but still many problems. Rev Soc Geol Esp. 327–348.

Rat, P., Amiot, M., Feuillée, P., Floquet, M., Mathey, B., Pascal, A., . . . Lamolda, M., others, 1983. Vue sur le Cretacé basco-cantabrique et nord-ibérique. Une Marge Son Arriere-Pays Ses Environ. Sedimentaires Memoires Geol. Univ. Dijon 9, 191.

Ravier, J., 1957. Le métamorphisme des terrains secondaires des Pyrénées. Université, Faculté des Sciences.

Razin, P., 1989, Evolution tecto-sédimentaire alpine des Pyrénées basques à l'ouest de la transformante de Pamplona, Province du Labourd. PhD thesis, University of Bordeaux 3, France, 464 p.

Reston, T.J., 2009. The structure, evolution and symmetry of the magma-poor rifted margins of the North and Central Atlantic: A synthesis. Tectonophysics 468, 6–27. https://doi.org/10.1016/j.tecto.2008.09.002

Reston, T.J., Krawczyk, C.M., & Hoffmann, H.-J., 1995. Detachment tectonics during Atlantic rifting: analysis and interpretation of the S reflection, the west Galicia margin. Geol. Soc. Lond. Spec. Publ. 90, 93–109. https://doi.org/10.1144/GSL.SP.1995.090.01.05

Ribes, C., Ghienne, J.-F., Manatschal, G., Decarlis, A., Karner, G.D., Figueredo, P.H., & Johnson, C.A., 2019. Long-lived mega fault-scarps and related breccias at distal rifted margins: Insights from present-day and fossil analogues. J. Geol. Soc. jgs2018-181. https://doi.org/10.1144/jgs2018-181

Roca, E., 1996. La cubeta mesozoica de las Columbrets: aportaciones al conocimiento de la estructura del surco de Valencia. Geogaceta 20, 1711–1714.

Roma, M., Ferrer, O., Roca, E., Pla, O., Escosa, F.O., & Butillé, M., 2018. Formation and inversion of salt-detached ramp-syncline basins. Results from analog modeling and application to the Columbrets Basin (Western Mediterranean). Tectonophysics 745, 214–228. https://doi.org/10.1016/j.tecto.2018.08.012

Rossi, P., Cocherie, A., Fanning, C.M., & Ternet, Y., 2003. Datation U-Pb sur zircons des dolérites tholéiitiques pyrénéennes (ophites) à la limite Trias–Jurassique et relations avec les tufs volcaniques dits « infra-liasiques » nord-pyrénéens. Comptes Rendus Geosci. 335, 1071–1080. https://doi.org/10.1016/j.crte.2003.09.011

Rouby, D., Raillard, S., Guillocheau, F., Bouroullec, R., & Nalpas, T., 2002. Kinematics of a growth fault/raft system on the West African margin using 3-D restoration. J. Struct. Geol. 24, 783–796.

Roux, J.-C., 1983. Recherches stratigraphiques et sédimentologiques sur les flyschs crétacés pyrénéens au sud d'Oloron (Pyrénées Atlantiques). Université Paul Sabatier de Toulouse (Sciences).

Ruiz, M., 2007. Caracterització estructural i sismotectònica de la litosfera en el domini Pirenaico-Cantàbric a partir de mètodes de sísmica activa i passiva. Universitat de Barcelona.

Sàbat, F., Roca, E., Muñoz, J.A., Vergès, J., Santanach, P., & Masana, E., 1997. Role of extension and compression in the evolution of the eastern margin of Iberia: The ESCI-València trough seismic profile. Rev. Soc. Geológica Esp. 8, 431–448.

Salas, R., Guimerà, J., Mas, R., Martín-Closas, C., Meléndez, A., & Alonso, A., 2001. Evolution of the Mesozoic central Iberian Rift System and its Cainozoic inversion (Iberian chain). Peri-Tethys Mem. 6, 145–185.

Saspiturry, N., Cochelin, B., Razin, P., Leleu, S., Lemirre, B., Bouscary, C., . . . Allanic, C., 2019a. Tectono-sedimentary evolution of a rift system controlled by Permian post-orogenic extension and metamorphic core complex formation (Bidarray Basin and Ursuya dome, Western Pyrenees). Tectonophysics 768, 228180. https://doi.org/10.1016/j.tecto.2019.228180

Saspiturry, N., Razin, P., Baudin, T., Serrano, O., Issautier, B., Lasseur, E., . . . Leleu, S., 2019b. Symmetry vs. asymmetry of a hyper-thinned rift: Example of the Mauléon Basin (Western Pyrenees, France). Mar. Pet. Geol. 104, 86–105. https://doi.org/10.1016/j.marpetgeo.2019.03.031

Saspiturry, N., Razin, P., Allanic, C., Issautier, B., Baudin, T., Lasseur, E., . . Leleu, S., 2020a, Closure of a hyperextended system in an orogenic lithospheric pop-up, Western Pyrenees: The role of mantle buttressing and rift structural inheritance: Terra Nova. 10.1111/ter.12457.

Saspiturry, N., Lahfid, A., Baudin, T., Guillou-Frottier, G., Razin, P., Issautier, B., Le Bayon, B., Serrano, O., Lagabrielle, Y., Corre, B., 2020b. Paleogeothermal Gradients across an Inverted Hyperextended Rift System: Example of the Mauléon Fossil Rift (Western Pyrenees). Tectonics. 10.1029/2020TC006206

Saspiturry, N., 2019. Evolution sédimentaire, structurale et thermique d'un rift hyper-aminci : de l'héritage post-hercynien à l'inversion alpine, Exemple du bassin de Mauléon (Pyrénées). PhD thesis, Bordeaux University, 444p.

Schettino, A., & Turco, E., 2011. Tectonic history of the western Tethys since the Late Triassic. Geol. Soc. Am. Bull. 123, 89–105. https://doi.org/10.1130/B30064.1

Serrano, O., Delmas, J., Hanot, F., Vially, R., Herbin, J.-P., Houel, P., & Tourlière, B., 2006. Le bassin d'Aquitaine: valorisation des données sismiques, cartographie structurale et potentiel pétrolier. Bureau de Recherche Géologique et minière.

Soares, D.M., Alves, T.M., Terrinha, P., 2012. The breakup sequence and associated lithospheric breakup surface: their significance in the context of rifted continental margins (West Iberia and Newfoundland margins, North Atlantic). Earth Planet Sci.Lett. 355–356, 311–326. https://doi.org/10.1016/j.epsl.2012.08.036.

Soares, D.M., 2014. Sedimentological and stratigraphical aspects of the syn- to post-rift transition on fully separated conjugate margins. PhD thesis, Cardiff University. 305p.

Soto, J.I., Flinch, F., & Tari, G., 2017. Permo-Triassic Salt Provinces of Europe, North Africa and the Atlantic Margins: Tectonics and Hydrocarbon Potential, in: In Soto et Al., Eds, Permo-Triassic Salt Provinces of Europe, North Africa and the Atlantic Margins. Tectonics and Hydrocarbon Potential. Elsevier.

Souquet, P., 1967. Le Crétacé supérieur Sud-Pyrénéen, en Catalogne, Aragon et Navarre. E. Privat.

Souquet, P., Debroas, E.-J., Boirie, J.-M., Pons, P., Fixari, G., Roux, J.-C., . . . Manivit, H., others, 1985. Le groupe du Flysch noir (albo-cénomanien) dans les Pyrénées. Bull Cent Rech Exlpo-Prod Elf-Aquitaine Pau 9, 183–252.

Suárez González, P., Quijada, I.E., Mas, J.R., & Benito, M.I., 2010. Nuevas aportaciones sobre la influencia marina y la edad de los carbonatos de la Fm Leza en el sector de Préjano (SE de La Rioja). Cretácico Inferior, Cuenca de Cameros. Geogaceta 7–10.

Teixell, A., Labaume, P., Ayarza, P., Espurt, N., de Saint Blanquat, M., & Lagabrielle, Y., 2018. Crustal structure and evolution of the Pyrenean-Cantabrian belt: A review and new interpretations from recent concepts and data. Tectonophysics 724, 146–170. https://doi.org/10.1016/j.tecto.2018.01.009

Teixell, A., Labaume, P., & Lagabrielle, Y., 2016. The crustal evolution of the west-central Pyrenees revisited: Inferences from a new kinematic scenario. Comptes Rendus Geosci. 348, 257–267. https://doi.org/10.1016/j.crte.2015.10.010

Ternet, Y., Majesté-Menjoulas, C., Canérot, J., Baudin, T., Cocherie, A., Guerrot, C., & Rossi, P., 2004. Carte géologique de la France au 1/50 000: Laruns-Somport, Orléans, France.

Thiébaut, J., Durand-Wackenheim, C., Debeaux, M., & Souquet, P., 1992. Métamorphisme des évaporites triasiques du versant nord des Pyrénées centrales et Occidentales. Bull. Société Hist. Nat. Toulouse 128, 77–84.

Thinon, I., 1999. Structure profonde de la marge Nord Gascogne et du Bassin armoricain. Université de Bretagne occidentale-Brest.

Thinon, I., Fidalgo-González, L., Réhault, J. P. and Olivet, J. L., 2001, Pyrenean deformations in the Bay of Biscay: Comptes Rendus de l'Académie des Sciences, Série IIa, v.332, p.561–568.

Thinon, I., Matias, L., Réhault, J.P., Hirn, A., Fidalgo-GonzÁlez, L., & Avedik, F., 2003. Deep structure of the Armorican Basin (Bay of Biscay): a review of Norgasis seismic reflection and refraction data. J. Geol. Soc. 160, 99–116. https://doi.org/10.1144/0016-764901-103

Tomassimo, A., & Marillier, F., 1997. Processing and interpretation in the tau-p domain of the ECORS Bay of Biscay expanding spread profiles. Mém. Société Géologique Fr. 171, 31–43.

Torné, M., Banda, E., & Fernandez, M., 1996. The Valencia Trough: Geological and geophysical constraints on the basin formation model., in: In P. A. Ziegler, & F. Horvath (Eds.), Structure and Prospects of Alpine Basins and Forelands, Mem. Nat Hist. Mus. pp. 103–128.

Torné, M., Pascal, G., Buhl, P., Watts, A.B., & Mauffret, A., 1992. Crustal and velocity structure of the Valencia trough (western Mediterranean), Part I. A combined refraction/ wide-angle reflection and near-vertical reflection study. Tectonophysics 203, 1–20. https://doi.org/10.1016/0040-1951(92)90212-O

Tugend, J., Manatschal, G., Kusznir, N.J., & Masini, E., 2015. Characterizing and identifying structural domains at rifted continental margins: application to the Bay of Biscay margins and its Western Pyrenean fossil remnants. Geol. Soc. Lond. Spec. Publ. 413, 171–203. https://doi.org/10.1144/SP413.3

Tugend, J., Manatschal, G., Kusznir, N.J., Masini, E., Mohn, G., & Thinon, I., 2014. Formation and deformation of hyperextended rift systems: Insights from rift domain mapping in the Bay of Biscay-Pyrenees. Tectonics 33, 1239–1276. https://doi.org/10.1002/2014TC003529

Vacher, P., & Souriau, A., 2001. A three-dimensional model of the Pyrenean deep structure based on gravity modelling, seismic images and petrological constraints. Geophys. J. Int. 145, 460–470. https://doi.org/10.1046/j.0956-540x.2001.01393.x

Vacherat, A., Mouthereau, F., Pik, R., Bernet, M., Gautheron, C., Masini, E., . . . Lahfid, A., 2014. Thermal imprint of rift-related processes in orogens as recorded in the Pyrenees. Earth Planet. Sci. Lett. 408, 296–306. https://doi.org/10.1016/j.epsl.2014.10.014

Valladares, I., 1980. Evolución de facies en el Jurasico calcareo del sector sur-occidental de la provincia de Burgos. Stud. Geol. Salamanticensia 16, 37–57.

Vargas, H., Gaspar-Escribano, J.M., López-Gómez, J., Van Wees, J.-D., Cloetingh, S., de La Horra, R., & Arche, A., 2009. A comparison of the Iberian and Ebro Basins during the Permian and Triassic, eastern Spain: A quantitative subsidence modelling approach. Tectonophysics 474, 160–183. https://doi.org/10.1016/j.tecto.2008.06.005

Vauchez, A., Clerc, C., Bestani, L., Lagabrielle, Y., Chauvet, A., Lahfid, A., & Mainprice, D., 2013. Preorogenic exhumation of the North Pyrenean Agly massif (Eastern Pyrenees-France). Tectonics 32, 95–106. https://doi.org/10.1002/tect.20015

Vergés, J., & García-Senz, J., 2001. Mesozoic evolution and Cenozoic inversion of the Pyrenean rift. Mém. Muséum Natl. Hist. Nat. 186, 187–212.

Vidal, N., Gallart, J., & Dañobeitia, J.J., 1997. Contribution of the ESCI-Valencia Trough wide-angle data to a crustal transect in the NE Iberian margin. Rev. - Soc. Geológica Esp. 417–429.

Vielzeuf, D., & Kornprobst, J., 1984. Crustal splitting and the emplacement of Pyrenean lherzolites and granulites. Earth Planet. Sci. Lett. 67, 87–96. https://doi.org/10.1016/0012-821X(84)90041-4

Wang, Y., Chevrot, S., Monteiller, V., Komatitsch, D., Mouthereau, F., Manatschal, G., . . . Martin, R., 2016. The deep roots of the western Pyrenees revealed by full waveform inversion of teleseismic P waves. Geology 44, 475–478. https://doi.org/10.1130/G37812.1

Whitmarsh, R.B., Manatschal, G., & Minshull, T.A., 2001. Evolution of magma-poor continental margins from rifting to seafloor spreading. Nature 413, 150–154. https://doi.org/10.1038/35093085

Wilson, R. C. L., G. Manatschal, and S. Wise (2001), Rifting along non-volcanic passive margins: Stratigraphic and seismic evidence from the Mesozoic successions of the Alps and western Iberia, in Nonvolcanic Continental Margins: A Comparison of Evidence From Land and Sea, edited by R. C. L. Wilson et al., Geol. Soc. Spec. Publ., 187, 29 – 452.

Zeyen, H., & Fernàndez, M., 1994. Integrated lithospheric modeling combining thermal, gravity, and local isostasy analysis: Application to the NE Spanish Geotransect. J. Geophys. Res. Solid Earth 99, 18089–18102. https://doi.org/10.1029/94JB00898

Ziegler, P.A., 1982. Triassic rifts and facies patterns in Western and Central Europe. Geol. Rundsch. 71, 747–772. https://doi.org/10.1007/BF01821101

Figure.1

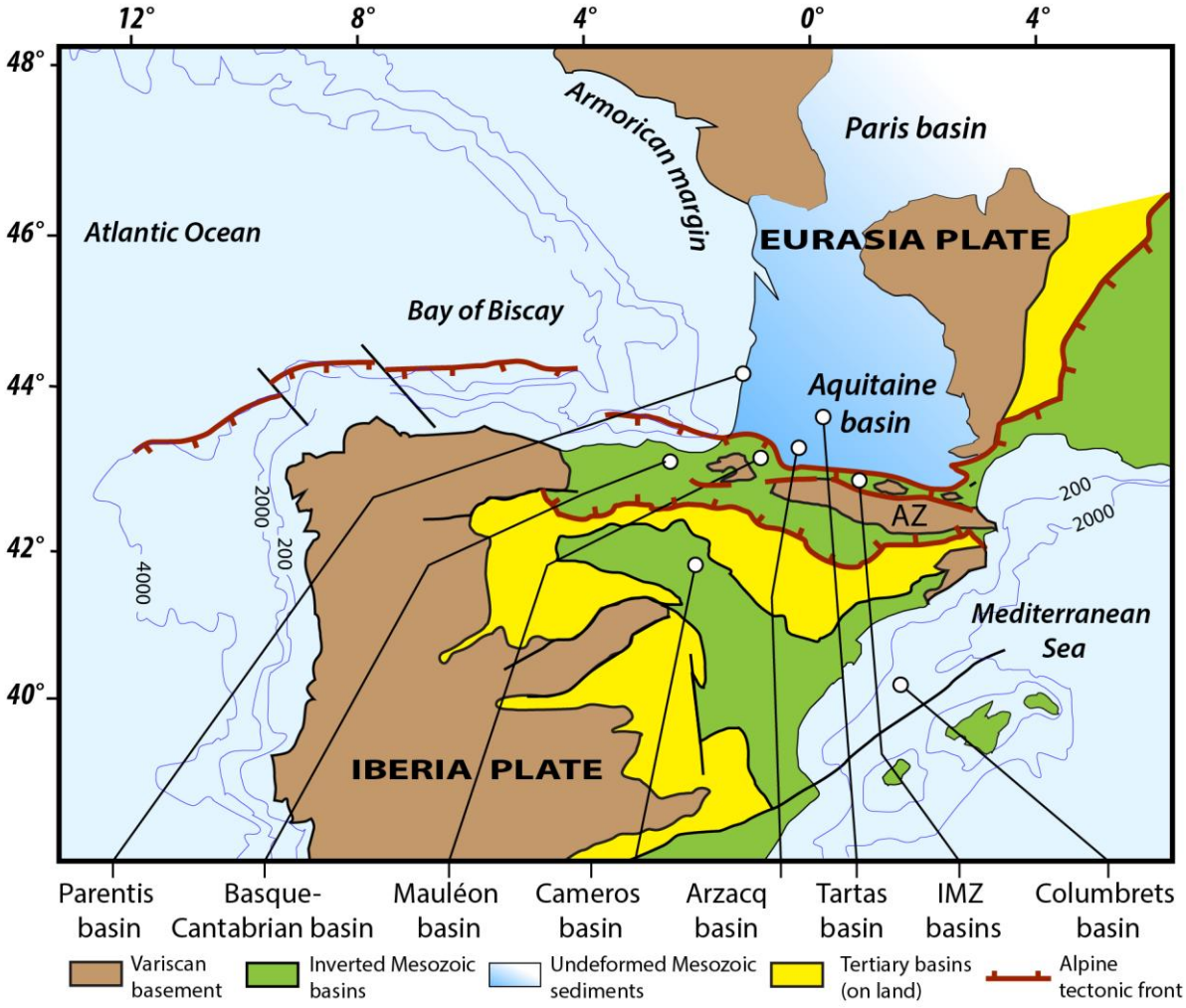

FIGURE 1 Simplified structural map of the Cantabrian-Pyrenean orogenic system and adjoining Iberia showing deformed and undeformed domains in the Eurasia plate and the locations of basins in this study (modified from Lagabrielle et al., 2020).

Figure.2

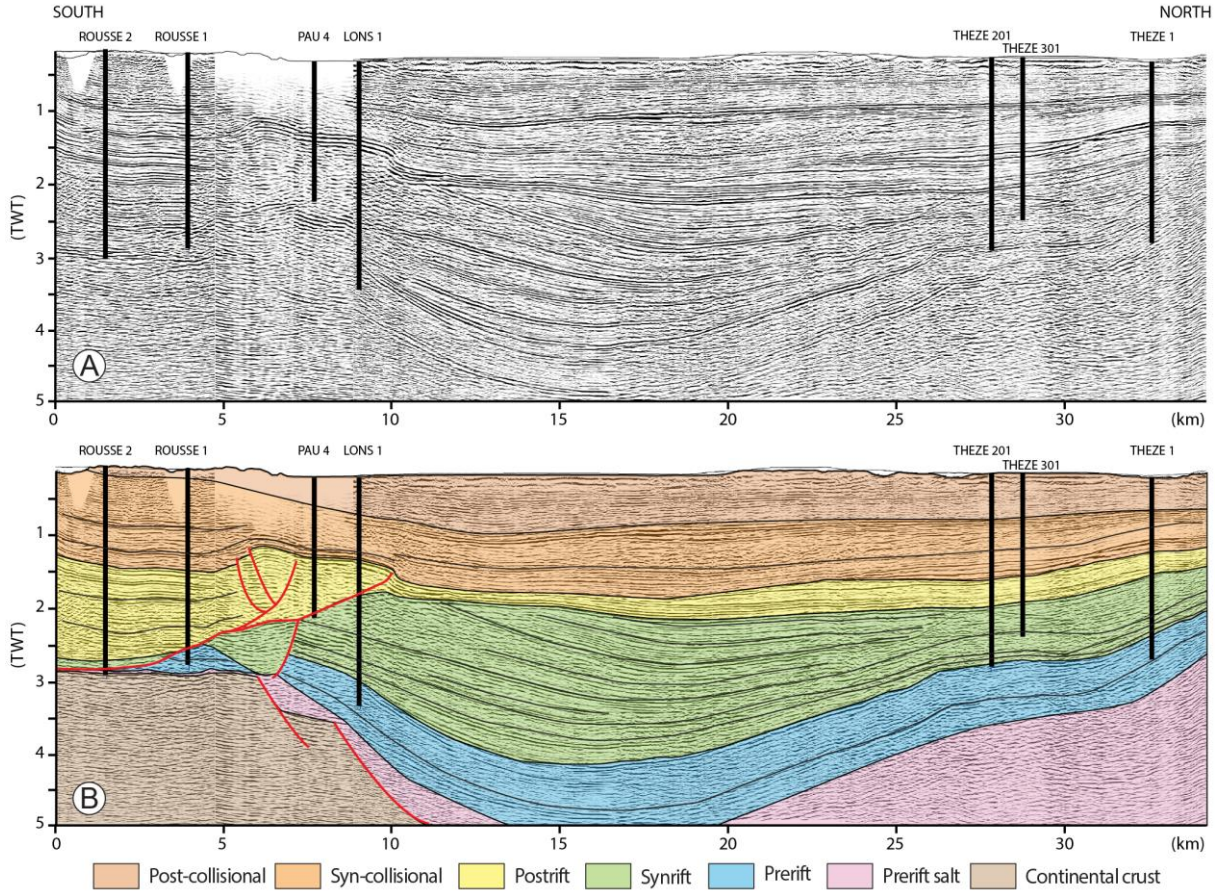

FIGURE 2 Interpretation of a South-North seismic reflection profile across the Arzacq basin: (A) Rousse-Thèze seismic reflection profile, calibrated using, from south to north, the Rousse-2, Rousse-1, Pau-4, Lons-1, Thèze 201, Thèze 301 and Thèze 1 boreholes (Issautier et al., 2020). (B) Interpreted section (modified from Issautier et al., 2020). The syn-rift sequence is characterized by a maximum time thickness of around 2.5 TWT seconds corresponding to a thickness of nearly 2000–3000 m. The depocenter of the syn-rift sequence in the Arzacq basin migrates south from its position, indicating a northward salt-controlled cover gliding during the rifting stage. The Arzacq syn-rift basin is characterized by a slight asymmetry of its depocenter.

Figure.3

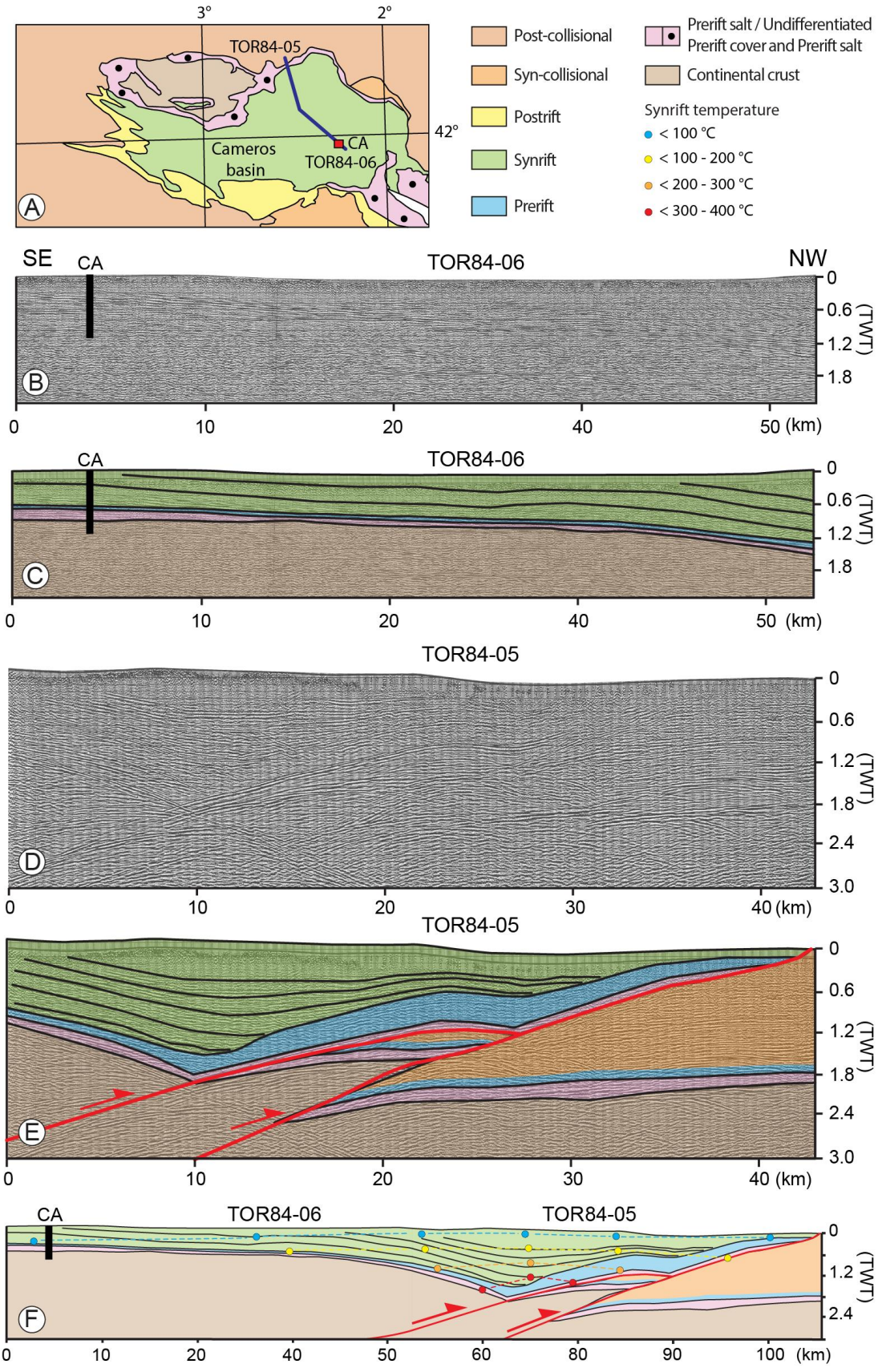
3°
2°
42°
TOR84-05
CA
TOR84-06
Cameros
basin
A
Post-collisional
Syn-collisional
Postrift
Synrift
Prerift
Prerift salt / Undifferentiated
Prerift cover and Prerift salt
Continental crust
Synrift temperature
< 100 °C
< 100 - 200 °C
< 200 - 300 °C
< 300 - 400 °C
SE
CA
TOR84-06
NW
B
0
10
20
40
50 (km)
0
0.6
1.2
1.8
(TWT)
CA
TOR84-06
C
TOR84-05
D
30
2.4
3.0
40 (km)
E
F
60
80
90
100

FIGURE 3 (A) Geological map of the Cameros basin (modified from Omodeo-Salé et al., 2014); (B-C) Interpretation of the SE-NW TOR84-06 seismic reflection profiles across the Cameros basin, location on Figure 3A (Omodeo-Salé et al., 2014), CA: Castelfrio 1 borehole; (D-E) Interpretation of the SE-NW TOR84-05 seismic reflection profiles across the Cameros basin, location on Figure 3A (Omodeo-Salé et al., 2014). (F) Line-drawing of the TOR84-05 and TOR84-06 seismic reflection profiles. The syn-rift sequence displays an onlap geometry on the marine Jurassic substrate towards the north. The depocenter of the syn-rift sequence in the Cameros basin migrates north from its position, indicating southward salt-controlled cover gliding during the rifting stage rooting at depth on a crustal structure. The Cameros syn-rift basin is characterised by a slight asymmetry of its depocenter. The syn-rift sequence is characterised by a maximum time thickness of around 1.5 TWT seconds corresponding to a thickness of nearly 1500–2000 m. Available syn-rift paleotemperatures from Rat et al. (2019) indicate that the base of the syn-rift basin reached temperatures of around 300–400 °C.

Figure.4

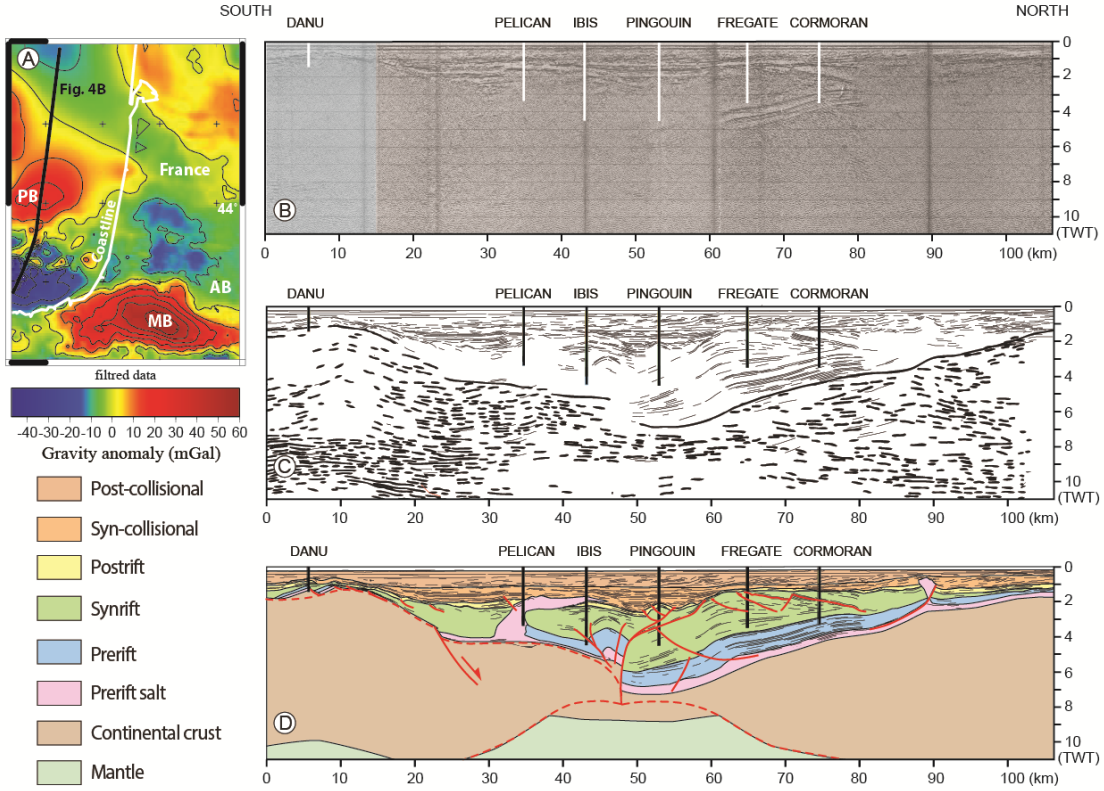

FIGURE 4 Parentis basin architecture. (A) Filtered Bouguer gravity anomaly map (Jammes, 2009); PB: Parentis basin Bouguer Anomaly; MB: Mauléon basin Bouguer Anomaly; AB: Arzacq basin. (B) Bay of Biscay ECORS profile, calibrated using, from south to north, the Danu, Pelican, Ibis, Pingouin, Fregate and Cormoran boreholes (in Jammes, 2009). (C) Line drawing of the sedimentary structures and deep crustal structures of the Bay of Biscay ECORS profile (in Jammes, 2009). (D) Interpreted Bay of Biscay ECORS profile (modified from Jammes, 2019). The depocenter of the syn-rift sequence in the Parentis basin migrates south from its position indicating northward salt-controlled cover gliding during the rifting stage, interpreted by Jammes (2009) and Tugend et al. (2014) as a northward-deepening décollement rooting at depth on a crustal detachment fault. The Parentis syn-rift basin is characterized by a mildly asymmetry of its depocenter. The syn-rift sequence is characterised by a maximum time thickness of around 4 TWT seconds corresponding to a thickness of nearly 3000–4500 m.

Figure.5

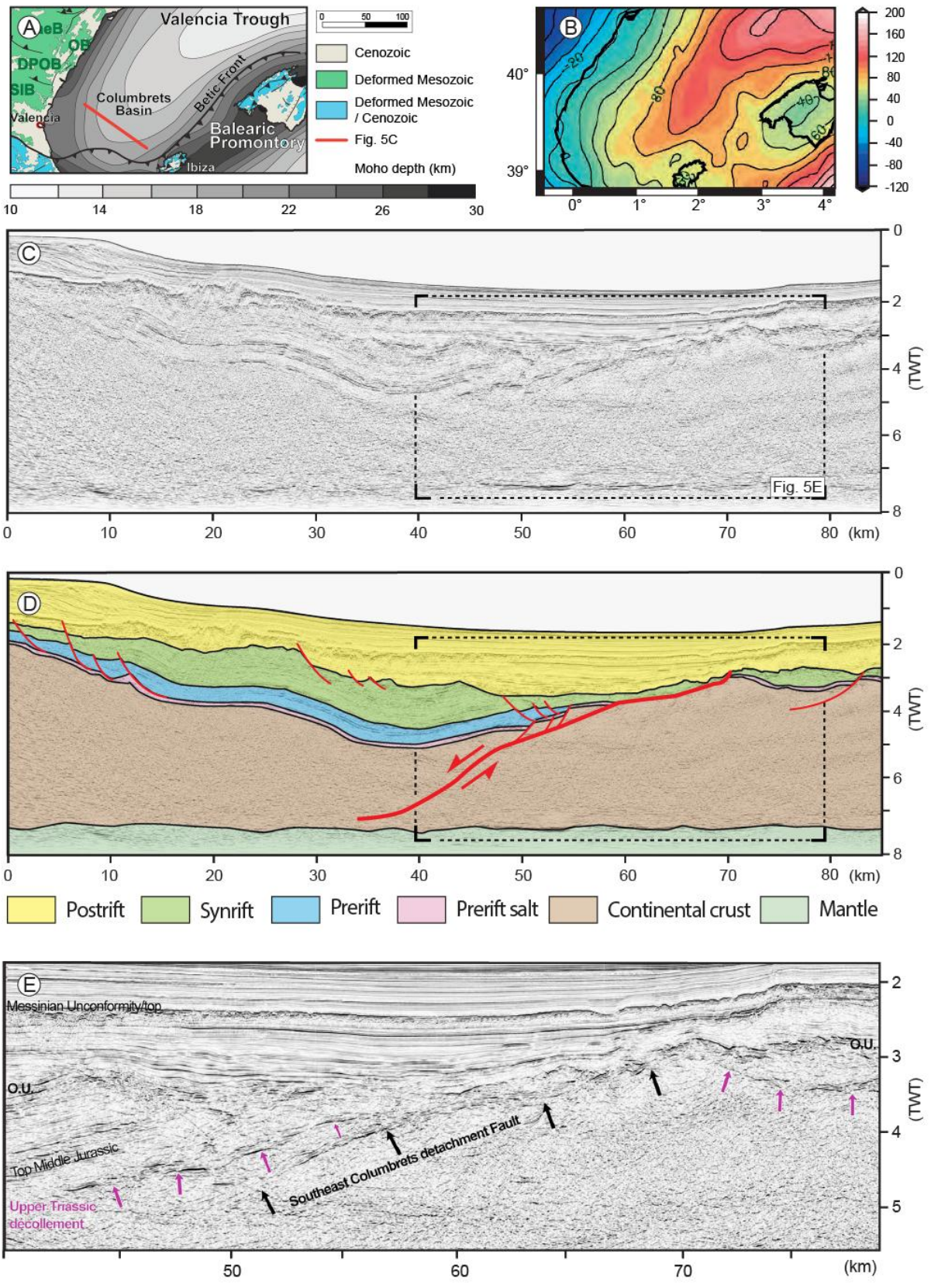
A
Valencia Trough
eB
OB
DPOB
SIB
Columbrets Basin
Betic Front
Balearic Promontory
Valencia
Ibiza
0 50 100
Cenozoic
Deformed Mesozoic
Deformed Mesozoic / Cenozoic
Fig. 5C
Moho depth (km)
10 14 18 22 26 30
B
40°
39°
0° 1° 2° 3° 4°
200 160 120 80 40 0 -40 -80 -120
C
Fig. 5E
0 10 20 30 40 50 60 70 80 (km)
0 2 4 6 8 (TWT)
D
Postrift
Synrift
Prerift
Prerift salt
Continental crust
Mantle
E
Messinian Unconformity/top
O.U.
Top Middle Jurassic
Upper Triassic décollement
Southeast Columbrets detachment Fault
50 60 70 (km)
2 3 4 5 (TWT)

FIGURE 5 (A) Geological and structural map of the Columbrets basin showing the Moho depth varying from 10 to 30 km depth (modified from Etheve et al., 2018). (B) Map of the Bouguer anomaly (modified from et al., 2015). (C) NW-SE SGV01-113 seismic reflection profile; location on Figure 5A (Etheve et al., 2018). (D) Interpreted SGV01-113 seismic reflection profile (modified from Etheve et al., 2018). The syn-rift sequence is characterised by a maximum time thickness of around 1.5 TWT seconds corresponding to a thickness of nearly 1500–2000 m; however, its true thickness was greater as the top of this sequence is affected by a major Tertiary erosional unconformity. The depocenter of the syn-rift sequence in the Columbrets basin migrates south from its position, indicating northward salt-controlled cover gliding during the rifting stage interpreted by Etheve et al. (2018) as a northward-deepening salt décollement rooting at depth on a ductile crustal detachment fault. (E) Detail of the southern part of the SGV01-113 seismic reflection profile showing the northward-deepening ductile crustal detachment fault (Etheve et al., 2018).

Figure.6

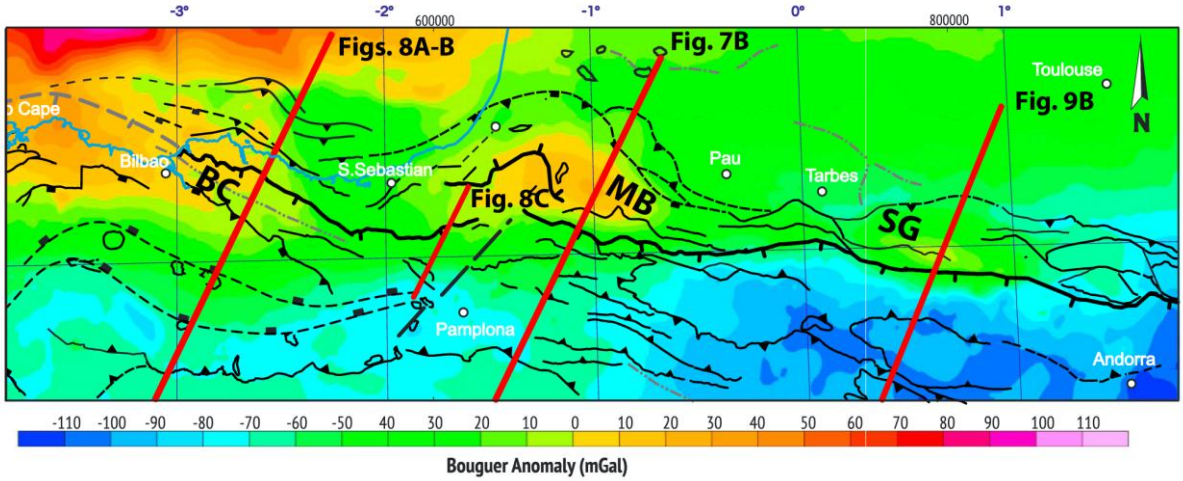

FIGURE 6 Bouguer anomaly map from the Basque-Cantabrian basin to the Central Pyrenees (Pedrera et al., 2017). BC, Basque-Cantabrian Bouguer anomaly; MB, Mauléon basin Bouguer anomaly; SG, Saint-Gaudens Bouguer anomaly.

Figure.7

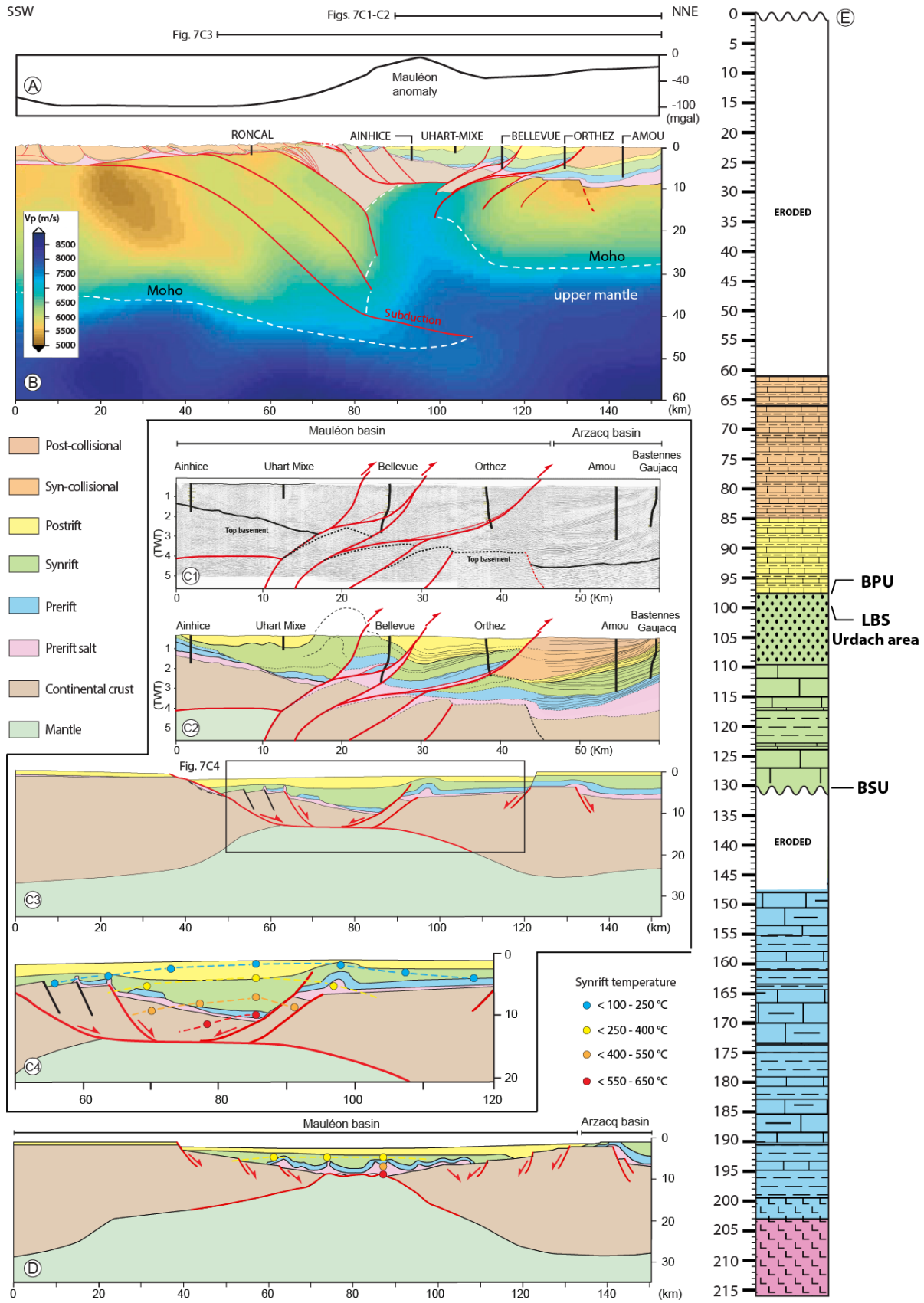
SSW
NNE
Figs. 7C1-C2
Fig. 7C3
Mauléon anomaly
(mgal)
RONCAL
AINHICE
UHART-MIXE
BELLEVUE
ORTHEZ
AMOU
Vp (m/s)
Moho
upper mantle
Subduction
(km)
Post-collisional
Syn-collisional
Postrift
Synrift
Prerift
Prerift salt
Continental crust
Mantle
Mauléon basin
Arzacq basin
Ainhice
Uhart Mixe
Bellevue
Orthez
Amou
Bastennes Gaujacq
Top basement
(TWT)
(Km)
Fig. 7C4
Synrift temperature
< 100 - 250 °C
< 250 - 400 °C
< 400 - 550 °C
< 550 - 650 °C
ERODED
BPU
LBS
Urdach area
BSU

FIGURE 7 Mauléon basin overall architecture. (A) Bouguer anomaly (Casas et al., 1997). (B) Mauléon basin lithospheric section (see location on Figure 6). The lowermost part corresponds to the Wang et al. (2016) Vp model showing the presence at shallow depth of continental lithospheric mantle. The uppermost part is materialized by the Saspiturry et al. (2020a) crustal-scale balanced cross-section calibrated using (from south to north) the Ronca, Ainhice, Uhart-Mixe, Bellevue, Orthez, Amou and Bastennes Gaujacq boreholes. (C1, C2) Geological section through the present-day Mauléon basin based on interpreted seismic lines and field data (modified from Saspiturry et al., 2019a). The Mauléon basin is exposed within a pop-up structure formed during N-S Pyrenean compression. (C3) Palinspastic restoration, to Santonian time, of the Saspiturry et al. (2020a) crustal-scale balanced cross-section. (C4) Detail of the palinspastic restoration of the Saspiturry et al. (2020a) crustal-scale balanced cross-section, with RSCM syn-rift paleotemperature of Saspiturry (2019). (D) Palinspastic restoration, to Santonian time, of the Teixell et al. (2016) crustal-scale balanced cross-section, with RSCM syn-rift paleotemperature of Corre (2017). (E) Stratigraphic chart showing the position of the key markers of the Mauléon basin. BSU, basal syn-rift unconformity; LBS, lithospheric breakup surface; BPU, basal post-rift unconformity.

Figure.8

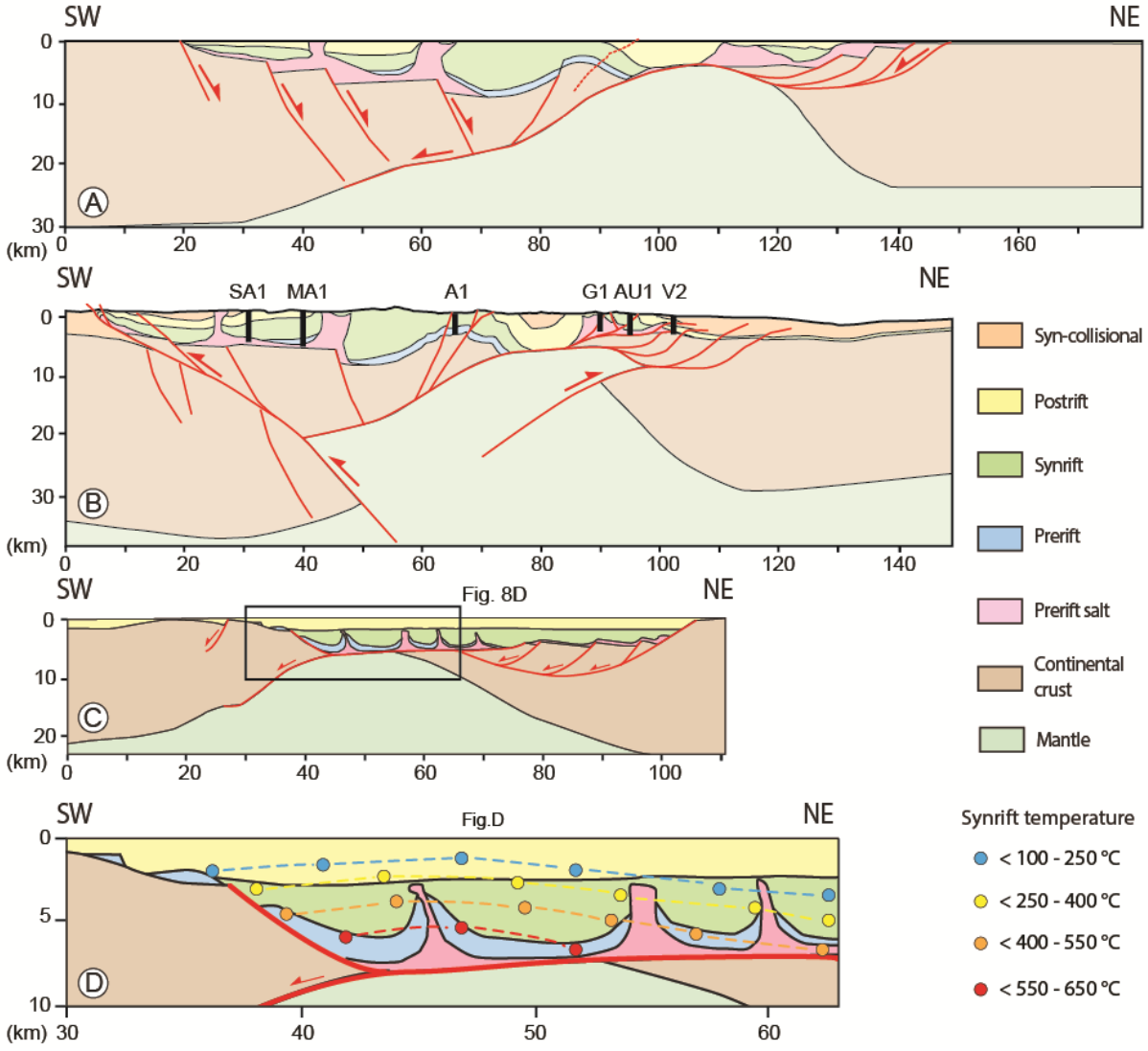

FIGURE 8 (A) Basque-Cantabrian basin palinspastic restoration, to Santonian time, of the Pedrera et al. (2017) crustal-scale balanced cross-section (see location on Fig. 6). (B) Basque-Cantabrian basin crustal-scale balanced cross-section (Pedrera et al., 2017), calibrated using (from south to north) the San Antonio 1 (SA-1), Marinda 1 (MA-1), Arratia 1 (A1), Gernika 1 (G1), Aulesti 1 (AU1) and Vizcaya C2 (V2) boreholes. (C) Schematic restoration of the eastern part of the Basque-Cantabrian basin in the "Nappe des Marbres" (Ducoux et al., 2019). (D) Detail of (C) with the RSCM syn-rift paleotemperatures measured by Ducoux et al. (2019).

Figure.9

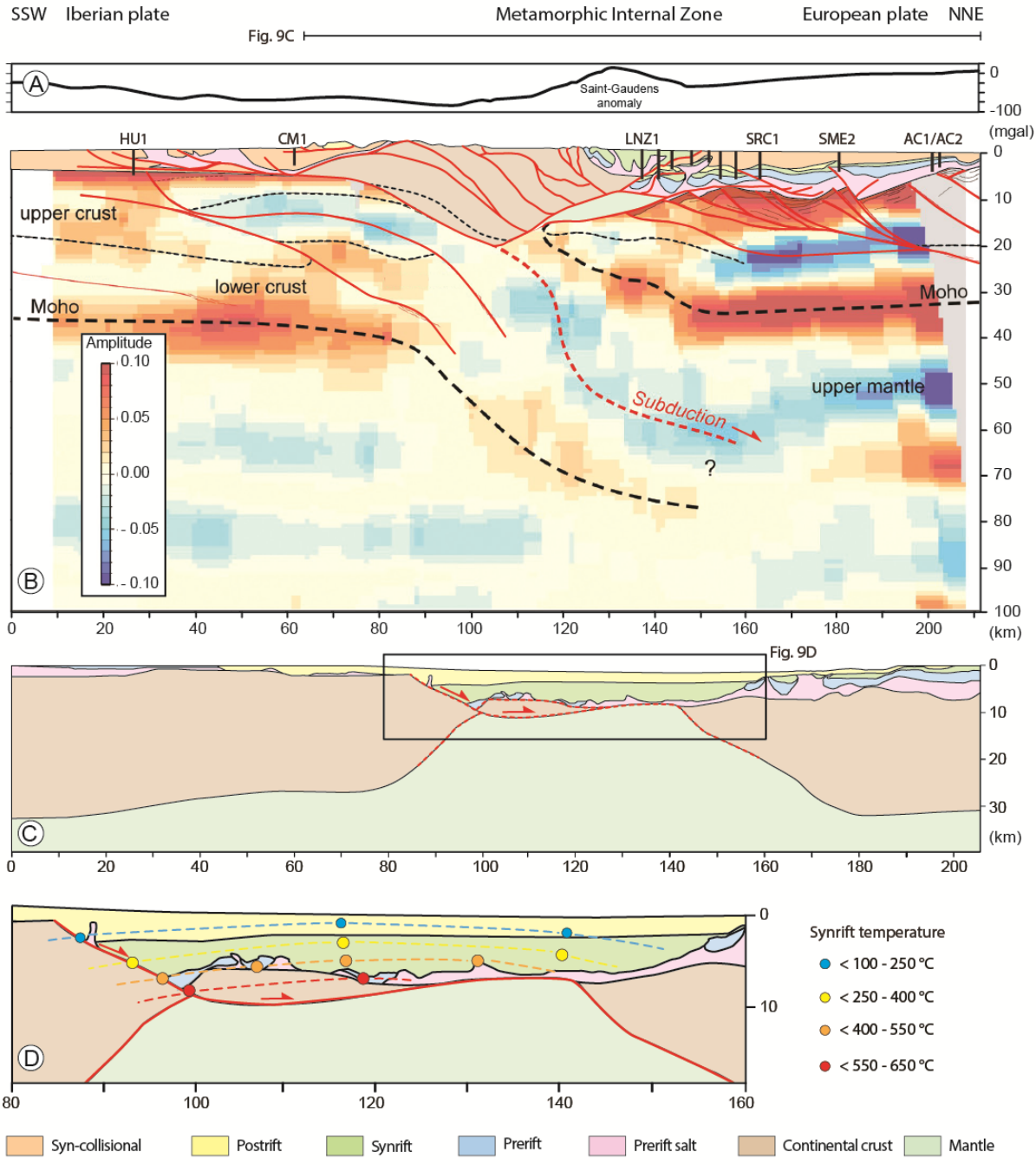

FIGURE 9 Metamorphic Internal Zone overall architecture. (A) Bouguer anomaly (in Espurt et al., 2019). (B) Metamorphic Internal Zone basin lithospheric section (see location on Figure 6). The lowermost part corresponds to the stack profile of receiver functions for the OROGEN West profile across the Central Pyrenean belt (in Espurt et al., 2019) showing the presence at

shallow depth of continental lithospheric mantle. The uppermost part is based on the Espurt et al. (2019) crustal-scale balanced cross-section calibrated using (from south to north) the Huesca 1 (HU-1), Campanue-1 (CM-1), Lannemezan 1 (LNZ1), Sariac 1 (SRC-1), Saint Médard 2 (SME-2), Auch 1 (AC-1) and Auch 2 (AC-2) boreholes. (C) Palinspastic restoration, to Santonian time, of the Espurt et al. (2019) crustal-scale balanced cross-section. (D) Detail of the palinspastic restoration of the Espurt et al. (2019) crustal-scale balanced cross-section, with RSCM syn-rift paleotemperatures.

Figure.10

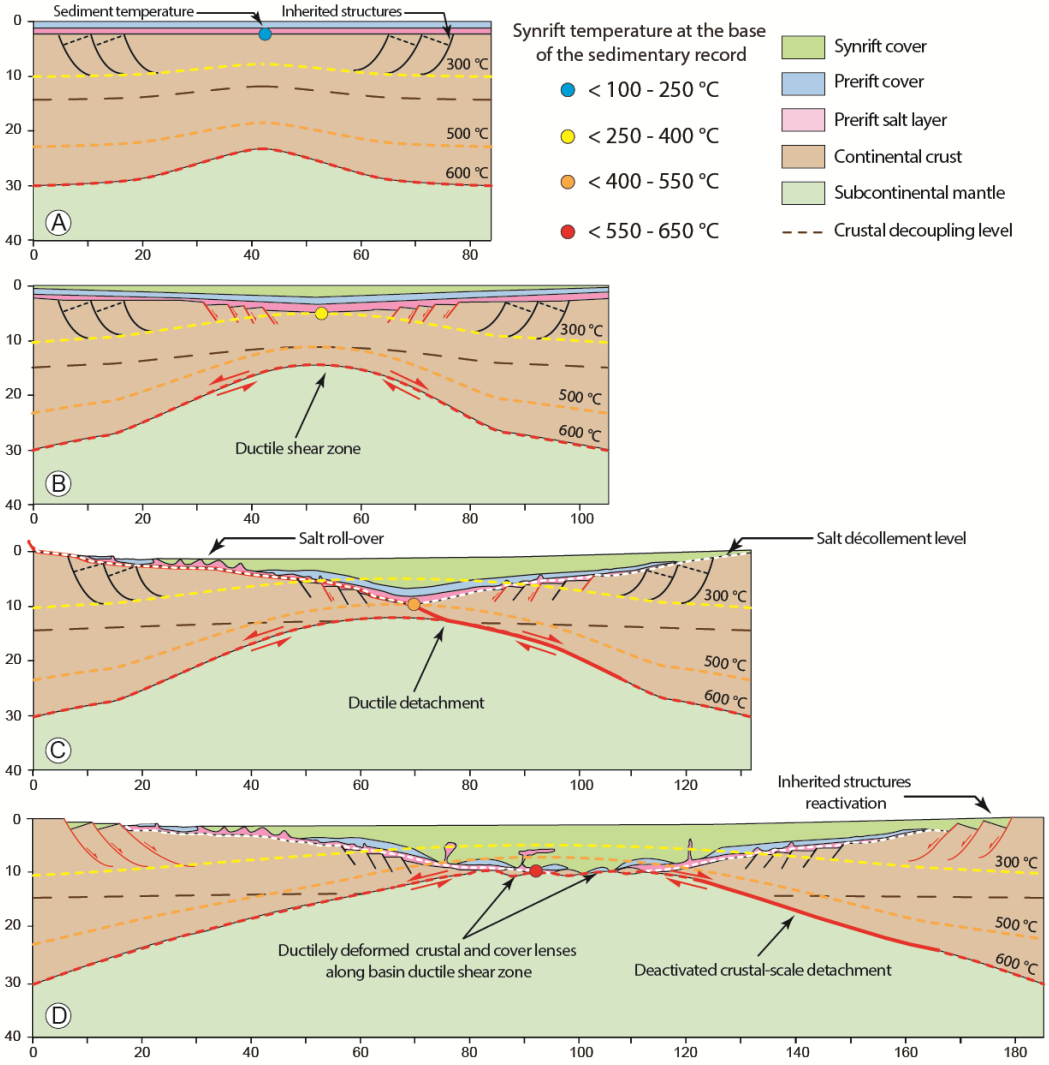

FIGURE 10 Conceptual model of the evolution of a smooth-slope type basin. (A) Inherited thin lithosphere. (B) Pure shear dominated thinning: formation of a symmetric basin characterized by shallow-water sediments. (C) Simple shear dominated thinning: basinward gliding of the pre-rift sedimentary cover along a major detachment connecting towards the surface with the Late Triassic salt décollement, leading to an asymmetrical basin shape. (D) Breakup stage resulting in the formation of a pseudo-symmetric basin undergoing brittle deformation on the proximal margins and ductile deformation in the basin core. No vertical exaggeration. Coloured dashed lines represent crustal isotherms; coloured circles indicate maximum sediment temperatures during HT/LP metamorphism.

1982 **Figure.11**

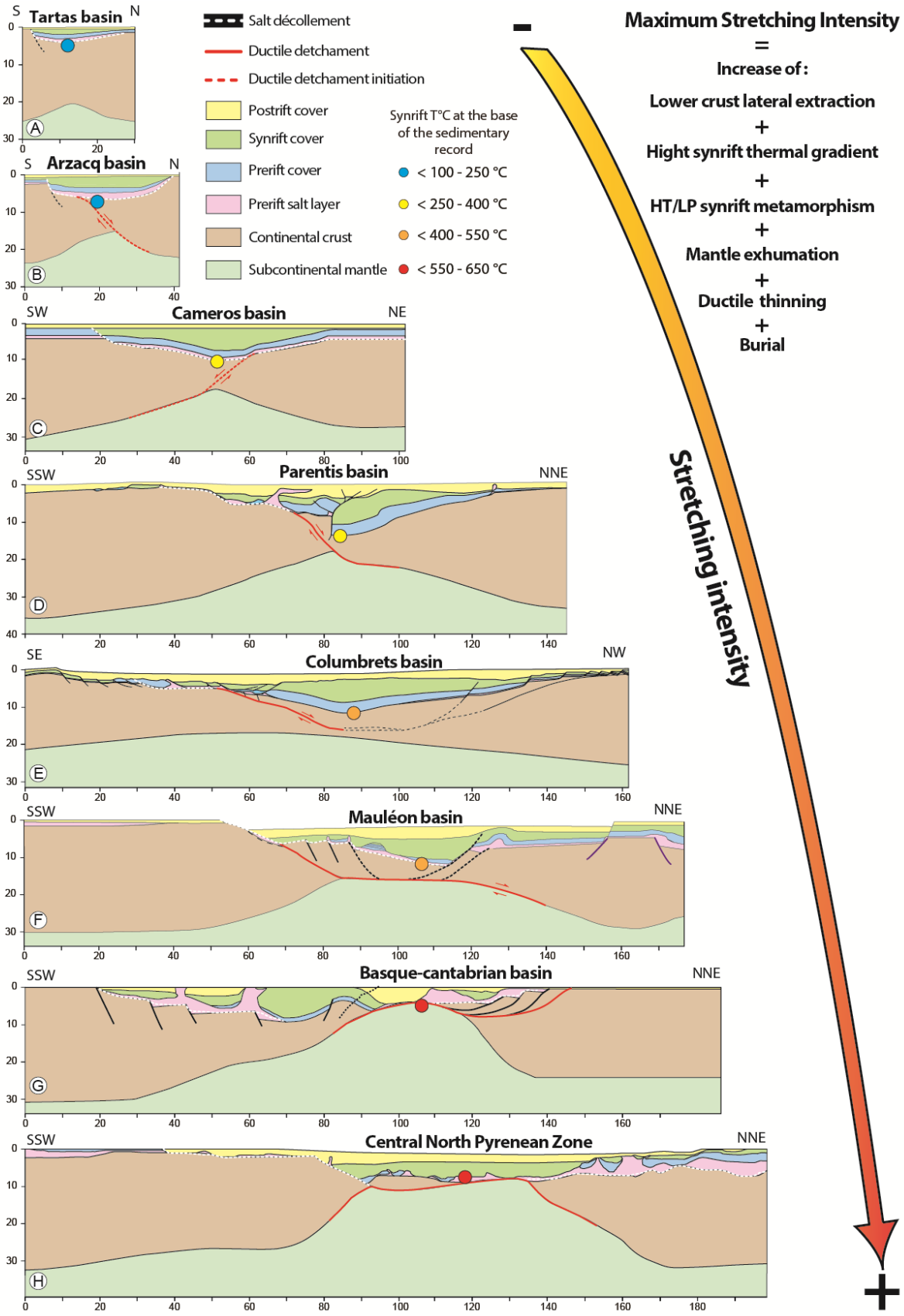

1983

FIGURE 11 Smooth-slope type basins classified according to the degree of continental crust extension: (A) Tartas sub-basin (Issautier et al., 2020); (B) Arzacq sub-basin (Issautier et al., 2020); (C) Cameros basin (modified after Casas-Sainz & Gil-Imaz, 1998); (D) Parentis basin (Tugend et al., 2014); (E) Columbrets basin (Etheve et al., 2018); (F) Mauléon basin (Saspiturry et al., 2019a); (G) Basque-Cantabrian basin (Pedrera et al., 2017); (H) Central North Pyrenean Zone basins (Espurt et al., 2019); locations in Figure 1. No vertical exaggeration. The large arrow indicates the degree of extension and the rise in peak metamorphic temperatures throughout the basin evolutionary sequence. Coloured circles indicate maximum sediment temperatures during HT/LP metamorphism.

1993 **Figure.12**

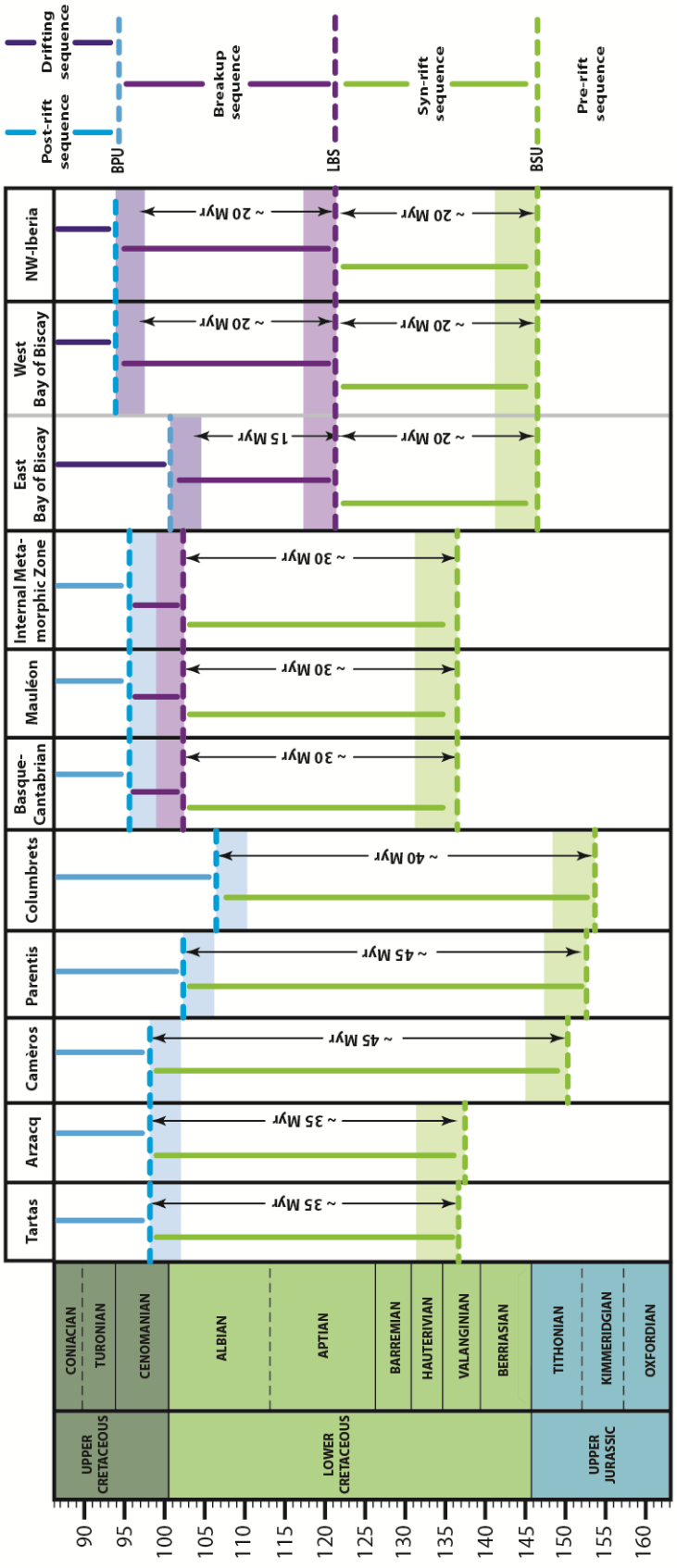

1994

FIGURE 12 Chronological chart showing the timing of the syn-rift, late syn-rift, breakup (mantle exhumation), post-rift and oceanic spreading events of the reviewed basins, the West Iberia basins and the Bay of Biscay margins. References used to define the timing of the different events: Tartas and Arzacq basins (Désaglaux & Brunet, 1990; Brunet, 1991; Serrano et al., 2006; Issautier et al., 2020), Camèros basin (Platt, 1990; Mas et al., 1993; Casas-Sainz & Gil-Imaz, 1998; Salas et al., 2001; Omodeo-Salé et al., 2014, 2017), Parentis basin (Brunet, 1994; Ferrer et al., 2008; Jammes et al., 2009; Tugend et al., 2015), Columbrets basin (Salas et al., 2001; Nebot & Guimerà, 2016; Etheve, 2016; Etheve et al., 2018; Roma et al., 2018), Basque-Cantabrian basin (Azambre & Rossy, 1976; Rat et al., 1983; Rat, 1988; García Mondéjar et al., 1996; Castañares et al., 1997; Castañares & Robles, 2004; Pedrera et al., 2017; Ducoux et al., 2019), Mauléon basin (Boirie, 1981; Fixari, 1984; Souquet et al., 1985; Jammes et al., 2009; Debroas et al., 2010; Masini et al., 2014; Teixell et al., 2016; Saspiturry et al., 2019a; Labaume and Teixell, 2020), Internal Metamorphic Zone basin (Lagabrielle & Bodinier, 2008; Lagabrielle et al., 2010, 2019; Clerc & Lagabrielle, 2014; Clerc et al., 2014, 2015; de Saint Blanquat et al., 2016; Teixell et al., 2018; Espurt et al., 2019), Northwest-Iberia margin (Soares et al., 2012; Pereira & Alves, 2012, Alves & Cunha, 2018; Alves et al., 2020), and Bay of Biscay margins (Montardet et al., 1979; Brunet 1994; Thinon, 1999; Thinon et al., 2001, 2003; Gong et al., 2008; Tugend et al., 2015). BSU, basal syn-rift unconformity; LBS, lithospheric breakup surface; BPU, basal post-rift unconformity. Coloured shaded areas represent time uncertainty of the BSU, LBS and BPU unconformities.

2015 **Figure.13**

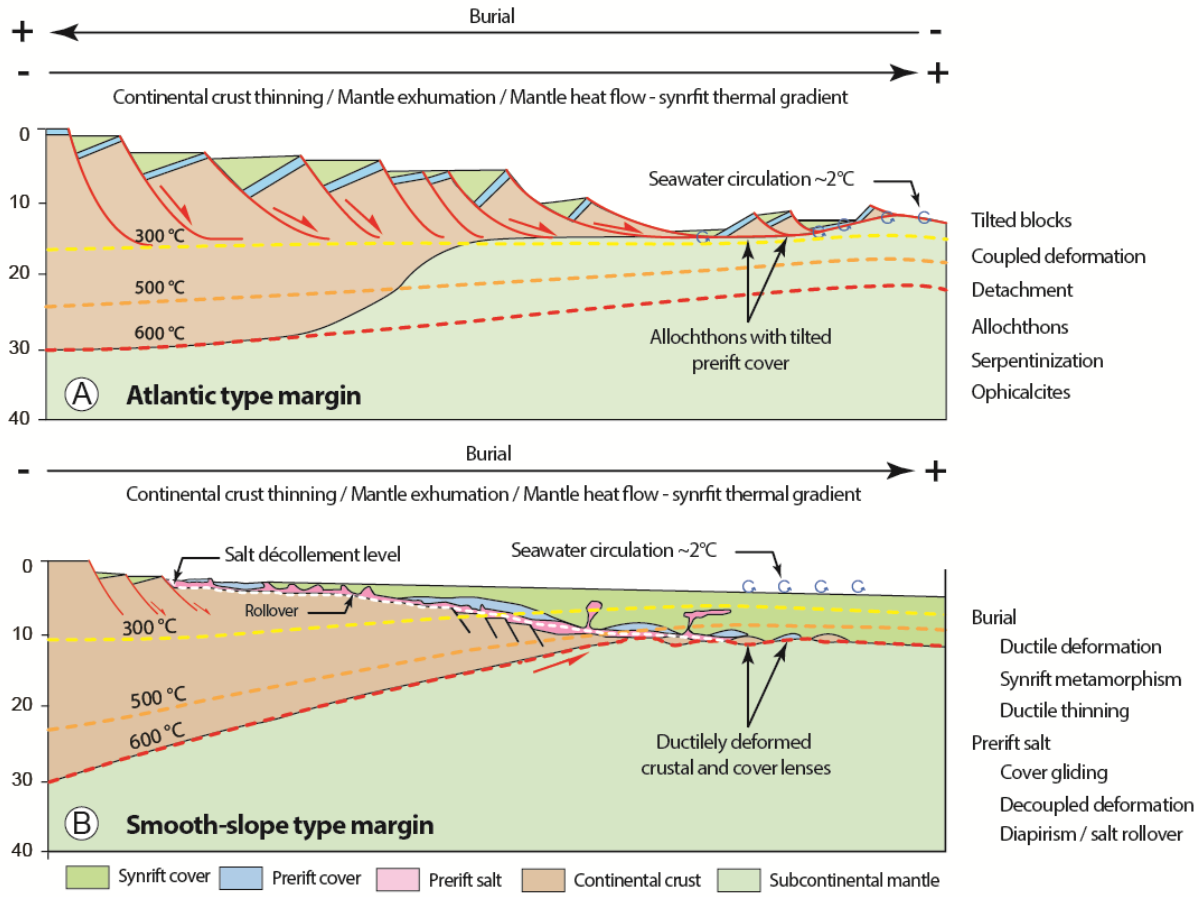

2016

2017 **FIGURE 13** Schematic diagrams showing (A) Atlantic-type margin architecture (section
2018 modified from Péron-Pinvidic et al., 2015) and (B) smooth-slope type margin architecture.
2019 Coloured dashed lines represent crustal isotherms; coloured circles indicate maximum
2020 sediment temperatures during HT/LP metamorphism.